GROUND WATER TRACER STUDIES IN COLUMBIA RIVER BASALT

A Thesis

Presented in Partial Fulfillment of the Requirements for the

Degree of Master of Science

with a

Major in Hydrology

in the

College of Graduate Studies

University of Idaho

by

Robin E. Nimmer

December, 1998

Major Professor: Dr. Dale R. Ralston

Authorization to Submit Thesis

This thesis of Robin E. Nimmer, submitted for the degree of Master of Science and titled "Ground Water Tracer Studies in Columbia River Basalt," has been reviewed in final form, as indicated by the signatures and dates given below. Permission is now granted to submit final copies to the College of Graduate Studies for approval.

Major Professor _____ Date _____

Dale R. Ralston

Committee Members _____ Date _____

James Osiensky

_____ Date _____

Ronald L. Crawford

Department
Administrator   _____ Date _____

John Oldow

College Dean   _____ Date _____

Earl Bennett

Final Approval and Acceptance by the College of Graduate Studies

_____ Date _____

Jean'ne M. Shreeve

ABSTRACT

Ground water contamination in a fractured rock aquifer is very difficult to remediate. An understanding of the transport mechanisms that occur in the fractures and the rock matrix is important in order to implement cleanup strategies such as *in situ* bioremediation. The objective of this study was to examine and compare responses of various tracers from tests in a basalt fracture zone aquifer.

Transport in fractured rock is affected by aquifer heterogeneities, advection, dispersion, molecular diffusion, matrix diffusion, channeling, transport in different channels, borehole storage and sorption; particulate transport may also be affected by filtration and sorption. Multiple well tracer tests using dissolved and particulate tracers were conducted to assist in the detection of these processes.

The field site for the tracer experiments is located in Moscow, Idaho at the University of Idaho Groundwater Research Site (UIGRS). Wells used in the tracer tests are located within a single fracture zone, the E-fracture, approximately 75 feet below land surface in the Wanapum Formation basalt of the Columbia River Basalt Group.

Five successful recirculating and nonrecirculating radially convergent tracer tests were conducted within the E-fracture zone using conservative or near-conservative tracers and particulate tracers. The tracers include fluorescein, bromide, iodide, veratryl alcohol, benzoic acid, polystyrene non-carboxylated fluorescent microbeads (6 micron) and *Bacillus thermoruber* spores.

The data from the tracer experiments were analyzed by basic analytical methods and type curve matching. Calculations generated from the experiments include: tracer velocity, hydraulic gradient, tracer mass recovery and dispersivity.

Results for the dissolved tracers showed a rapid increase in concentration, multiple peaks and a long breakthrough curve tail. The particulate tracers peak breakthrough arrived prior to that of the dissolved tracers.

The fluorescein data were applied to type curves by a curve matching process using the Brenner solution and the Sauty (1980) method. Most of the data points do not fall on the type curves and the calculated dispersivity values are estimations only.

The tracer test results indicate transport is governed by preferential pathways and may be affected by aquifer heterogeneity, advection, dispersion, molecular diffusion, matrix diffusion, channeling, transport in different channels, borehole storage and sorption; although, matrix diffusion and sorption are not likely. The particulate tracers may also be affected by density and filtration.

ACKNOWLEDGEMENTS

DEDICATION

I dedicate this work to my parents, Jim and Sue Kromm, and my husband, Nuri.

TABLE OF CONTENTS

LIST OF FIGURES

LIST OF TABLES

CHAPTER 2
BACKGROUND REVIEW

INTRODUCTION

Transport of ionic, organic, microbial and particle tracers in a fractured rock aquifer is controlled by the tracer characteristics and the unique pattern of fractures and joints within the block of rock being tested. Hydraulic analysis of ground water flow in fractured rock usually is based on one of the following conceptual models: discrete fractures, double porosity or equivalent porous medium models. The density of fractures and measurement scale influence the test results and control which conceptual model is used as the basis for data analysis. Transport in a fractured medium is influenced by several processes including fracture roughness, channeling, reaction and retardation processes, sorption and density effects. Particulate transport in fractured media is also affected by filtration. In addition, microorganism transport may be affected by more microbial-specific processes.

Also reviewed in this chapter are different types of tracer tests and various ground water tracers. Both single and double well tracer tests are discussed. The types of tracers include conservative and near conservative dissolved tracers and microbial and particle tracers.

TRANSPORT PROCESSES IN FRACTURED ROCK

Water movement in fractured rock is more complex than in a porous medium due to the extreme heterogeneity and complicated structure of the medium. In most fractured media, flow and transport occur mainly in the fractures while most of the storage is in the blocks or matrix. The blocks may include more than 99% of the rock volume and thus most of the water in storage. Block porosity includes both primary porosity and secondary porosity related to microfractures. Solute transport processes in fractured rock are similar to a porous medium by advection and hydrodynamic dispersion but are dominated by specific fracture features.

Fractured Rock Flow Classifications

Analysis of ground water flow in fractured rock usually is based on one of the following conceptual models: discrete fractures, double porosity or equivalent porous medium models (Li, 1991). In the discrete fracture model, the primary porosity of the blocks is insignificant and the characteristics of discrete fractures govern hydraulic properties including their "continuity, density, geometry (shape, orientation, aperture and scale) and interconnectedness" (p. 63). Solute moves through fractures with storage in the porous rock matrix in a double porosity system. Generally in this system, advection dominates transport through the fractures while diffusion dominates transport within the rock matrix and between the fractures and rock matrix (Novak, 1993). The third fractured rock conceptual model is the equivalent porous medium or continuum model; the rock system behaves as a porous medium due to abundant fracturing.

Dverstorp et al. (1992) compared tracer migration in a sparsely fractured rock using a discrete fracture network model to results from a three-dimensional field experiment at the Stripa Mine in Sweden. Parallel plates and tubes were used to represent the flow channels. The authors suggested that the discrete fracture model is superior to many other models because it allows for quantitative values of fracture size, aperture, orientation and other model parameter values. The model allows for the testing of the importance of different parameters and assumptions. However, only a single fracture was simulated which may not represent fracture networks. Average medium properties should not be used for analysis of transport over the entire fracture because of channeling and other network effects.

The double porosity model has been applied to field data in a number of studies. Reeves et al. (1991) modeled data from a field study in fractured dolomite at the Waste Isolation Pilot Plant (WIPP) in New Mexico using a single porosity fracture model, a single porosity model which combines the porosity of the fractures and blocks and a double-porosity model. The authors concluded that the double porosity model best matched the data. Ostensen (1998) also conducted tracer experiments at the WIPP site. He modeled the data using a double porosity model and discovered that matrix diffusion was insignificant in retarding the tracer. In another study, Novak (1993) successfully applied a two-dimensional

double porosity model with reactions to results from an experiment in a single fracture and adjacent block matrix.

Berkowitz et al. (1988) conducted a study of contaminant transport in fractured rock. Their results showed that discrete fracture models have limited application to field related investigations because there may be hundreds or thousands of fractures in a system and the location and characteristics of each fracture must be known. Supporting this hypothesis, their experimental breakthrough curves matched equivalent porous medium model breakthrough curves quite well.

Two authors provided guidelines as to when an equivalent porous medium model may be applied to results from tests in fractured rock. Pankow et al. (1986) concluded that the equivalent porous medium model is appropriate when the rock medium has a small fracture spacing, the connectivity of the fractures is great, and the block porosity is high. Tsang et al. (1988) stated the equivalent porous medium model should not be used when channeling is observed.

Scale of Measurement

The scale of measurement should be considered when selecting the appropriate model to represent solute and particulate transport (Li, 1991; NRC, 1996). Neretnieks (1993) stated that the measurement scale depends upon the fracture frequency, the length and orientation of the fractures, and other geometrical characteristics of the fractures. Several parameters that are affected by scale include: the permeability of the individual fractures, (Neretnieks, 1993), fluid velocity (Abelin, 1991a) and dispersivity.

The measurement scale is divided into sections by Berkowitz et al. (1988) who described four different scales. These include:

"very near field" scale: one fracture close to the source
"near field" scale: the number of interconnected fractures is low, near the source
"far field" scale: the fractures and porous matrix continue to behave separately, far from the source
"very far field" scale: the entire system behaves as an equivalent porous medium. The fractures act as large pores.

The "very near field" and "near field" scale data responded to discrete fracture models. The

"far field" scale data are represented by a double porosity system, and the "very far field" scale data are represented by an equivalent porous medium model.

Li (1991) provided a similar scale classification. In a large-scale test (tens to hundreds of meters), the system often behaves as a double porosity system or an equivalent porous medium; in a small-scale test, the fractures often behave as a discrete fractured medium or a double porosity medium. For example, the fractured basalt of the Columbia River Basalt Group behaves as discrete fractures when testing at a small scale; however, at a larger test scale, the basalt behaves as a double porosity system and at a still larger scale the basalt behaves as an equivalent porous medium (Li, 1991).

Effects of Fracture Roughness and Orientation

Many tracer test analyses apply a simplistic model that assumes parallel and flat fracture walls with a constant fracture aperture (e.g. Neretnieks, 1983; Cliffe et al., 1993). This model is called the parallel plate model. The advantage of the parallel plate model is it allows for analytical solutions to the one-dimensional advection-dispersion equation to be used in evaluating solute transport (Grisak and Pickens, 1980; Tang et al., 1981; Sudicky and Frind, 1982).

However, a number of authors (Tsang and Tsang, 1987; Raven et al., 1988; Brown, 1989; Thompson, 1991; Thompson and Brown, 1991; Fetter, 1993; Neretnieks, 1993) have suggested that the parallel plate model is inadequate for describing transport in a fractured porous media. Most fractures have rough surfaces and partial contact (Neretnieks, 1993; Ge, 1997), which physically and chemically affect solute and particulate transport (Neretnieks, 1993). Tsang and Tsang (1987) discovered many fractures are constricted by filling material or closed due to normal stress. Approximations become less accurate at a higher normal stress (>10 MPa) across the fracture parallel plate. Tsang and Tsang (1987) determined that the parallel plate model can accurately be applied only when the applied stress is low, meaning when fracture is mostly open. Brown (1987) presented a model for flow in isotropic rough-surfaced fractures and suggested that the parallel-walled fracture model becomes less accurate when the fracture aperture decreases and tortuosity increases.

Thompson and Brown (1991) discovered that the direction of the fracture roughness is more important than the degree of roughness when determining transport characteristics from their studies. The average solute transport rates significantly increase if the roughness is orientated parallel to the flow direction. This becomes more apparent as the surface contact area increases. Solute transport slows if the surface roughness is orientated normal to the direction of flow.

Zones of mobile and stagnant fluid are formed within a single fracture due to tortuous flow over rough surfaces (see Figure 1.). (Turner, 1958; Aris, 1959; Coats and Smith, 1964; Raven et al., 1988). The mobile zone contains an "inertial core" which carries most of the tracer at higher flow velocities. Stagnant zones are located along irregularities in the fracture walls where vortices and eddies form resulting from non-laminar flow. Solute in the mobile zone diffuses into the stagnant zone and is stored there until the concentration of solute in the mobile zone decreases and is then released back into the flowing water. Raven et al. (1988) discovered that at low fluid velocities dispersivity is larger than high fluid velocities because the tracer is more evenly distributed between the stagnant zones and the "inertial core" but at higher velocities the opposite is true because more of the tracer lies within the "inertial core". Thompson (1991) found evidence of stagnant zones in a fracture by the coexistence of high dispersivity values with low velocities.

The advection-dispersion model was modified to include mass transport in a single fracture by incorporating transient solute storage in the immobile zones (i.e. diffusion into the stagnant zones), referred to as the Advection Dispersion with Transient Solute Storage Model (ADTS) (Turner, 1958; Aris, 1959; Coats and Smith, 1964; Raven et al., 1988). Raven et al. (1988) applied data from induced gradient tracer tests in fractured rock to the advection-dispersion (AD) model and the ADTS model. From the breakthrough curves the early time experimental data match both models well; however, after approximately two hours, they more closely fit the ADTS model until the end of the experiment at 24 hours. This does not necessarily indicate transient solute storage exists in stagnant zones but rather that it is a possible reason for the skewness of the breakthrough curve tail that is sometimes seen in short-duration, (<100 hours) single-fracture tracer tests. The ADTS model provides lower longitudinal dispersivities and higher average fluid velocities in comparison with the AD

fluid velocity profile   "Inertial core"   mobile fluid zone

Q

immobile fluid zone   vortices and eddies
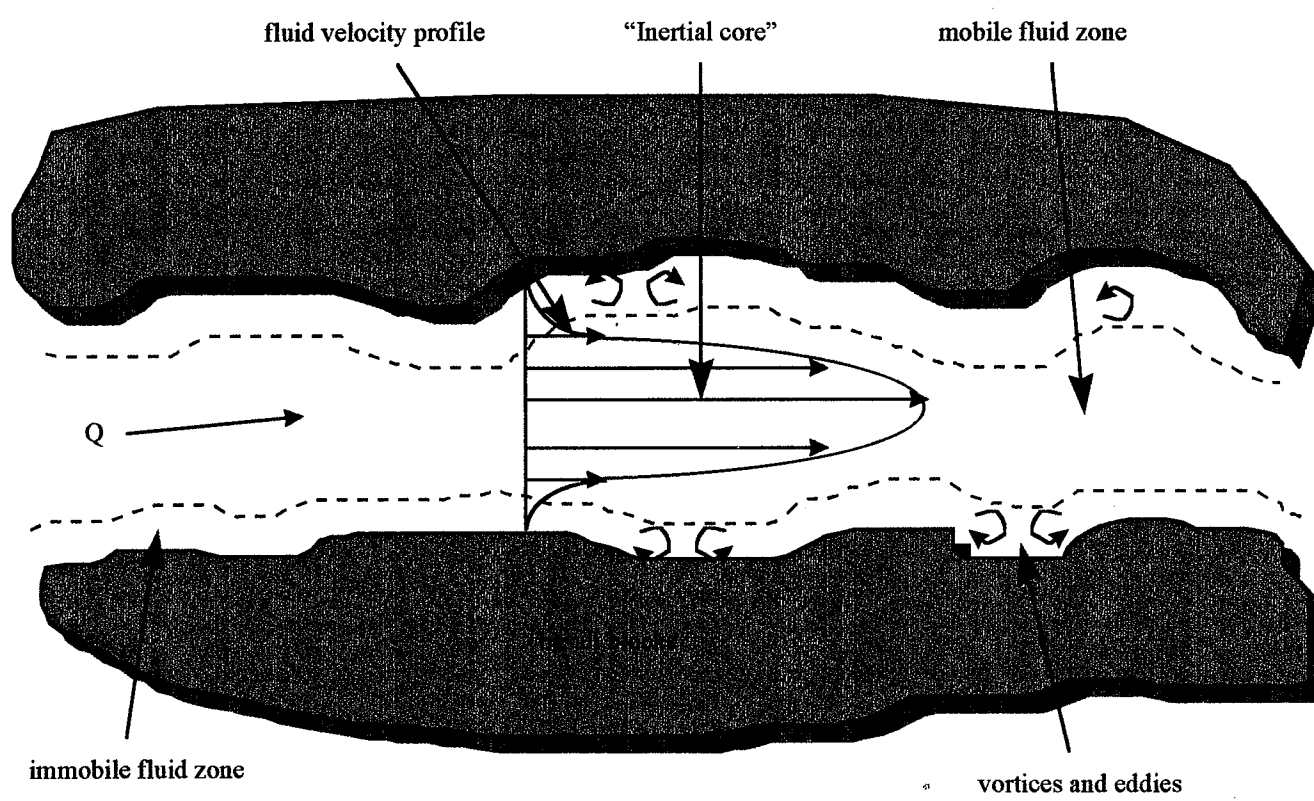
Figure 1.   Cross Section of a Single Fracture (from Raven et al., 1988)

model. Therefore, in a natural gradient test the AD model might best fit the data because of the lower velocity and higher dispersivity. In this situation the ADTS model would overestimate the velocity and thus underestimate the dispersivity. Significant channeling and matrix diffusion are not considered in the model.

For comparison purposes, the one-dimensional AD equation is

$$\frac{\partial C}{\partial t} = D_L \frac{\partial^2 C}{\partial x^2} - v \frac{\partial C}{\partial x}$$

where $\dfrac{\partial C}{\partial t}$ = change in concentration with time

$\dfrac{\partial C}{\partial x}$ = change in concentration with distance

D_L = coefficient of longitudinal hydrodynamic dispersion

v = average linear velocity

The AD equation, modified to the ADTS equation, is

$$\frac{\partial C}{\partial t}\phi + \frac{\partial C_s}{\partial t}(1-\phi) = D_L \frac{\partial^2 C}{\partial x^2} - v \frac{\partial C}{\partial x}$$

where ϕ = mobile or flowing fraction within the total fracture

$\dfrac{\partial C_s}{\partial t}$ = change in concentration in the solute storage zone with time

Channeling Effects

Tsang and Tsang (1989) stated that transport in fracture channels and channelized transport are two separate processes. In the literature both may be referred to as channeling but in this thesis channeling refers to channelized transport only. A fracture channel is a "long narrow region of enlarged aperture formed at the intersection of two fractures or by processes such as shearing" (NRC, 1996, p. 273.). Transport in fracture channels refers to a substance moving through a fracture channel that is fixed in place and orientation. In channelized transport, a channel is a narrow pathway of least resistance; there may be multiple channels within a single fracture that vary in space and time based upon the direction and rate of flow. Channelized transport is the movement of a substance through these zones of least resistance.

A detailed discussion of channeling or channelized transport is provided because it is a major mechanism controlling solute and particulate transport in fractured media.

Channelized transport occurs when fluid in a single fracture moves through preferential tortuous channels (Tsang and Tsang, 1987; Tsang et al., 1988). Preferential channels may make up as little as 20 % of the total fracture network (Rasmuson and Neretnieks, 1986). Moreno et al. (1988), Tsang et al. (1991) and NRC (1996) attributed channelized transport to non-uniform velocity distributions caused by highly variable apertures in a fracture. Raven et al. (1988) and Abelin et al. (1991b) suggested this process is caused by fracture roughness in addition to the contact area effects of the apertures. Channeling effects grow for a fracture with less than ten percent contact area (Thompson, 1991). Tsang and Tsang (1989) stated that channeling occurs in fractures with highly variable apertures and originates due to variable permeability within the porous medium. Dverstorp et al. (1992) determined that the degree of channeling is controlled by the permeability distribution and the geometry of the fractures.

Channeling causes regions of higher velocities within a fracture (Moreno et al., 1988) with most of the flow occurring on only a portion of the fracture surface (Cliffe et al., 1993). Solute velocities caused by channeling are two to three times greater than the average velocity. These higher velocity zones cause dispersion to decrease (Abelin et al., 1991b) and may limit the contact between the solute and rock surface thus limiting many chemical and physical reactions (Moreno et al., 1988; Tsang and Tsang, 1989).

Channeling is found to be an extensive process in many fractured rock tracer experiments; therefore, various channel models have been employed in the interpretation of solute transport, the simplest being the pure channel (PC) model (NRC, 1996). The PC model is a one-dimensional solute transport model with flow occurring through disconnected channels. This model is applicable when transport occurs in a single channel that does not intersect other channels. An experimental breakthrough curve may be dissected into several smaller component curves representing transport in single channels. With the application of an analytical model to the component curves, the average velocity, dispersivity and dilution factors can then be calculated for each channel. This model is popular because many tracer tests conducted in fractured rock have multiple breakthrough peaks. By applying the PC

model with component curves, each peak can be attributed to flow in a different channel. However, the application of component curves harbors some ambiguity especially with breakthrough curves with long tails because a variety of non-unique component curves can be created that may not necessarily represent actual channels. The channels found from the curve matching process are for specific flow geometries and may change with different flow regimes. The PC model generates a different dispersivity than the AD model because the velocity is greater in the channels (Moreno et al., 1985; Moreno and Neretnieks, 1993).

Moreno and Neretnieks (1993) investigated whether the advection-dispersion (AD) model is adequate to describe transport when channeling is prominent by applying field data to the advection-dispersion model (AD) and a pure channeling model (PC). The AD model accounts for mixing in the channel while the PC model does not account for mixing. The flow regime for channels which do not frequently intersect is likely to be represented by several independent channels, each with its own flow rate. Moreno and Neretnieks (1993) determined that the PC model provided the most accurate results. The authors concluded that if flow channels are commonly intersecting, the system could be described by the AD model; if however, the channels are not intersecting, the system should be described by a number of independent channels and the PC model applied.

Cliffe et al. (1993) conducted five single-fracture tracer experiments in shale and analyzed the breakthrough curves by applying the advection-dispersion model (AD), an AD model with matrix diffusion, and a two-channel model. The field results were first compared with results from the AD model with identification of disparities. The other two models were then employed. The authors concluded that although the two-channel model oversimplified the actual situation, this model best fit the data implying that channeling played a dominating role and that matrix diffusion was negligible.

Moreno and Neretnieks (1993) applied the AD model, PC model, and an altered form of the PC model - a network channeling model, to analyze their field data. The AD and PC models are two extremes for describing fracture transport and thus a network channeling model was formed to describe field data more accurately. In the network channeling model, the individual channels are connected to form a three-dimensional channel network that allows for mixing along the flow paths. This model uses the advection plus matrix diffusion model

minus the dispersion term which would be overestimated due to the velocity distribution among the channels. The authors found that the network channeling model best described their data.

Reactions and Retardation

Reactive constituents may affect solute and particulate migration in the ground water system. Reaction types include redox, adsorption/absorption, complexation, microbial, precipitation, biodegradation and radioactive decay (Fetter, 1993). The latter three reaction types may decrease the contaminant concentration but may not slow the rate of contaminant movement (Fetter, 1993). Precipitation may clog pathways which result in a reduced aquifer permeability or altered flow paths.

Retardation results in the solute moving at a slower rate through an aquifer system than the average ground water velocity. Retardation is sensitive to fracture width, fracture porosity, matrix porosity, diffusion and sorption (Novak, 1993). Freeze and Cherry (1979) stated that fractures with smaller apertures experience greater retardation. The two largest retardation processes on transport in fractured rock are sorption and matrix diffusion (Moreno and Neretnieks, 1993; Moreno et al, 1985).

Both molecular and matrix diffusion retard transport movement in fractured rock. Diffusion is the process by which "ionic or molecular constituents move under the influence of their kinetic activity in the direction of their concentration gradient" (Freeze and Cheery, 1979, p. 103). Molecular diffusion occurs from solute in the mobile zone into water stored in stagnant zones in rough walled fractures (Raven et al., 1988; Abelin et al., 1991a) and into dead-end fractures (NRC, 1996) when the concentrations are highest in the mobile zone. Matrix diffusion occurs from the solute in the major fractures to smaller fractures, pore spaces and joints in the rock matrix (Neretnieks, 1980). When the concentration in the pathway becomes less than the surrounding area, the process is reversed causing significant tailing of breakthrough curves during tracer tests (Novakowski et al., 1985).

Matrix diffusion may be a major retardation factor for solute movement in fractured rock (Grisak and Pickens, 1980; Neretnieks, 1980; Neretnieks, 1983; Moreno and Neretnieks, 1993; Novak, 1993; Novakowski and Lapcevic, 1994; NRC, 1996). It may be orders of

magnitude more effective in slowing plume migration when compared to retardation by fracture surface reactions alone; although, the magnitude depends upon the amount of rock matrix available to the solute (Neretnieks, 1980) and the length of contact time between the solute and matrix blocks (NRC, 1996). Abelin et al. (1991a) concluded that fractures with large surface areas have a greater rate of matrix diffusion and induce a larger matrix diffusion value than smaller surface areas. Even at low block porosities, Abelin et al. (1991b) and Neretnieks et al. (1982) found that matrix diffusion retards solute transport; however, Malowzewski and Zuber (1992) stated that matrix diffusion is insignificant at high transport velocities when low block porosities exist.

A matrix diffusion term may be added to the advection-dispersion equation (AD) to more accurately describe solute transport in a fractured medium. Moreno and Neretnieks (1993) determined the AD equation works well for homogeneous media, but often does not provide an accurate description of heterogeneous media including fractured rock. The advection-dispersion equation is modified for fracture transport by Braney et al. (1991) and Jackson et al. (1991) in Cliffe et al. (1993) to include matrix diffusion, which becomes

$$\frac{\partial C}{\partial t} = D_L \frac{\partial^2 C}{\partial x^2} - v \frac{\partial C}{\partial x} + F$$

where F = flux of the tracer or solute between the rock matrix and the fracture
The flux is

$$F = \frac{2D_i}{h} \frac{\partial C^m}{\partial w}$$

where D_i = intrinsic diffusion coefficient in the rock
h = fracture aperture (averaged)
C^m = concentration of tracer in the rock matrix
w = coordinate normal to the fracture (normally set equal to zero)

Sorption is another retardation process that affects solute transport and includes adsorption, absorption, chemisorption and ion exchange (Fetter, 1993). Adsorption is the process by which substances attach themselves to a solid surface. Absorption is the exchange of solute from solution into the aquifer material by diffusion. Chemisorption occurs when a chemical reaction holds the solute onto a solid surface. Lastly, ion exchange includes both cation and anion exchange. Cation exchange is when a positively charged molecule is

adsorbed on a clay mineral surface and is replaced by cations in the surrounding solution. Anion exchange is the attraction of a negatively charge molecule to a positively charged surface.

Sorption is both reversible and irreversible which exhibit different responses on a breakthrough curve. Most sorption reactions are fast and reversible (Fetter, 1993). In a reversible reaction a substance sorbs onto a material and later desorbs. Desorption is much slower in comparison to sorption (Hendry et al., 1997). Sorption occurs during the early portion of a tracer test while desorption occurs in the latter portion of the test and thus is seen by a significant tail in the breakthrough curve. An irreversible reaction causes the tracer to be permanently immobilized and therefore results in a large amount of tracer loss. This causes lower than average tracer concentrations and a later breakthrough curve peak. If both reversible and irreversible sorption occur, a later breakthrough peak may be seen with a significant breakthrough curve tail.

Sorption in fractured rock may be expressed differently than in a porous medium. In fractured rock where porosity in the matrix is negligible, the retardation equation representing sorption is (linear sorption isotherm) (Burkholder, 1976 in Freeze and Cherry, 1979)

$$R = \frac{\bar{v}}{v_c} = 1 + \frac{2K_a}{b}$$

where R = retardation factor
$\bar{v}$ = average linear ground water velocity
v_c = velocity of the $C/C_o = 0.5$ point on the concentration profile
K_a = distribution coefficient for fractured rock
b = fracture aperture width

A fractured rock sorption term replaces the porous medium term in the advection-dispersion equation which becomes

$$\frac{\partial C}{\partial t}\left(1 + \frac{2K_a}{b}\right) = D_L \frac{\partial^2 C}{\partial x^2} - v \frac{\partial C}{\partial x}$$

The distribution coefficient for fractured rock (K_a) is the mass of solute on the solid phase per unit area of solid phase divided by the concentration of solute in solution. Whereas for a porous medium the distribution coefficient is the mass of solute on the solid phase per unit

mass of solid phase divided by the concentration in the solution. The distinction is made because sorption on fractured media is affected more by surface area than mass.

Sorption quantification is by equilibrium sorption isotherms and kinetic (nonequilibrium) sorption processes (Fetter, 1993). Equilibrium sorption isotherms include linear, Freundlich and Langmuir. The linear and Freundlich isotherms allow for an unlimited number of sorption sites, which in reality is not true. The focus of the Langmuir sorption isotherm is that a surface possesses a finite number of sorption sites. Irreversible first-order, reversible linear, and reversible non-linear kinetic sorption models are types of kinetic sorption models. The bilinear adsorption model is also a kinetic sorption model and is the nonequilibrium version of the Langmuir. Equilibrium sorption isotherms are used when sorptive processes are rapid with respect to the flow velocity and equilibrium is reached. A kinetic sorption model (nonequilibrium) is used when sorptive processes are slow with respect to the flow velocity and equilibrium is probably not reached; these are heterogeneous surface reactions.

TRANSPORT CHARACTERISTICS OF PARTICULATES

The study of particulate (microbial and particle) transport is of great importance for understanding their migration as contaminants or their use in enhanced *in situ* bioremediation. Certain bacteria and viruses, such as fecal bacteria and E.coli, may be contaminants. Particles may also be contaminants; for example, heavy metals may attach themselves to clay or organic particles (Domenico and Schwartz, 1990). On the other hand bacteria and spores may be used to degrade contaminants and specific particles may be used to deliver them and nutrients in the subsurface (Brown, 1998). The transport of particulates is influenced by similar processes (i.e. advection, dispersion, channeling, etc.), but are governed more specifically by preferential pathways, filtration, sorption and density effects. Microbial transport is also affected by a number of more distinct processes.

In forced gradient tests, microorganisms and particles travel along high velocity preferential pathways. Particulates are transported only through fractures which can pass their size. These are only a small percentage of the total fracture network; therefore, the effective porosity is less which in turn increases the average velocity. This phenomenon is referred to

as the porosity exclusion effect. Dissolved tracers also follow these preferential pathways but follow other pathways with slower velocities as well. Consequently, the center of mass for the particulate tracers will arrive prior to the center of mass of the conservative tracer. The initial rise of the breakthrough curve for the dissolved tracer and the particulate tracer should occur at approximately the same time. Table 1 lists several forced gradient tracer experiments

SOURCE	CONSERVATIVE TRACERS	MICROBIAL TRACERS	PARTICLE TRACERS	TEST ENVIRONMENT
Wood and Ehrilch (1978)	bromide and iodide	yeast - *Saccharomyces cerevisiae*		sand and gravel aquifer
Pyle and Thorpe (1981) in Davis et al. (1985)	rhodamine WT	bacteria- *E. coli*		?
Bales et al. (1989)	?	virus - *bacteriophage*		sandy soil and fractured tuff
Harvey et al. (1989)	bromide	DNAPI stained bacteria	microspheres	sandy aquifer
Gannon et al. (1991)	chloride	bacteria - *Pseudomonas, Achromobacter, Bacillus, Enterobacter*		soil
McKay et al. (1993)	bromide	virus- *bacteriophage*		fractured rock
Reimus et al. (1994)	iodide		microspheres	fractured tuff
Petrich (1995)	bromide		microspheres	sandy aquifer
Pang et al. (1998)	chloride and rhodamine WT	spores -*Bacillus subtilis*		alluvial gravel aquifer
Brown (1998)	bromide	spores- *Clostridium bifermentans*	microspheres	sandy aquifer

Table 1. Summary of Particulate Tracer Work in Forced Gradient Tests.

conducted using microbial and particle tracers in conjunction with conservative tracers. In each experiment the breakthrough curve peak for the particulate arrived prior to that for the

conservative tracer.

Particulate transport is affected by filtration. Filtration can decrease the aquifer permeability and may severely alter or block the transport pathway. Most microorganisms and particles are filtered as they are transported through the subsurface. The smaller the aperture of the fracture, the fewer large sized particles are transported. This was demonstrated in forced gradient tests by Harvey (1989) in Harvey and Garabedian (1991), Petrich (1995) and Brown (1998) who employed different sized particles during their experiments. They discovered the particle recovery varied inversely with particle size.

McDowell-Boyer et al. (1986) described filtration as a combination of three processes: surface filtration, straining filtration and physical-chemical filtration. Surface filtration occurs when pore spaces or fractures are too small to support the transport of larger particulates and a surface cake or mat is formed. Sakthivadivel et al. (1972) in McDowell-Boyer et al. (1986) found the ratio of the media grain diameter to the diameter of the particulate (d_m/d_p) to be the most significant filtration factor. Surface cakes form when the ratio is less than ten. Straining filtration occurs when particulates are small enough to become lodged in between the pore spaces or fractures. Sakthivadivel et al. (1966) in McDowell-Boyer et al. (1986) found strained particulates could not be re-suspended even if flow rates were increased or reversed. Finally, physical-chemical filtration incorporates particle-media collision mechanisms and particle-media attachment mechanisms. Physical-chemical filtration is the dominant process of particulate retention.

Particle-media collision mechanisms include sedimentation, interception and Brownian motion (McDowell-Boyer et al., 1986). Sedimentation occurs when particulates fall out of the fluid streamlines by density effects and collide with the media. Interception occurs when a particulate is transported along fluid streamlines and collides with the media. Lastly, Brownian motion is the random movement of particulates in a liquid or gas by the impact of molecules surrounding them. For very small particulates (less than a few micrometers) Brownian motion is the dominant particle-media collision mechanism.

Particle-media attachment mechanisms include electrostatic, London-van der Waals, and hydrodynamic forces (McDowell-Boyer et al., 1986). Electrostatic force is the dominant attachment force between charged particles and the charged media. London-van der Waals

force is the dipole-dipole attractions between atoms and molecules and is affected by the ionic strength of the liquid. Finally, hydrodynamic forces squeeze water out of the pore spaces to allow the attachment of particles to the media.

Reversible and irreversible sorption cause retardation or loss of particulates during transport (Harvey and Garabedian, 1991). Reversible sorption is the equilibrium partitioning of bacteria (or other particles) between the liquid phase and the fracture walls (Hendry et al., 1997). Some bacteria have cells that produce adhesive substances. These bacteria anchor themselves to a porous medium and over time become difficult to remove causing irreversible sorption (Hendry et al., 1997).

Particulate sorption and desorption are affected by several mechanisms. These mechanisms include the surface roughness of the fracture, fluid dynamics, substratum chemistry and solute chemistry (Harvey et al., 1993). Fontes et al. (1991) discovered that sorption is affected by the ionic strength and pH of the solution on the charge density and electrostatic repulsion. Hendry et al. (1997) found that desorption may be a function of bacterial residence time on the media.

In column studies, Hendry et al. (1997) discovered the breakthrough curve for the vegetative bacterium, *Klebsiella oxytoca*, had an attenuated peak and a substantial tail with respect to the chloride breakthrough curve. The authors attempted to exclude all other transport variables during the experiments and concluded the attenuated peak was caused by irreversible sorption and the significant tail was caused by reversible sorption.

Bacterial sorption may be incorporated into the advection-dispersion equation. If adsorption is considered the dominant process in addition to advection and dispersion, a one-dimensional bacterial transport equation for a homogeneous medium may be employed (Hendry et al., 1997). This equation, a modification to the AD equation, is

$$\frac{\partial C}{\partial t} + \frac{\rho(1-\varepsilon)}{\varepsilon} \frac{\partial S}{\partial t} = D_L \frac{\partial^2 C}{\partial x^2} - v \frac{\partial C}{\partial x} - k_{irr} C$$

where $\rho(1-\varepsilon)$ = dry bulk density of the porous media

$\frac{\partial S}{\partial t}$ = change in concentration of bacteria sorbed to the porous matrix (solid phase) with time

$\dfrac{\partial C}{\partial t}$ = change in bacterial concentration with time

$\dfrac{\partial C}{\partial x}$ = change in concentration with distance

D_L = coefficient of longitudinal hydrodynamic dispersion
v = average linear velocity
C = bacterial concentration in solution (CFU mL^{-1})
k_{irr} = irreversible adsorption rate constant (t^{-1})

Bacteria undergo irreversible and kinetically reversible sorption. Both may be described by a first-order kinetic reaction:

$$\frac{\partial S}{\partial t} = \frac{\varepsilon C}{(1-\varepsilon)\rho} k_f - k_r S$$

where k_f = forward rate constant (t^{-1})
k_r = reverse rate constant (t^{-1})
S = bacterial concentration sorbed to the porous matrix (solid phase)

Unknowns for the two equations above are v, D_L (α), k_f, k_r and k_{irr}. If a conservative tracer is used in conjunction with a microbial tracer, the average velocity and dispersion can be calculated from the conservative tracer data. The three sorption terms can then be estimated by trial-and-error. Sorption terms calculated at one scale may not be applicable at another scale.

Particulates that are denser than water tend to fall out of suspension resulting in a large tracer loss. This is more pronounced at slower flow velocities, particularly under a natural gradient. A significant breakthrough curve tail may result from particulates that fall out of suspension but return to the flow stream by an increase in velocity.

Tracer results in some natural gradient field tests suggest that the peak breakthroughs for microorganisms and particles are attenuated with respect to dissolved tracers. Harvey et al. (1989) conducted a natural gradient field tracer test using chloride and different types (i.e. non-carboxylated latex, polyacrolein and carboxylated) and sizes of microspheres. They discovered the bacteria-sized microsphere breakthrough peaks were retarded with respect to the chloride peak in a sandy aquifer. This result was likely related to particle settling at lower ground water velocities and to a smaller degree, sorption. The non-carboxylated latex spheres were the first to arrive followed by the polyacrolein spheres (carbonyl surface groups are

attached) and finally by the carboxylated latex spheres. The carboxylated latex spheres have a net charge which attracts them to other charged substances thereby retarding the sphere transport. The authors concluded that particle size, and more importantly, surface characteristics of the particle, affect transport. Harvey et al. (1993) also found bacteria and bacteria-sized carboxylated latex microspheres were retarded with respect to bromide in a natural-gradient test in a sandy aquifer.

Some authors have found similar peak breakthrough times for the microbial and conservative tracers. Reasons for this may be described by a combination of the previously described transport processes. Atkinson et al. (1973) applied a fluorescent dye, pyranine, and *Lycopodium* spores in underground streams in limestone for a natural gradient test. The authors found the breakthroughs peaked at similar times. In the same aquifer, Buchtela et al (1968) in Atkinson et al. (1973) found the spore breakthrough peak arrived before the fluorescein peak. In another study, Fontes et al. (1991) discovered the bacterial tracer arrived at nearly the same time as chloride in forced gradient column tests in a sand environment. Harvey and Garabedian (1991) found similar results using bromide as the conservative tracer in a small-scale, natural gradient test in a sandy aquifer.

A limited number of studies have been conducted to determine the effect of aquifer heterogeneities on microbial transport. Small-scale tracer experiments were conducted in a layered sandy aquifer and in laboratory columns by Harvey and Garabedian (1991) and Fontes et al. (1991), respectfully. They found that microbial and conservative tracers react dissimilarly to physical heterogeneties in aquifer material.

Microorganism transport may be affected by a number of more microbial-specific processes; these include microbial growth, death, starvation, predation, motility and chemotaxis. Microbial growth may increase the problems associated with filtration (i.e. reduction in permeability) and result in an increased recovery. Death, starvation, and predation of the microbes result in a tracer loss. Bacteria are either motile or nonmotile. Motility is the flagella (long, hair-like tail) attached to the bacterium (Chapelle, 1993). Breakthrough may occur much faster for the motile bacteria caused by the forward swimming motion of the flagella. Chemotaxis may also affect microbial transport, which is the movement of an organism in relation to chemicals.

TRACER TESTS

Ground water tracer tests are conducted for a variety of reasons. The tests can provide information on aquifer properties and parameters including preferential flow paths, velocity, residence time, effective porosity, dispersivity and dispersion. Fracture connection and contaminant sources may also be determined. The design of the tracer experiment is dependent upon the purpose of the test, the site itself (number of wells, distance between wells, etc.) and the availability of equipment.

There are two main types of ground water tracer tests, these are single well and two well tests. Single well tests include injection/withdrawal, borehole dilution and "push pull" tests. Two well tracer techniques include both natural gradient and induced gradient tests. Divergent and convergent tests are types of induced gradient tests.

Single Well Tests

A type of single well tracer test is the injection/withdrawal technique (Davis et al., 1985; Fetter 1993). This technique involves the injection of a known volume of conservative tracer into a well, followed by two to three well volumes of water to flush the tracer out of the well column and into the formation. A small tracer volume is best so as not to disturb the flow system. The tracer is allowed to migrate for a period of time and is then removed by pumping the same well at a constant rate great enough to overcome the natural gradient. Samples are collected during the withdrawal process. The distance traveled can be calculated as well as the pore velocity and the longitudinal dispersion coefficient.

Istok et al. (1997) developed another type of single well test called a "push pull" test to determine the microbial activity *in situ*. A conservative tracer as well as degradable tracers (e.g. perfluorocarbons or glucose) are mixed with water collected from the injection well. This cocktail is then injected back into the well. The tracers are allowed to migrate into the aquifer. After a period of time the well is pumped and samples are collected. The amount of microbial activity is characterized by the concentrations of the conservative tracer with respect to the concentrations of the reactive or degradive tracers.

The borehole dilution technique is also a type of single-well tests (Freeze and Cherry, 1979; Davis et al., 1985; NRC, 1996). This method involves injecting a slug of tracer into a

packed-off interval in the well, mixing it within the borehole, and measuring how the concentration decreases over time. The direction and magnitude of the tracer velocity in the horizontal direction can be calculated. A disadvantage of this method is that several assumptions must be made for an accurate interpretation including no vertical flow and a homogeneous gravel pack. This type of test is best suited for a well with no screen or gravel pack.

There are several advantages to single well tests. They are inexpensive because less tracer is required, they have a less complex flow regime, more of the tracer can be retrieved and they are easier to analyze.

Two Well Techniques

In a natural gradient test, tracer is injected in one well and measurements are taken in another well without disturbing the flow field (Davis et al., 1985; Domenico and Schwartz, 1990). This type of test is ideal for studying natural flow conditions (NRC, 1996). Mackay et al. (1986) and LeBlanc et al. (1991) conducted large-scale natural gradient tracer tests in a sand aquifer. Natural gradient tests can be conducted at the local (2-5 m) and intermediate (5-100 m) scales (Domenico and Schwartz, 1990). Disadvantages of this method include: the direction of flow must be known or a large number of observation wells is required to intercept the tracer (more so in a heterogeneous environment), more time is required to recover the tracer than for forced gradient tests, and a larger amount of tracer may be necessary due to the great amount of tracer loss (Davis et al., 1985; Domenico and Schwartz, 1990; NRC, 1996).

There are several potential problems with the monitoring well(s) in fractured rock. These are: difficulty collecting *in situ* measurements due to dilution in the borehole (unless a packer is used), difficulty in capturing the tracer due to channelized transport in fractured rock, monitoring wells not located in fractures connected to the tracer injection well and wells not located in fractures with large enough apertures to allow for decent sample collection (NRC, 1996).

Forced gradient or radial flow techniques use two wells with an imposed velocity on the aquifer (Davis et al., 1985; Domenico and Schwartz, 1990; NRC, 1996). Porosity,

dispersivity and dispersion can be calculated. The advantages of a forced gradient test are: the amount of tracer needed is less than a natural gradient test because there is less tracer loss, and the higher gradient increases the tracer travel time and reduces the length of the test. This technique is further divided into two types of tests: radially divergent and radially convergent tests.

In a radially divergent test, water is continuously injected into a recharging well (Davis et al., 1985; Domenico and Schwartz, 1990; NRC, 1996). After steady state conditions are reached a tracer is injected as a slug or a continuous injection in the same well. The monitoring well(s) is not pumped or is pumped at a small enough rate to collect a sample without altering the flow pattern. The advantages to this test are: if a number of monitoring wells are used a larger extent of the aquifer may be analyzed than with a convergent test, and the tracer is pushed into the formation quickly which may more accurately be represented by a simple model as compared to a slow injection which causes greater challenges to modeling (NRC, 1996). The disadvantages of a radially divergent test include: a large amount of water is needed for the recharging well, and the recharging water may clog the fractures (NRC, 1996). Problems associated with the monitoring well(s) are the same as those mentioned for natural gradient tests.

In a radially convergent test, water is continuously pumped from a well until steady state conditions are met (Davis et al., 1985; Domenico and Schwartz, 1990; NRC, 1996). A tracer is then injected as a slug or continuous injection into a different well followed by two to three well volumes of water to flush the tracer into the formation. Samples are collected from the pumping well. Packers may be employed to isolate the screened interval in a cased well or distinct fractures in an uncased hole. The advantages to a radially convergent test are that they do not have the problems with the monitoring wells as in natural gradient or radially divergent tests, and ideally more of the tracer mass can be recovered than in the other two-well tests (NRC, 1996).

Another version of a radially convergent tracer test is to have multiple tracer injection wells with one pumping well (NRC, 1996). Different tracers which do not interfere with one another are placed in different injection wells. This provides information for a larger area of the aquifer.

A recirculating tracer test is a two-well radially convergent test (called a doublet) in which one well is pumped while the other is recharged, ideally at the same rate (Davis et al., 1985; Domenico and Schwartz, 1990; NRC, 1996). The recharged water may or may not come from the pumping well. After steady state conditions are reached, a slug of tracer is injected into the recharging well, or if multiple wells are used as monitoring wells along a transect, the tracer could be injected into the well closest to the recharging well in the transect. The advantage of a recirculating test over other convergent tests is a higher hydraulic gradient. The disadvantages are the longer flow lines and the recycled tracer which may yield numerous breakthrough peaks if using recharge water from the pumping well. A way to avoid recirculation of the tracer is to inject water from another source.

TRACERS

A variety of different tracers are applied in ground water tracer tests including dissolved and particulate tracers. Dissolved tracers may be conservative or non-conservative. A conservative tracer is one that does not react physically, chemically or biologically and is used to represent the average ground water flow. A non-conservative tracer reacts physically, chemically or biologically with the aquifer material and does not represent the average ground water flow. Conservative and non-conservative tracers include ionic species, fluorescent dyes, organic compounds, radioactive isotopes and gases. Particulate tracers include both microorganisms and particles.

The selection of the tracer is dependent upon the purpose of the test, the aquifer, the ground water chemistry and microbiology, and the availability of equipment. A variety of different tracers are employable if the purpose of the tracer experiment is to determine if various fractures are connected. A sorptive tracer may be used if the purpose of the experiment is to test how a sorptive fertilizer is transported. Finally, if *in situ* bioremediation is a potential cleanup technology for a contaminated site, a tracer test using microbial tracers or similar sized particle tracers may be conducted to determine the fate and transport of microorganisms.

Conservative and Non-Conservative Tracers

The ionic tracers, bromide, chloride and iodide, are considered to be conservative (Davis et al., 1985). They are available the form of salts such as potassium bromide and lithium iodide. Unlike chloride, bromide and iodide usually have low background levels in the ground water. Bromide is the most widely used tracer because it is biologically stable, not sorbed by aquifer material and not lost by precipitation (Schmotzer et al., 1973). However, Boggs and Adams (1992) found bromide, and possibly other anions, sorb in the presence of iron oxides and kaolinite in addition to a low pH. Chloride has increased density effects above 3000 ppm and may slightly sorb onto some soils. Iodide tends to sorb more than chloride and may be affected by biological activity. Other ionic tracers include fluoride, lithium, ammonium, magnesium and potassium. Analysis is conducted by an ion selective electrode or by liquid chromatography.

Fluorescent dyes are widely used ground water tracers (Davis et al., 1985) and may or may not be considered conservative. There are several types of fluorescent dyes which include blue fluorescent dyes (amino G acid and photine CU), green fluorescent dyes (fluorescein, lissamine FF, and pyrane) and orange fluorescent dyes (rhodamine B, rhodamine WT, rhodamine B and sulfo rhodamine B). Fluorescent dyes are inexpensive, easy to use, simple to analyze, and some have a low toxicity. Other dyes have very low detection limits (depending on the analysis instrument) and can be visually detected at low levels (i.e. fluorescein can be seen at only 0.3 mg/L). However, the dyes are affected by sediment, pH, temperature, salinity, $CaCO_3$ level, sorption, photochemical and biological decay. Each fluorescent dye responds uniquely to various types of processes; for example, fluorescein is strongly affected by pH and photochemical decay whereas rhodamine B is strongly sorbed. Fluorescent dyes are also affected by "quenching", the process by which other molecules reabsorb the fluorescent light rendering erroneously high concentrations. Analysis is conducted by a fluorometer or a fluorescent spectrometer. Smart and Laidlaw (1977) provide a thorough discussion on fluorescent dyes.

Sabatini and Austin (1991) applied fluorescein and rhodamine WT (RWT) as adsorbing tracers to mimic adsorbing pesticides in batch and column studies in sand. Chloride was used as the base-line (conservative) tracer. They discovered the peak breakthrough for

fluorescein arrived prior to the pesticide but not significantly behind chloride. The RWT peak breakthrough was found after the pesticides. Both dyes were found to sorb more to organic phases than non-organic. The authors stated their results may not pertain to other aquifer environments.

In other studies, fluorescein was used as a non-sorbing tracer and rhodamine WT as a sorbing tracer. Ptak and Schmid (1996) used both tracers in a heterogeneous sand and gravel, aquifer field scale test. They found RWT had a significant tail which may have been caused by sorption. The authors concluded that fluorescein was " practically non-sorbing" and RWT was clearly a sorptive tracer. They stated that fluorescein is the least sorptive tracer of all the fluorescent dyes. Kanwar et al. (1997) used RWT as a sorbing tracer to mimic the transport of atrazine through soil. Käss (1992) in Ptak and Schmid (1996) stated that fluorescein can be accepted as a "quasi-ideal" tracer in most cases meaning it is fairly conservative.

Several research groups found RWT acts as a conservative tracer despite the conclusions of many other authors (i.e. Sabatini and Austin, 1991; Ptak and Schmid, 1996, Shiau et al., 1993; and Everts and Kanwar, 1994). Pang et al. (1998) discovered RWT acts similarly with bromide. Aulenbach et al. (1978) found RWT acts similarly with tritium, a conservative tracer.

Organic compounds (other than fluorescent dyes) are used as ground water tracers, but are not as popular (Davis et al., 1985). They may or may not be considered conservative. Some examples include veratryl alcohol, silicic acid, borac acid, benzoic acid, phosphoric acid, acetic acid, ethanol, sugars and glycerol (Davis et al., 1985). These tracers have many disadvantages: sorption, rapid decomposition, high detection limits, density effects, toxicity and high background concentrations. Organic tracers may be used as degradative tracers in "push pull" single wells tests. Analysis is performed by colorometric or chromatographic methods. Sugars and glycerol at high concentrations can be detected by optical refraction techniques.

Inert natural gases are applicable as conservative ground water tracers (Davis et al., 1985). These include helium, neon, krypton and xenon. They have low background levels and do not participate in chemical reactions or ion exchange. Krypton and xenon may however be sorbed onto clay and organic material. Temperature, gas pressure and salinity

affect the amount of gas allowed to dissolve. Special attention must be given toward the sample collection and preservation. The samples are analyzed by gas chromatography or mass spectrometry.

Radioisotopes were used as tracers; these however, are no longer allowed in most instances due to environmental concerns (Davis et al., 1985). Some may be conservative (ie. tritium) while others are not (ie. strontium). Some examples of radioactive isotopes used as tracers are ^2H, ^3H, ^{32}P, ^{51}Cr, ^{60}Co, ^{82}Br, ^{85}Kr, ^{131}I and ^{198}Au. Those that give off gamma rays were the most widely used due to the ease of detection and counting. Advantages of radioactive tracers are the ease of detection at low levels; some are not prone to sorption. Most of the isotopes are chosen because they have very short half lives; ^{181}I, for example, has a half life of 8.1 days and ^{82}Br has a half life of 35.4 hours. Previously distributed atmospheric radionuclides may act as tracers as well. These include ^3H from the detonation of nuclear bombs in the 1950's, ^{14}C, ^{32}Si, ^{36}Cl and ^{39}Ar. Great care must be taken when collecting samples with radioactive isotopes. Analysis is performed by down-hole devices or special laboratories.

Microbial and Particle Tracers

Microorganisms are used as ground water tracers to better understand their transport characteristics in representing pathogenic bacteria or microorganisms for use in bioremediation. These tracers include bacteria, yeast, viruses and spores (Davis et al., 1985). Table 2 lists the microbial tracers and their size ranges. Analysis is performed in a laboratory by a variety of methods including plate counts or microscopy.

Tracer	Size (μm)
bacteria	1-10
spores	0.5-33
yeast	2-3
viruses - animal (enteric)	0.2-0.8
- plant	0.2-0.8
- bacterial	0.2-1.0

Table 2. Microbial Tracers and Their Size Distribution (Davis et al., 1985).

Bacteria are the most commonly used microbial ground water tracer (Keswick et al., 1982). Some of the most commonly used bacteria are *Escherichia coliform* (E. coli), *Streptococcus faecalis, Bacillus stearothermophilus, Serratia marcescens* and *Seratia indica.* Other bacteria include *Chromobacterium violaceum, Bacillus subtilis* (Wood and Erlich, 1978) and *Klebsiella oxytoca* (Hendry et al., 1997). Advantages of bacterial tracer use are their ease of growth and detection (Keswick et al., 1982). A disadvantage is that some strains are naturally found in the ground water. A strain must be selected that is not indigenous to the environment where the tracer experiment is being conducted.

Spores are bacteria in the resting stage. Some examples of spores used in ground water tracer experiments include L*ycopodium* (33 μm) (Davis et al., 1985), *Bacillus* (0.5-3 μm) and *Clostridium* (0.5-3 μm) (Brown, 1998). *Lycopodium* spores are best used in karst regions due to their very large size. Spores can remain in the dormant stage for great lengths of time while waiting for the right environmental conditions (i.e. pH, temperature, food) to stimulate their growth. Brock et al. (1994) found spores have a greater resistance for chemicals, radiation and drying than the original cells.

Yeasts are another form of microbial tracer (Davis et al., 1985). An example is *Saccaromyces cerevisiqe* (Davis et al., 1980). Advantages of yeast tracers are the low cost, ease of detection and low health hazard. Skilton and Wheeler (1988) indicate that yeasts are a poor microbial tracer because of their relatively large size.

Viruses are also used as tracers. Kewsick et al. (1982) stated that bacterial viruses are the most popular microbial tracer. However, Davis et al. (1985) found that viruses have limited popularity because most virus detection is difficult and human viruses are generally not used due to health risks. In ground water studies, phages have been found to travel up to 1,600 meters (Keswick et al., 1982). *Bacteriophages* are viruses that are parasitic to bacteria (Chapelle, 1993). Examples of *bacteriophages* are: *Serratia marcescens,* E*nterobacter cloacae* and *Escherichia coli* (Skilton and Wheeler, 1988). The advantages of *bacteriophages* are numerous: they do not cause disease; they are easy to distinguish amongst themselves due to a number of different bacterial hosts thus numerous types can be used simultaneously; they are unlikely to have any background levels; they have very low detection

rates; and because they are very small they are not as affected by filtration (Keswick et al., 1982; Skilton and Wheeler, 1988).

Particles have also been used as ground water tracers to represent similar sized microorganisms in the ground water, nutrient delivery capsules or contaminant particles. The mostly widely used particle tracers are microbeads or microspheres. They may be purchased in a variety of diameters and fluorescent colors. Carboxylated latex beads have a surface charge whereas non-carboxylated latex beads do not and therefore should not sorb to aquifer material. The microbeads are very stable, meaning they do not undergo degradation or break apart during normal transport. Analysis is conducted by filtering the sample through a black nucleopore filter, preparing the slide and counting the beads under a microscope with a fluorescent light.

CHAPTER 3
DESCRIPTION OF TEST FIELD SITE

INTRODUCTION

The field work for this study was conducted at the University of Idaho Groundwater Research Site (UIGRS) located on the western edge of campus in Moscow, Idaho. Figure 2 is the site location map and Figure 3 is a plan view map of the UIGRS. Paradise Creek borders the site to the north and Perimeter Drive borders it to the east. This site was chosen over other university owned sites for a variety of reasons. The selection criteria included the presence of a fractured rock aquifer at shallow depths, presence of existing wells, proximity to campus and availability for research. Much research has been conducted at this site including a site characterization by Li (1991) and a ground water microbial analysis by Zheng (1992).

REGIONAL GEOLOGIC SETTING

The UIGRS is situated in the Moscow-Pullman basin which is on the eastern margin of the Columbia River Basalt system (Li, 1991; Provant, 1995). Miocene basalt flows cover the irregular surface of the Precambrian bedrock with interbedded and overlying sedimentary deposits (Lum et al., 1990). The basin is bound to the northwest by Belt Supergroup metamorphics of Smoot Hill, Kamiak Butte, and Randall Butte area, to the north and east by Idaho Batholith granite of the Palouse Range and to the south by granite and gneiss along the western edge of Paradise Ridge and Bald Butte. The basin is open to the west.

Lava originated from fissures located in southeastern Washington and northeastern Oregon and flowed into the basin (Li, 1991; Provant, 1995). The thickness of a single basalt flow ranges from a few feet to hundreds of feet. Under northwestern Moscow the total thickness of the basalt and sediments is approximately 1400 feet (Ralston, 1998). Sediment interbeds in the basalt are minimal towards Pullman where the depth to basement rocks is approximately 2000 feet (Lum et al., 1990).

In the western portion of the basin the thickness of the basalt and sediments may be over 3000 feet. The flows thin toward the basin margins and dip slightly toward the west and northwest with little deformation.
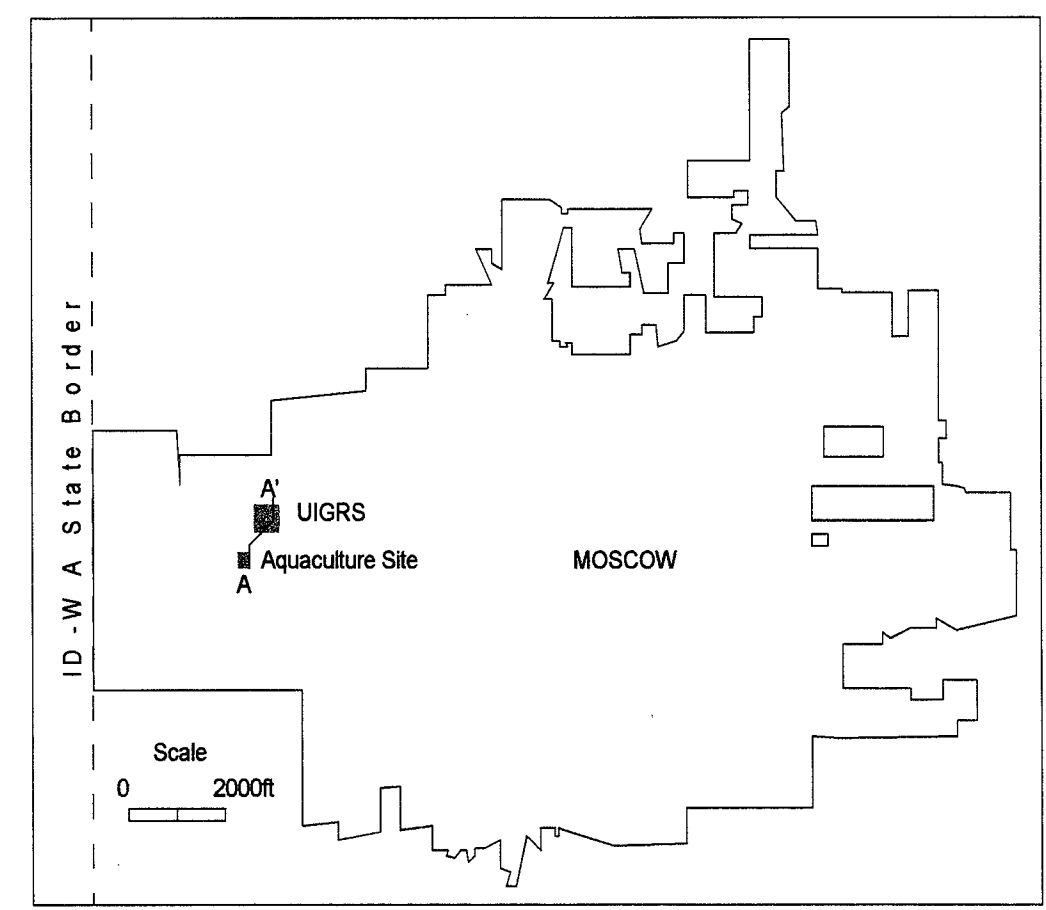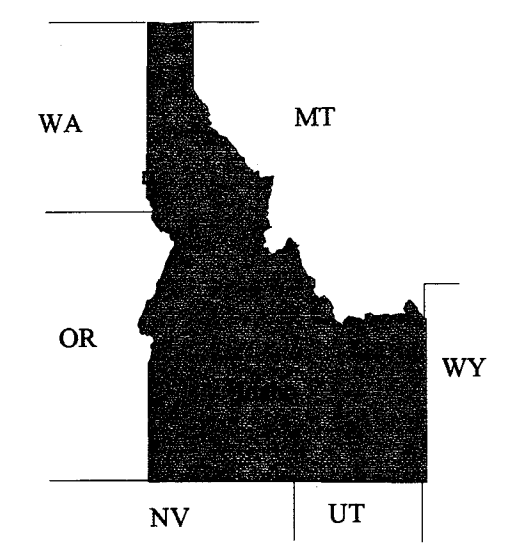
Figure 2. Location Maps of the UIGRS (A-A' is a cross section in Figure 4.)
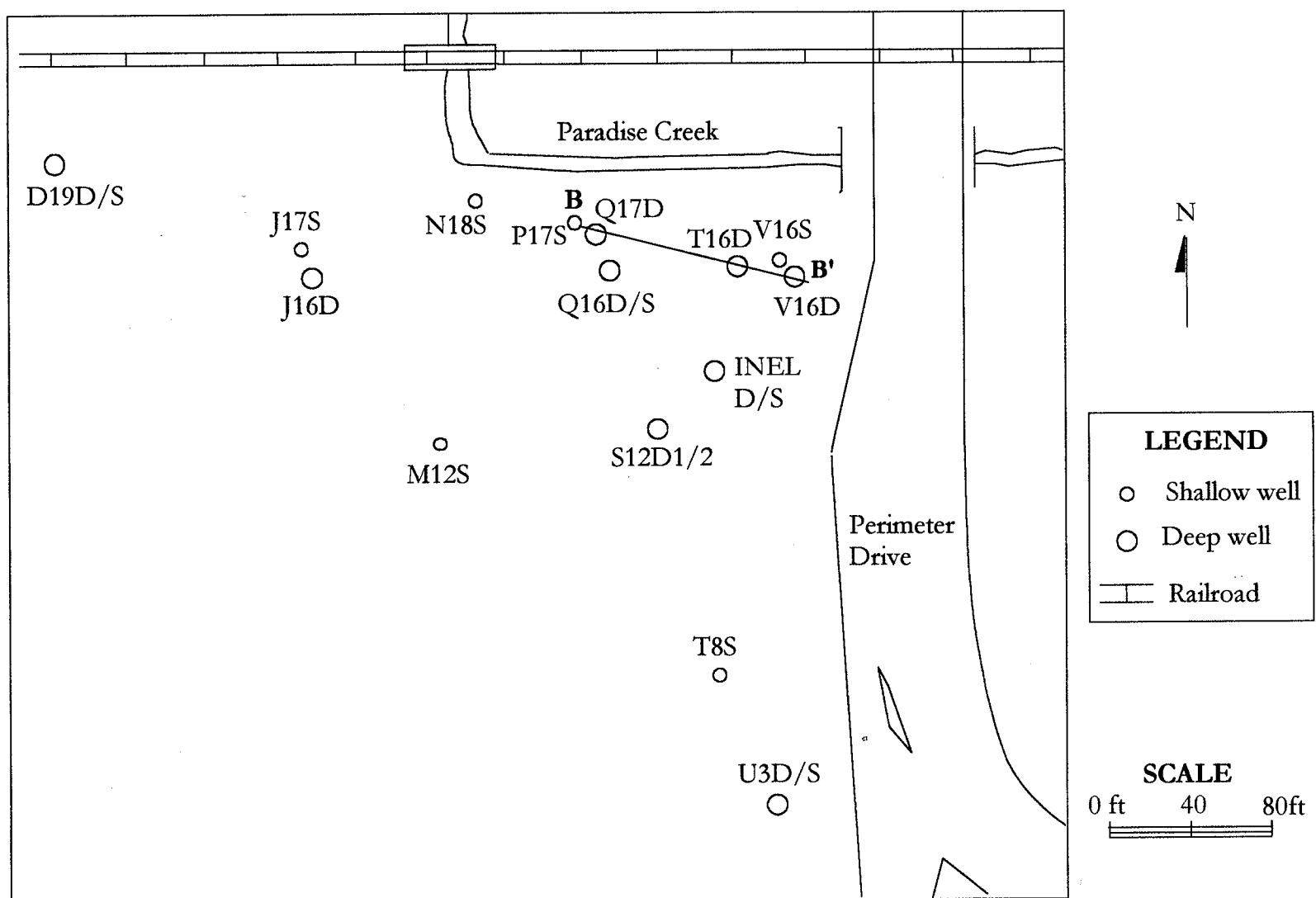
Figure 3. Map of the University of Idaho Groundwater Research Site (UIGRS) (modified from Li, 1991)
         B - B' is a cross section in Figures 8, 9, 11 and 12.

Stratigraphy and Lithology of the Moscow-Pullman Basin

There are three main stratigraphic units within the Moscow-Pullman basin. From the bottom up these are the crystalline basement rock, Columbia River basalts with associated sediments, and surficial sediments. The crystalline basement rock consists of Precambrian orthoquartzite and Cretaceous granite intrusions (Provant, 1995). The overlying Miocene aged Columbia River Basalt Group is comprised mostly of basalt with sediments deposited between some of the flows. Palouse loess and alluvium of the Pleistocene age make up the uppermost stratigraphic unit. Figure 4 is a geologic cross section through the University of Idaho Aquaculture site and the UIGRS.

The Columbia River Basalt Group is comprised of two major formations in the basin. These are the Grande Ronde and Wanapum Formations. They are hydrologically, geochemically and possibly even microbiologically different from one another.

The basal basalt unit of the Columbia River basalts under Moscow is the Grande Ronde Formation. It is comprised of lava flows which erupted approximately 15.6 to 17.0 million years ago (Provant, 1995). Each flow has an average thickness between 40 and 80 feet; although, greater thicknesses have been found (Li, 1991). Within the basin, the total thickness of this formation is between zero and 2500 feet (Li, 1991).

The Wanapum Formation is the upper basalt unit with only the Priest Rapids Member present in the basin. This formation is the result of lava flows dating 14.5 million years. The Lolo flow of the Priest Rapids Member is the uppermost basalt unit in the basin; it has a range in thickness from 160 to 200 feet (Provant, 1995).

Sediments within the Columbia River Basalt Group comprise the Latah Formation (Provant, 1995). The sediments range from clay and silt size particles to sand and fine gravel size particles and are derived from fluvial and lacustrine environments controlled by the basalt deposition. There are three basic areas where these sediments are found. The uppermost sediments in this formation are called the sediments of Bovill. These sediments do not underlie basalts or in between basalt flows and are not present at all locations. The first sedimentary interbed of the Latah Formation separates the Wanapum and Grande Ronde basalt formations and is equivalent to the Vantage Horizon or Vantage Member in the Ellensburg Formation in central Washington. Other sedimentary interbeds separate the
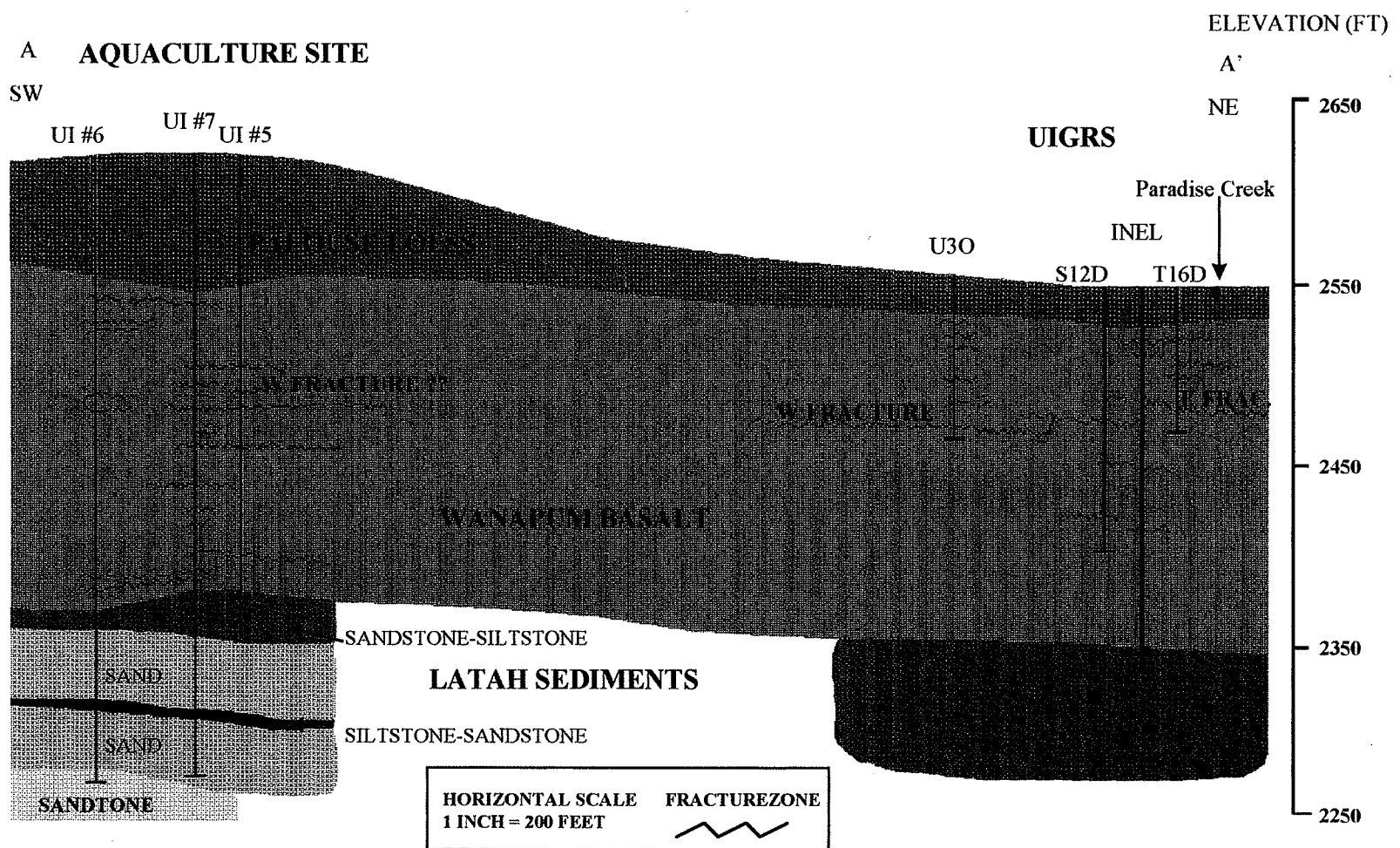
A **AQUACULTURE SITE**

Figure 4. North-South Cross Section Through Aquaculture Site and UIGRS Area (modified from Kopp, 1994).
See Figure 2 for Location of Cross Section.

different flows in the Grande Ronde Formation and are loosely called the sediments of Moscow as are the older sediments beneath the Grande Ronde basalt in the Moscow-Pullman basin (Pierce, 1998).

The uppermost stratigraphic unit of the basin includes alluvial sediments and Palouse loess (Li, 1991; Provant, 1995). Paleosols mixed with eolian volcanic, glacio-fluvial and glacio-lacustrine sediments comprise the Palouse Formation which has a thickness up to 150 feet (Provant, 1995). The loess is composed of a silty loam with mostly quartz and feldspar in addition to minute percentages of sand. Alluvial sediments are the most recent and consist of reworked loess, basalt and granitic fragments or mixtures of them. They are derived from stream deposits and slope-wash. The thickness of this unit may be up to several hundred feet (Li, 1991).

Structure of a Columbia River Basalt Flow

The structural characteristics of a basalt unit are formed by the cooling and emplacement of the flow (Bush and McFadden, 1994). A typical Columbia River Basalt flow consists of (from top to bottom) a vesicular flow top, entablature, colonnade and pillows (Figure 5). Static conditions during the cooling of a flow are necessary to form this structure. Vesicles are found in several portions of a flow but are most abundant in the flow top. They are formed from trapped gas bubbles within the cooling magma. The colonnade is comprised of large columns formed in the basal section of a flow. These columns have diameters from one to 16 feet with an average of about three feet and a length of up to 245 feet with an average between 50 and 100 feet. The entablature is comprised of smaller columns in the upper section of a flow and on the average makes up 20% of the flow thickness but can range between zero and 100% of the flow thickness. Columns in the entablature are usually less than three feet in diameter and are less consistent in orientation. They are often bundled together to form fans, synforms, antiforms or other odd shaped structures. A distinct contact is formed where the colonnade-entablature meet, creating an extensive horizontal fracture zone that can be several kilometers long. This contact is usually found in the bottom 2/3rds of a flow because cooling occurs from the top down and from the bottom up, but most rapidly

Vessicular Top

Entablature

Colonnade

Pillows
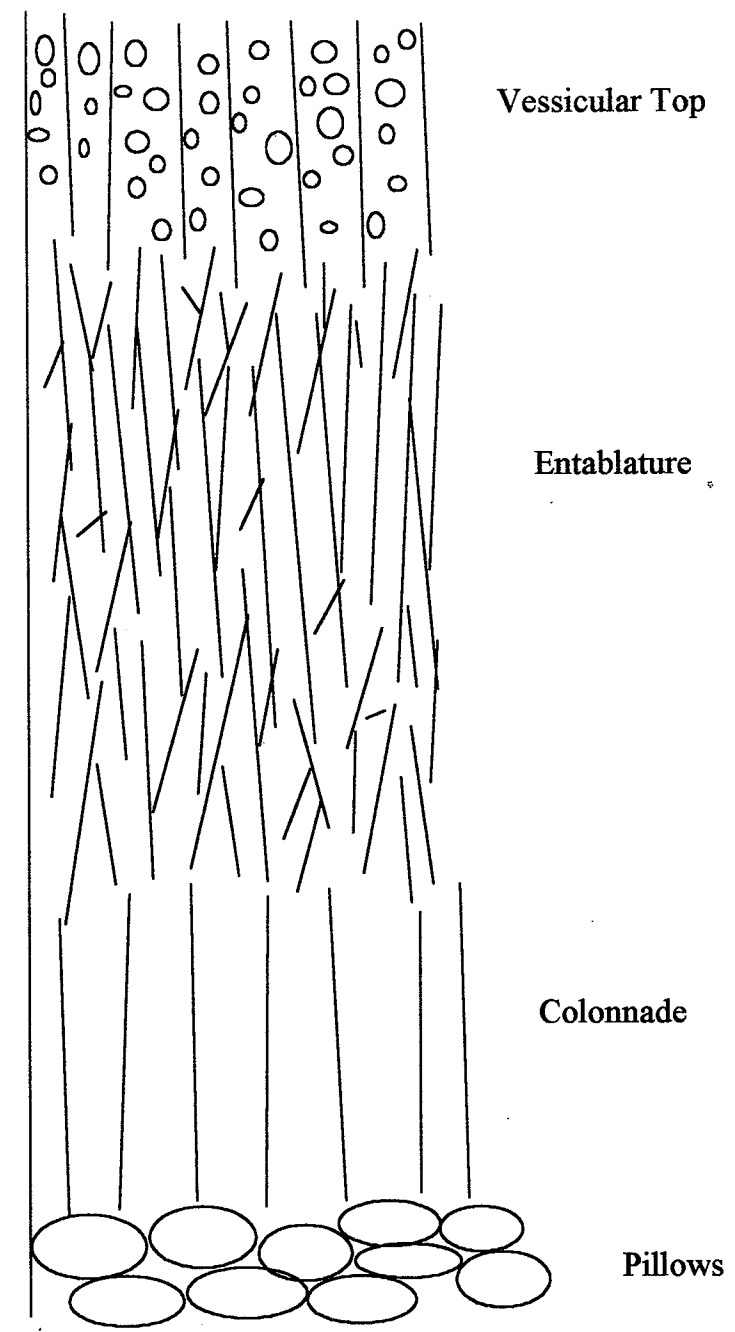
Figure 5. Physical Characteristics of a Typical Basalt Flow

from the top down (Bush, 1998). Multiple sequences of colonnade and entablature can occur in a single flow.

The structure of the Lolo flow is somewhat different than the above and varies laterally as well (Li, 1991). The top of the flow is oxidized. The upper section of the flow consists of large blocks and subhorizontal fractures. A hackly entablature then grades in the center portion of the flow to alternating entablature and colonnade structures. Large diameter columns of the colonnade make up the bottom of the flow.

Each basalt flow has its unique structure (Bush, 1998). Many flows have several lobes or fingers at the advancing front which may intermingle and stack. These lobes may cross within hours, days or years and disrupt the typical basalt structure. When a flow encounters a body of water or an earthquake occurs during the cooling process, the flow takes on a different structure. Fractures are formed and terminated by each other. These alterations make stratigraphic interpretation somewhat difficult.

REGIONAL HYDROGEOLOGIC SETTING

There are two regional aquifers within the Moscow-Pullman basin. An upper aquifer is associated with the Wanapum Formation and a lower aquifer is associated with the Grande Ronde Formation.

The aquifer located in the Wanapum Formation consists mainly of fractured basalt but includes the underlying sediments. Many domestic and a limited number of municipal wells are located in this aquifer. Wells have depths ranging from 200 to 400 feet with a depth to water between 50 and 80 feet (Ralston, 1998).

The lower aquifer is located in the Grande Ronde Formation and includes fractured basalt as well as some sediments. Most municipal wells are located in this aquifer. Well depths are between 500 to 1400 feet; the depth to water varies from 250 to 300 feet (Ralston, 1998).

UIGRS GEOLOGIC SETTING

The general geology of the University of Idaho Groundwater Research Site (UIGRS) is similar to the regional geology with differences mainly in stratigraphic thicknesses. The

primary focus of the research at the UIGRS is on the Wanapum basalts and the overlying sediments. The following discussion includes a description of the shallow alluvium and Latah Formation, the basalt of the Lolo flow and the lithology of the fracture zone in which the experiments were conducted.

Sediment Stratigraphy and Lithology

The uppermost stratigraphic unit at the UIGRS consists of unconsolidated soil and sediments. This unit includes Pleistocene Palouse loess underlain by alluvium. The loess consists of black soil, clay and silt and has a thickness up to 13 feet. The alluvium is composed of sand and gravel and probably was deposited by an ancient Paradise Creek channel. The grain size of the alluvium varies laterally as does the thickness, ranging between 0 and 10 feet, and lies in the interval from 8 to 18 feet.

The other sedimentary stratigraphic unit at the UIGRS is the "Vantage equivalent" interbed of the Latah Formation which underlie the Wanapum basalt. These sediments consist of sand layers with silt zones and are laterally continuous for at least several thousand feet (Kopp, 1994). The thickness of this formation is approximately 200 feet (Kopp, 1994).

Stratigraphy and Lithology of the Lolo Flow

Basalt of the Lolo Flow of the Wanapum Formation underlies the alluvium at the UIGRS and is the focus of this thesis. This basalt lies at a depth between about 15 and 200 feet. It consists of mostly dense basalt with subhorizontal fractures, numerous microfractures, vertical joints and vesicles which are formed as the result of cooling patterns. Most of the wells in the basalt are completed in subhorizontal fractures in the upper third of the flow at depths ranging from 70 to 90 feet. Less continuous horizontal fractures, vertical joints that may connect horizontal fractures, and at a smaller scale, microfractures and vesicles are found at a variety of depths. Only two wells penetrate the Lolo flow at the UIGRS below a depth of 100 feet. These are INEL-D and D19D (Figure 3).

Test Fracture Lithology

Two major subhorizontal fracture zones were identified by Li (1991) underlying the UIGRS; he called these the E- and W-fracture zones. The zones are laterally continuous over tens to hundreds of feet and may be connected by vertical fractures. At most sites the fractures are located at depths of 70-90 feet with some depths reaching 140 feet.

The E- and W-fracture zones are examples of subhorizontal fractures that occur at numerous sites in the Lolo flow. Figure 6 is a photograph taken of a quarry wall along the Moscow-Pullman highway of a horizontal fracture zone (middle of the photograph) which is a stratigraphic equivalent to the E- and W-fracture zones. The fracture zone is laterally continuous and varies in thickness. Vertical joints connect the horizontal fractures and the less fractured blocks of basalt.

At a smaller scale, microfractures and vesicles form a portion of subhorizontal fracture zones in the Lolo flow. Figure 7 is a smaller scale photograph of a fractured system in the quarry wall shown in Figure 6. As seen in Figure 7 the dark gray areas of the basalt represent a clean break with no visible signs of weathering; the brown discoloration is a mineral alteration caused by water movement or storage within microfractures. This large basalt block probably broke away from the outcrop along the microfractures because these are the zones of greatest weakness. Small vesicles caused by trapped gas bubbles during cooling can also be seen in the rock (far left).

UIGRS HYDROGEOLOGIC SETTING

The E- and W-fracture aquifers at the UIGRS are penetrated by a total of nine wells. Nine additional wells penetrate the shallow sediments, one well is screened in a fracture zone other than the E- and W-fractures, and one well is completed in the Latah Formation sediments below the Lolo flow. Table 3 provides information about well construction and Table 4 provides ground water level data and well capacity information.

The E-fracture aquifer dips less than 10 degrees to the west and is located in the center, northeast portion of the UIGRS (Li, 1991). The aquifer is penetrated by five wells (Q17D, Q16D, T16D, V16D and S12D1) but is missing in other areas. The fracture zone is 0.5 to 3 feet thick and is located approximately 64 to 79 feet below land surface with the

Figure 6. Photograph of Large Scale Horizontal Fracture Zone.
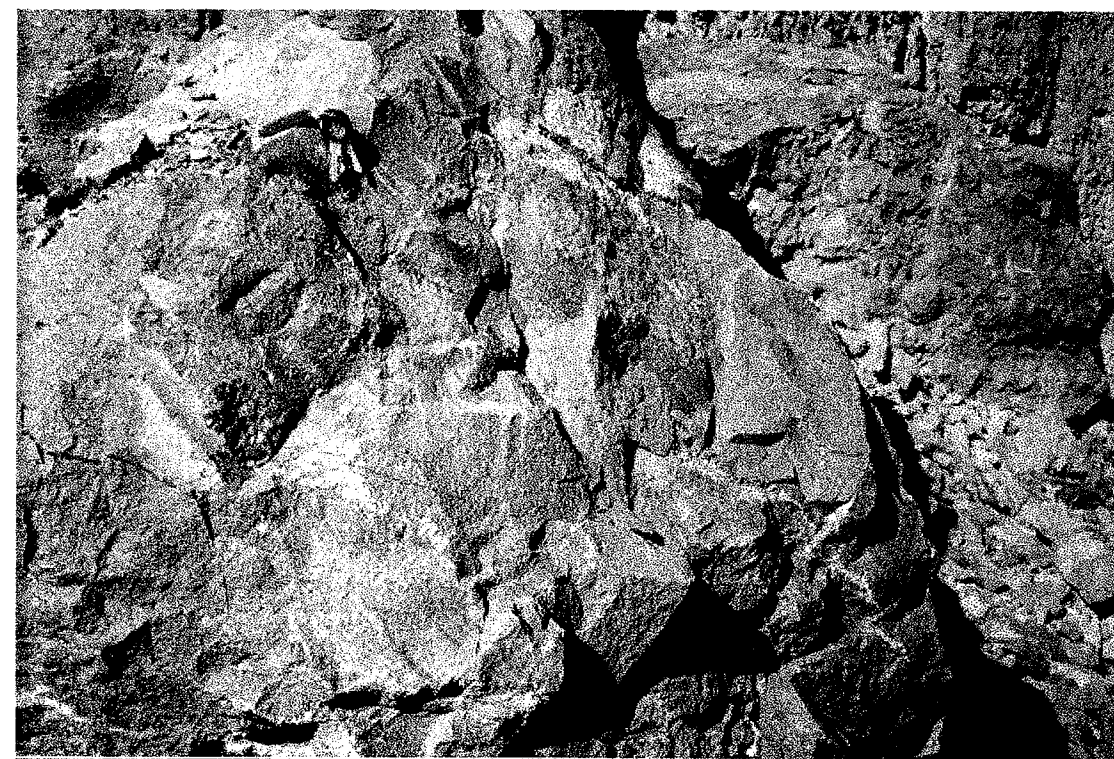
Figure 7. Photograph of Small Scale Basalt Features.

WELL NO.	GROUND ELEV. (AMSL) (ft)	TOTAL DEPTH (ft)	BOREHOLE DIAMETER (in)	SURFACE CASING DEPTH (ft)	SURFACE CASING DIAMETER (in)	PVC LINER DEPTH (ft)	PVC LINER DIAMETER (in)	PERFORATION (PVC)	PERF. INTERVAL (ft)	SANDPACK INTERVAL (ft)	SEAL
Q17D	2544.98	100	4	30	6	81	4	Hacksaw slots	76-79	73-81	C&B
Q16D	2545.10	80	8	20	8	73	4	40-slot screen	70-72.5	69-73	B
Q16S	2545.10	80	8	20	8	27	1.25	Hacksaw slots	26-27	25-27.5	B
T16D	2543.61	80	4	22	6	70	4	Hacksaw slots	65-69	59-70	C&B
V16D	2543.46	70	4	20	6	70	4	40-slot screen	65-67.5	63-70	C&B
S12D1	2545.95	146	6	23	6	127	1.25	Hacksaw slots	119-126	117-129	B**
S12D2	2545.95	146	6	23	6	75	1.25	Hacksaw slots	65-74	64-75	B
T16D	2543.61	80	6	22	6	70	4	Hacksaw slots	65-69	59-70	C+B
D19D	2542.74	140	6	20	6	140	4	40-slot screen	137-139	133-140	C+B
U3D	2547.65	83	8	18	8	83	4	40-slot screen	81-83	79-83	B
U3S	2547.65	83	8	18	8	34	1.25	Hacksaw slots	33-34	32-35	B
J16D	2545.60	68	8	18	8	68	4	40-slot screen	65-67.5	63-68	B
J16S	2545.60	68	8	18	8	20	1.25	Hacksaw slots	19-20	18-21	B
J17S	2545.50	16	6	5	6	16	2	20-slot screen	14-16	12-16	B
V16S	2543.05	10	3	2	4	10	1	open bottom	10	9-10	B
P17S	2544.70	10	3	2	4	10	1	open bottom	10	9-10	B
N18S	2544.02	17	6	3	4	16	2	20-slot screen	13-16	12-17	B
T8S	2546.50	15	6	4	6	15	2	20-slot screen	13-15	12-15	B
**M12S	2546.65	17	6	4	6	16	2	20-slot screen	13-16	12-16	B
*INEL-D	2545	205	8	19	8	202	2	20-slot screen	192-202	190-205	B
*INEL-S	2545	205	8	19	8	100	2	20-slot screen	90-100	88-103	B

*Data from Kopp (1994)   B - Bentonite   C&B - Cement and Bentonite mix   B** - Bentonite Pellets or Plugs
**Referred to as H12S in Li (1991)

Table 3. Well Construction Information (Li, 1991; Kopp, 1994)

WELL NO.	GROUND ELEV. (AMSL) (ft)	TOTAL DEPTH (ft)	BOREHOLE DIAMETER (in)	SURFACE CASING DEPTH (ft)	SURFACE CASING DIAMETER (in)	PVC LINER DEPTH (ft)	PVC LINER DIAMETER (in)	PERFORATION (PVC)	PERF. INTERVAL (ft)	SANDPACK INTERVAL (ft)	SEAL
Q17D	2544.98	100	4	30	6	81	4	Hacksaw slots	76-79	73-81	C&B
Q16D	2545.10	80	8	20	8	73	4	40-slot screen	70-72.5	69-73	B
Q16S	2545.10	80	8	20	8	27	1.25	Hacksaw slots	26-27	25-27.5	B
T16D	2543.61	80	4	22	6	70	4	Hacksaw slots	65-69	59-70	C&B
V16D	2543.46	70	4	20	6	70	4	40-slot screen	65-67.5	63-70	C&B
S12D1	2545.95	146	6	23	6	127	1.25	Hacksaw slots	119-126	117-129	B**
S12D2	2545.95	146	6	23	6	75	1.25	Hacksaw slots	65-74	64-75	B
T16D	2543.61	80	6	22	6	70	4	Hacksaw slots	65-69	59-70	C+B
D19D	2542.74	140	6	20	6	140	4	40-slot screen	137-139	133-140	C+B
U3D	2547.65	83	8	18	8	83	4	40-slot screen	81-83	79-83	B
U3S	2547.65	83	8	18	8	34	1.25	Hacksaw slots	33-34	32-35	B
J16D	2545.60	68	8	18	8	68	4	40-slot screen	65-67.5	63-68	B
J16S	2545.60	68	8	18	8	20	1.25	Hacksaw slots	19-20	18-21	B
J17S	2545.50	16	6	5	6	16	2	20-slot screen	14-16	12-16	B
V16S	2543.05	10	3	2	4	10	1	open bottom	10	9-10	B
P17S	2544.70	10	3	2	4	10	1	open bottom	10	9-10	B
N18S	2544.02	17	6	3	4	16	2	20-slot screen	13-16	12-17	B
T8S	2546.50	15	6	4	6	15	2	20-slot screen	13-15	12-15	B
**M12S	2546.65	17	6	4	6	16	2	20-slot screen	13-16	12-16	B
*INEL-D	2545	205	8	19	8	202	2	20-slot screen	192-202	190-205	B
*INEL-S	2545	205	8	19	8	100	2	20-slot screen	90-100	88-103	B

*Data from Kopp (1994) B - Bentonite C&B - Cement and Bentonite mix B** - Bentonite Pellets or Plugs
**Referred to as H12S in Li (1991)

Table 3. Well Construction Information (Li, 1991; Kopp, 1994)

WELL NO.	YEAR COMPLETED	WATER LEVEL ELEV. (AMSL) ANNUAL HIGH (ft)	WATER LEVEL ELEV. (AMSL) ANNUAL LOW (ft)	MAX. WELL YIELD (gpm)	SPEC. WELL YIELD (gpm/ft)	DATUM MARKER FOR WATER LEVEL	DATUM ELEV. (ft)
Q17D	1987	2540.3	2536.6	7-10	0.25	Top of 6" casing	2545.95
Q16D	1990	2540.6	2536.8	2	not available	Top of 8" casing	2546.96
Q16S	1990	2540.5	2536.6	<1(?)	not available	Top of 8" casing	2546.96
T16D	1988	2540.4	2536.7	7-10	0.3-0.4	Top of 6" casing	2545.24
V16D	1987	2540.7	2537.0	40-50	3.25	Top of 6" casing	2544.41
S12D1	1989	2540.4	2535.4	<1	not available	Top of 6" casing	2546.93
S12D2	1989	2520.3	2519.3	<1	not available	Top of 6" casing	2546.93
D19D	1987	2519.8	2518.9	30-50	0.2-0.3	Top of 6" casing	2543.76
U3D	1990	2521(?)	2519.3	1-2?	not available	Top of 8" casing	2548.62
U3S	1990	2544.1	2541.2	1-2?	not available	Top of 8" casing	2548.62
J16D	1990	2521(?)	2519.3	40-60	0.4-0.5	Top of 8" casing	2546.68
J16S	1990	2540.5	2536.4	<1	not available	Top of 8" casing	2546.68
J17S	1990	2540.1	2536.2	<1	not available	Top of 2" casing	2546.64
V16S	1988-1990	2541.0	2536.7	<0.5	not available	Top of 1" casing	2544.86
P17S	1988-1990	2540.0	2536.3	<0.5	not available	Top of 1" casing	2546.27
N18S	1988-1990	2539.7	2536.2	<1	not available	Top of 2" casing	2546.16
T8S	1988-1990	2541.0	2537.5	<0.2	not available	Top of 2" casing	2547.98
**M12S	1988-1990	2540.5	2537.3	<0.2	not available	Top of 2" casing	2547.84
*INEL-D	1992	not available	not available	not available	not available	Top of 8" casing	2546.4
*INEL-S	1992	not available	not available	not available	not available	Top of 8" casing	2546.4

*Data from Kopp (1994)   **Referred to as well H12S in Li (1991)

Table 4. Ground Water Level and Well Yield Capacity Data at the UIGRS (Li, 1991; Kopp, 1994)

exception of S12D1 which has a depth of 127 feet. The depth to water in the first four wells is about 5-10 feet. The E-fracture aquifer acts as a confined, heterogeneous and anisotropic aquifer with well yields from <1-30 gallons per minute (gpm) and specific well yields between 0.3 to 3.3 gpm per foot of drawdown. This variability indicates a variable hydraulic conductivity.

The W-fracture aquifer is the stratigraphic equivalent to the E-fracture aquifer on the western and southern area of the UIGRS (Li, 1991). Four wells penetrate the W-fracture aquifer: D19D, J16D, U3D and S12D2. The W-fracture zone is also missing at other areas of the site. This aquifer ranges in depth from 70 to 165 feet in a z-shape and is approximately 0.5 to 1.0 foot thick. The W-fracture aquifer also is penetrated by a well at the Aquaculture Research Site located about 800 feet to the southwest. It consists of several sub-horizontal fracture zones with vertical connecting fractures. The depth to water ranges from about 18 to 31 feet (García Pardo, 1993). This aquifer is also confined, heterogeneous and anisotropic with well yields ranging from less than 1 to 60 gpm and specific well yields of less than 0.5 gpm per foot at the well of greatest yield.

Differentiation of the E- and W-fracture systems is based on water level elevations, hydraulic responses, microbiology and water chemistry (Li, 1991; Zheng, 1993). Water level elevations in wells completed in the W-fracture are approximately 20 feet lower than the E-fracture wells. Aquifer tests conducted in the E-fracture show a rapid drop in water levels in the E-fracture wells but drawdown takes hours to affect wells in the W-fracture. Microbial communities are different between the fractured aquifers. Microbes of the different aquifers utilized different laboratory substrates; microbes of the E-fracture aquifer utilized several more substrates than microbes in the W-fracture aquifer. Geochemically, the ammonia and nitrate ratio was different for W- and E-fracture aquifers. However, there were some variations in the microbial and geochemical data even within each aquifer caused by the heterogeneous nature of the site.

Li (1991) and García Pardo (1993) found a good hydraulic connection between the shallow aquifer, E-fracture aquifer and Paradise Creek. Both of these aquifers respond to changes in stream stage. The W-fracture shows almost no connection to the shallow aquifer and Paradise Creek and a limited hydraulic connection to the E-fracture aquifer. However,

the W-fracture aquifer does show some hydraulic connection to the Vantage Equivalent sediments (Li, 1991; García Pardo, 1993; Kopp, 1994). Pumpage of wells completed in the Vantage Equivalent sediments under the Lolo flow at the Aquaculture Research Facility impacted water levels in the W-fracture aquifer wells.

Li (1991) concluded the E-fracture behaves as an equivalent porous medium and the W-fracture behaves as a double porosity medium based on a series of aquifer tests. He found that the Hantush and modified Hantush leaky aquifer models were applicable to the E-fracture aquifer with the modified Hantush method pertinent to the early time data. Transmissivity values for the E-fracture range from 14 to 580 ft^2/d with an average of 80 ft^2/d. Storativity values for this fracture aquifer are between $2x10^{-5}$ and $5x10^{-4}$ with an average of $9x10^{-5}$. The W-fracture aquifer is best modeled by the Moench double-porosity with fracture skin model. Early time deviation may be explained by the fractured rock with double-porosity model. Transmissivity values vary from 0.5 to 3 ft/d and storativity values range from $5x10^{-7}$ and $5x10^{-5}$. No aquifer tests were conducted in the shallow aquifer.

CHAPTER 4
DESIGN AND DESCRIPTION OF TESTS

INTRODUCTION

This chapter provides a description of five tracer tests conducted at the UIGRS and information about the tracer test mechanics. A detailed description of how each tracer test was carried out is provided. The field instrumentation, the selection of the tracers, and the method of sample analysis are discussed.

DESCRIPTION OF TRACER EXPERIMENTS

Two different groups of ground water tracer experiments were employed for the hydrogeologic analysis of the E-fracture aquifer: 1) radially convergent two-well recirculation tests which use a pumping-recharging well pair; tracer was injected into the recharging well and 2) radially convergent tests in which one well was pumped with another used as the tracer injection well. The two well recirculation tests involve tracer movement over larger areas but are more difficult to interpret because of tracer recirculation. A radially convergent test involves a smaller area but is easier to interpret.

A total of five complete tracer tests were conducted in the E-fracture aquifer at the UIGRS. A number of other tests were run in the development of field procedures. Three experiments were conducted using the radially converging recirculation technique and are symbolized by the roman numeral I. Two radially converging tests were conducted and are symbolized by the roman numeral II. Each roman numeral is followed by the number for the order in which the tests were conducted. It is important to note the recirculation experiments were carried out prior to the radially converging experiments, except Test I-3 which was the last test conducted.

Detailed information about each tracer test is listed in Tables 5 to 8. Table 5 provides the general tracer test information (i.e. test type, test date, wells used, etc.). Table 6 lists information about each tracer used including the injection amount, injection concentration and the injection time. Table 7 describes sampling information (i.e. sample collection method, frequency, containers and storage). Lastly, Table 8 provides information about sampling

	TEST I-1	TEST I-2	TEST I-3	TEST II-2	TEST II-4
Test Type	recirculating convergent	recirculating convergent	recirculating convergent	convergent	convergent
Test Date	9/12/96	9/20/96	10/17/97	10/29/96	3/26/97
Main Pumping Well Pump Depth (ft):	V16D 53	V16D 53	V16D 63	Q17D 63	Q17D 63
Ave. Main Pumping Rate (gpm)	~3.0	~3.0	4.7	2.8	2.9
Recharging Inj. Well	Q17D	Q17D	Q17D	NA	NA
Time Recirculation Ceased (min)	t=294	t=120	t=321	NA	NA
Tracer Injection Well	Q17D	Q17D	Q17D	Q16D	Q16D
Monitoring Wells (including main pumping well)	Q16D, T16D and V16D	Q16D, T16D and V16D	Q16D, T16D, V16D and S12D2	Q17D	Q17D
Length of Pumping Before Tracer Inj. (hrs.)	48	12	3	17	2
Means of Injection	60 cc syringe	60 cc syringe	peristaltic pump	peristaltic pump	peristaltic pump
Injection Tubing Diameter (ID) (in)	1/8	1/8	1/8	1/8	1/8
Tracer Injection Rate (mL/min)	40	40	(Fl) 176 (I) t 150 (VA) 153 (spores) 212 (beads) 214	200	(Fl) 568 (BA/VA) 640 (spores) 617 (beads) 570 (Br) 667

NA - not applicable

Table 5. General Tracer Test Information for Tests Conducted at the UIGRS.

	TEST I-1	TEST I-2	TEST I-3	TEST II-2	TEST II-4
Fluorescein inj. amt.: inj. conc.: inj. time:	16.02 g in 60 mL 2.67×10^5 mg/L t=0 min	16.02 g in 60 mL 2.67×10^5 mg/L t=0 min	40.00 g in 250 mL 1.60×10^5 mg/L t=0 min	267.0 g in 1000 mL 2.67×10^5 mg/L t=0 min	15.00 g in 500 mL 3.00×10^5 mg/L t=0 min
Iodide inj. amt.: inj. conc.: inj. time:	NA	NA	350 g (KI) in 500 mL 7.00×10^5 mg/L (KI) t=19.08 min	NA	NA
Benzoic Acid inj. amt.: inj. conc.: inj. time:	NA	NA	NA	NA	100 g in 1100 mL 9.09×10^5 mg/L t=364.17 min
Veratryl Alcohol inj. amt.: inj. conc.: inj. time:	NA	NA	400 g in 600 mL 6.67×10^5 mg/L t=34.9 min	NA	100.00 g in 1100 mL 9.09×10^5 mg/L t=364.2 min
Bacillus thermoruber spores inj. amt.: inj. conc.: inj. time:	NA	NA	10^9 spores/mL in 2L 2×10^{12} spores t=64.0 min	NA	10^8 spores/mL in 1L 10^{11} spores t=239 min
YG Microbeads inj. amt.: inj. conc.: inj. time:	NA	NA	2.11×10^8 beads/mL (16 mL beads) in 234 mL H_2O 3.37×10^9 beads t=83.5 min.	NA	NA
PC Red Microbeads inj. amt.: inj. conc.: inj. time:	NA	NA	NA	NA	2.11×10^8 beads/mL (8 mL beads) in 492 mL H_2O 1.69×10^9 beads t=269 min

NA - not applicable

Table 6. Tracer Information for Tests Conducted at the UIGRS.

	TEST I-1	TEST I-2	TEST I-3	TEST II-2	TEST II-4

Fractomette Alpha 2000 fraction collector
  wells
  frequency
	Q16D and T16D
	5 min
		T16D and V16D
		5 min
			NA	Q17D
				5 min
					NA

Golden Retriever fraction collector
  wells
  frequency
	V16D
	5 min
		Q16D
		5 min
			NA	NA	NA

Hand Sampling
  wells
  frequency
	NA	NA	Q16D ~ 10 min
			T16D ~ 10-20 min
			V16D - see text
				NA	Q17D - see text

Sample Containers	15 mL glass test tubes	15 mL glass test tubes	15 mL glass test tubes (Q16D and S12D2) 500 mL Pyrex glass sample jars (T16D and Q16D)	15 mL glass test tubes	500 mL Pyrex glass sample jars 15 mL glass test tubes for Br
Sample Storage	room temperature (cooler)	room temperature (cooler)	5°C cold room	room temperature (cooler)	5°C cold room

NA - not applicable

Table 7. Sampling Information for Tests Conducted at the UIGRS.

	TEST I-1	TEST I-2	TEST I-3	TEST II-2	TEST II-4
12V Pumps wells - rate (mL/min) continuous or grab	T16D - failed Q16D - failed grab	T16D - failed Q16D ~ 1.14×10^4 continuous	S12D2 - 1.14×10^4 grab	NA	NA
Peristaltic Pumps wells - rate (mL/min) continuous or grab	NA	NA	Q16D - 300 T16D - 263 grab	NA	NA
Packer Design 1 wells	Q16D and T16D	Q16D and T16D	NA	Q16D	NA
Packer Design 2 wells	NA	NA	NA	NA	Q16D
Packer Design 3 wells	NA	NA	Q16D and T16D	NA	NA
Aardvark Packer wells	NA	NA	Q17D	NA	NA
Electric Sounder wells	Q16D, Q17D, T16D and V16D	Q16D, Q17D, T16D and V16D	Q16D, T16D and V16D	Q16D and Q17D	Q16D and Q17D
Pressure Transducers wells	Q17D and V16D	Q17D and V16D	Q16D, Q17D, T16D and V16D	Q16D and Q17D	Q16D and Q17D

NA - not applicable

Table 8. Sampling Pumps in Monitoring Wells, Packers and Water Level Measurement Devises for Tests Conducted at the UIGRS.

pumps, packers and water level measurement devises. Discussions about each test are provided in the following sections.

DESCRIPTION OF RECIRCULATING CONVERGENT TESTS

Tests I-1, I-2 and I-3 were recirculating convergent tracer tests. The first two experiments were very similar and are described in a single section. The similarities of their basic design are provided before each test is discussed.

The design of the recirculation tracer test experiments was controlled by the unique characteristics of the selected wells. Wells V16D and Q17D were chosen as the recirculation well pair and wells Q16D and T16D were used as monitoring wells; T16D is located between the recirculation well pair and Q16D is just off this transect (see Figure 8). This setup was chosen because a transect with multiple wells was desired to better interpret the hydrogeology of the E-fracture.

Water was pumped from well V16D by a 3.5-inch submersible pump attached to 1.25-inch ID steel riser pipes. Discharge was controlled by a valve near the top of the well casing and monitored by an inline flow meter. The pumped water was routed into well Q17D using about 100 feet of 1.5-inch ID PVC pipe. A t-connector in the recirculation pipe provided an avenue for sample collection from well V16D. A butterfly valve was used to control flow through the sampling port.

Tests I-1 and I-2

Tests I-1 and I-2 were conducted as pretests for the multi-tracer experiments. The objective of Test I-1 was to evaluate various injection and sampling schemes and to gain information about the fracture hydrogeology. Test I-2 was conducted because the 12-volt pumps in wells T16D and Q16D failed during Test I-1. Figure 8 is a cross section of the E-fracture and the tracer test setup used for these two experiments.

Water was pumped from well V16D and discharged at a depth of five feet below the top of the casing in well Q17D. This depth was chosen because at a depth greater than five feet the pressure would force the piping system apart. A constant rate dole valve was placed inline to keep the flow at a specific discharge rate of three gallons per minute (gpm).

Figure 8. Cross Section of the E-Fracture During Tests I-1 and I-2 .

Depth

— 0
— 10
— 20
— 30
— 40
— 50
— 60
— 70
— 80ft

B

B'

Q17D

Q16D

T16D

V16D

E-fracture aquifer

LEGEND

Pump
Water pipe
Discharge valve
Dole valve
Flow meter
Well screen
Packer Design 1
Pressure transducer
Tracer inj. line
Air line
Sample line
12V pump
Data logger
Peristaltic pump
Fraction collector

Map

N

B   Q17D
        T16D
Q16D   B'
            V16D

Scale
40ft   0   40ft

Well diameters and equipment are not to scale.

LEGEND

- Pump
- Water pipe
- Discharge valve
- Dole valve
- Flow meter
- Well screen
- Packer Design 1
- Pressure transducer
- Tracer inj. line
- Air line
- Sample line
- 12V pump
- Data logger
- Peristaltic pump
- Fraction collector

Well diameters and equipment are not to scale.

Figure 8. Cross Section of the E-Fracture During Tests I-1 and I-2 .

Well V16D was pumped at a rate of three gpm. This rate was chosen because it is the maximum amount of water well Q17D can accept without overflowing. The pumping well was pumped to steady state conditions before the tracer was injected. A pumping period of 48 hours occurred prior to the tracer injection in Test I-1 because setup problems delayed the injection.

Wells Q16D and T16D were used as monitoring wells. Twelve-volt pumps were used to collect samples from these wells. The pumps were submerged to a depth of 20 feet; each was connected to 1/2-inch ID tubing above and below the pump to supply the water to the surface. The pump intake tube was located in the center of the screened interval. A packer (Packer Design 1, described in the Field Instrumentation section of this chapter) was placed at the top of the well screen to prevent the tracer from diffusing up the well column. The pump tubing at the surface was split with a y-connector. One line was used as the back pressure relief line; water was allowed to discharge on the ground. This line was necessary because the rate of the sample collection by the fraction collector was so small a large back pressure stressed the pump motor. The other line from the y-connector was attached to 1/2-inch ID tubing that was ultimately reduced to 1/32-inch ID tubing for the fraction collector. Valves were placed within the tubing to control discharge.

Fluorescein was used as the tracer in experiments I-1 and I-2 and injected into well Q17D within the screened interval. Approximately 16 g of fluorescein was mixed with deionized water and sodium hydroxide to form a 60-mL solution. The tracer was injected into the injection line for well Q17D using a 60-mL syringe. The tracer was followed by a 60-mL injection of deionized water and two minutes of forced air from an air compressor. The water was to move the tracer out of the tubing and the air flush was to completely clear the line. In Test I-1 the injection line was to be removed after the injection because sorption of the tracer on the tubing was thought to be a problem; however, upon partial line removal it was noticed some of the tracer remained in the line. The line was then flushed with approximately one liter of water to ensure the tracer was forced into the formation. The line was removed from the well. Sorption onto the tracer injection line was determined to be negligible; in later tests this line remained in the well during the duration of the experiment. Recirculation ceased and the water pumped from well V16D was discharged near the creek to prevent the recirculation of

the tracer after a color change was noticed in the samples. Water levels changed in all the wells following the recirculation portion of the test.

Samples were collected by two fraction collectors. Wells V16D and T16D shared a collector and another was used for well Q16D. Water was directed to a fraction collector which housed a number of 15-mL test tubes. The collector was programmed to move the test tubes on five minute intervals. Water dripped into a test tube for a five minute time period after which the fraction collector moved to the next test tube.

Water levels were measured by two methods: 1) an electric sounder and 2) a data logger which registered and stored readings from pressure transducers. Water levels in all the wells in the E-fracture were measured using the electric sounder; the pumping and recharging well pair were equipped with pressure transducers.

Test I-3

As in the other two recirculation tests, well V16D was pumped during Test I-3 and the water was recirculated into well Q17D. Figure 9 is a cross section of the test setup. A commercial packer was placed directly above the screened interval in the injection well (Q17D) to reduce the amount of tracer circulating up the well column. Tracer injection and mixing lines passed through the packer. The end of the injection line was placed at the top of the well screen and the end of the mixing line was placed near the bottom of the screen. The piping system or recirculation pipe (RP) was connected to the packer riser pipe at the top of the well casing. Three orifices in the piping system were created near the recirculation well for outlets of a pressure transducer and two small tubes which were placed inside the pipe. One was placed at the junction where the packer and the RP meet for the pressure transducer. The other two orifices were about a foot from the junction within the RP; one was for the injection line and the other for the mixing line. Valves were placed in each of the two tubes to prevent outflow.

A discharge rate of about five gpm was adopted in this test. Water was pumped from well V16D and discharged into the screened interval below the packer in well Q17D. The five-gpm rate was chosen because at lower rates the pressure was not great enough for the pressure transducer to register readings in the data logger for the recirculation well.
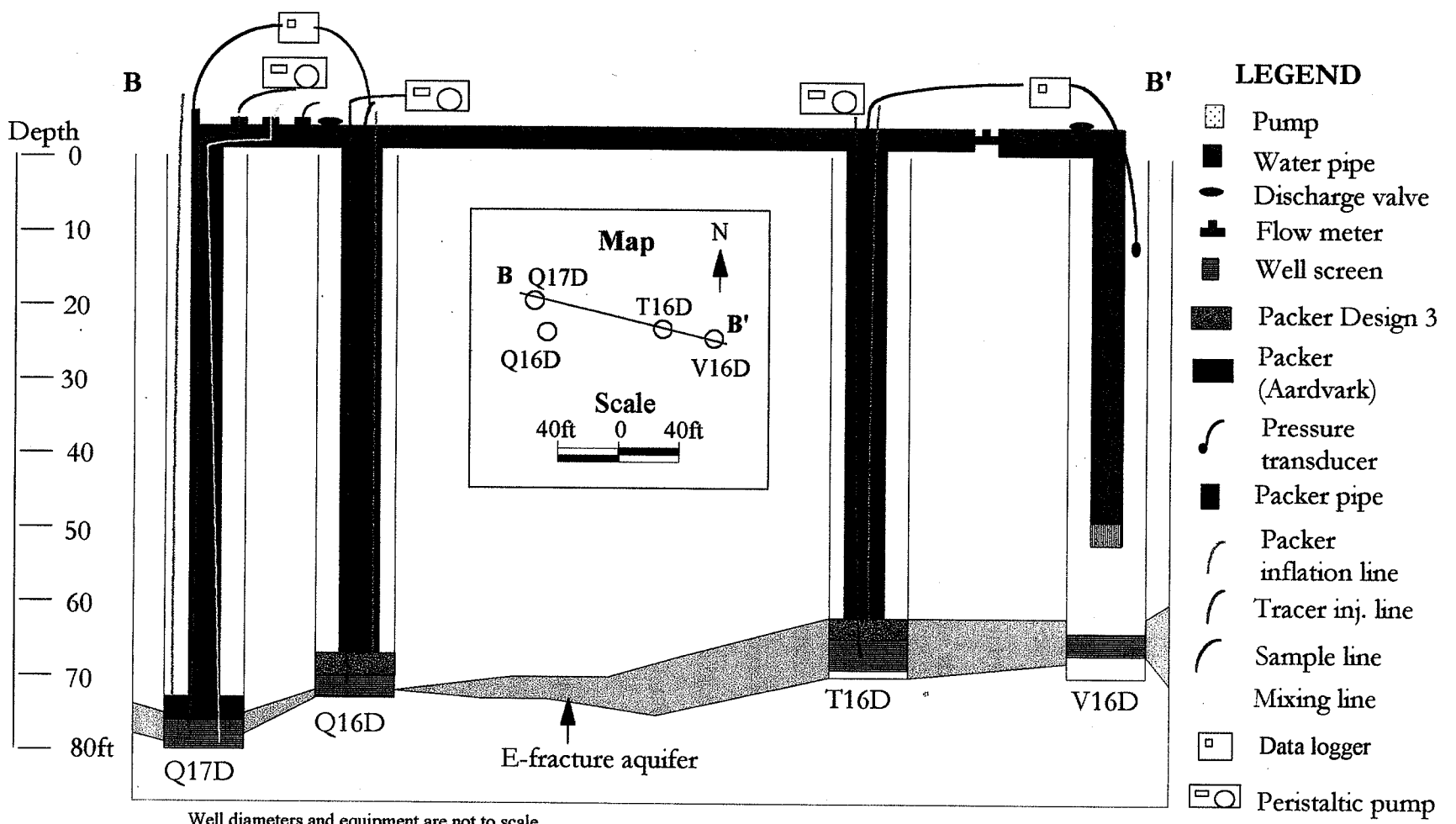
Figure 9. Cross Section of the E-Fracture During Test I-3.

Depth
- 0
- 10
- 20
- 30
- 40
- 50
- 60
- 70
- 80ft

B

B'

Q17D

Q16D

E-fracture aquifer

T16D

V16D

Map

N

B Q17D

T16D

B'

Q16D

V16D

Scale

40ft   0   40ft

LEGEND

- Pump
- Water pipe
- Discharge valve
- Flow meter
- Well screen
- Packer Design 3
- Packer (Aardvark)
- Pressure transducer
- Packer pipe
- Packer inflation line
- Tracer inj. line
- Sample line
- Mixing line
- Data logger
- Peristaltic pump

Well diameters and equipment are not to scale.

Recirculation continued throughout the experiment because a steady hydraulic gradient was important in this test.

Both dissolved and particulate tracers were injected in this experiment. In their order of injection they included: fluorescein, iodide (KI form), veratryl alcohol (VA), *Bacillus thermoruber* spores (~1 μm) and YG Polystyrene microbeads (6 μm). The dissolved tracers were injected prior to the spores and microbeads because the particulates could plug the fractures and alter the flow paths. The microbeads were injected last because they have a larger size than the spores. A time lag between 10 and 30 minutes followed each injection before the next tracer was injected in order to allow for a more complete dispersal of each.

The tracers were injected at varying rates (see Table 5) into well Q17D by a peristaltic pump in a four step process (Figure 10). Step 1 was to inject the tracer. The line was then flushed with approximately 10 mL of water following each tracer injection. Step 2 was to attach the mixing line to the injection line by the peristaltic pump creating a loop. The tracer was then mixed at the same rate as the injection within the screened interval by recirculating the water within the well for three minutes. An initial concentration sample was collected from this loop following mixing. Steps 3 and 4 were to flush each of the two lines with tap water for one minute to force out any remaining tracer in the line. Finally, both lines were clamped off.

A packer (Packer Design 3, see Field Instrumentation section of this chapter) was placed at the top of the well screen in monitoring wells, Q16D and T16D. The packers were used to limit the tracer diffusion within the well column. A packer was not used in well S12D2 because the well diameter is only 1.25 inches and a packer for this size well was not available.

Samples were collected from the pumping well, V16D, and three monitoring wells, Q16D, T16D and S12D2, by a variety of pumps at varied frequencies. A t-connector within the recirculation pipe was connected to a 1/2-inch (ID) tubing which provided an avenue for pumping well (V16D) sample collection. The sampling frequency after tracer injection started for well V16D was every five minutes. After about two hours, the frequency was increased to 2.5-minute intervals following a rapid rise in the observed fluorescein concentration. The sampling frequency was reduced to three minute intervals about 4.5 hours after the tracer
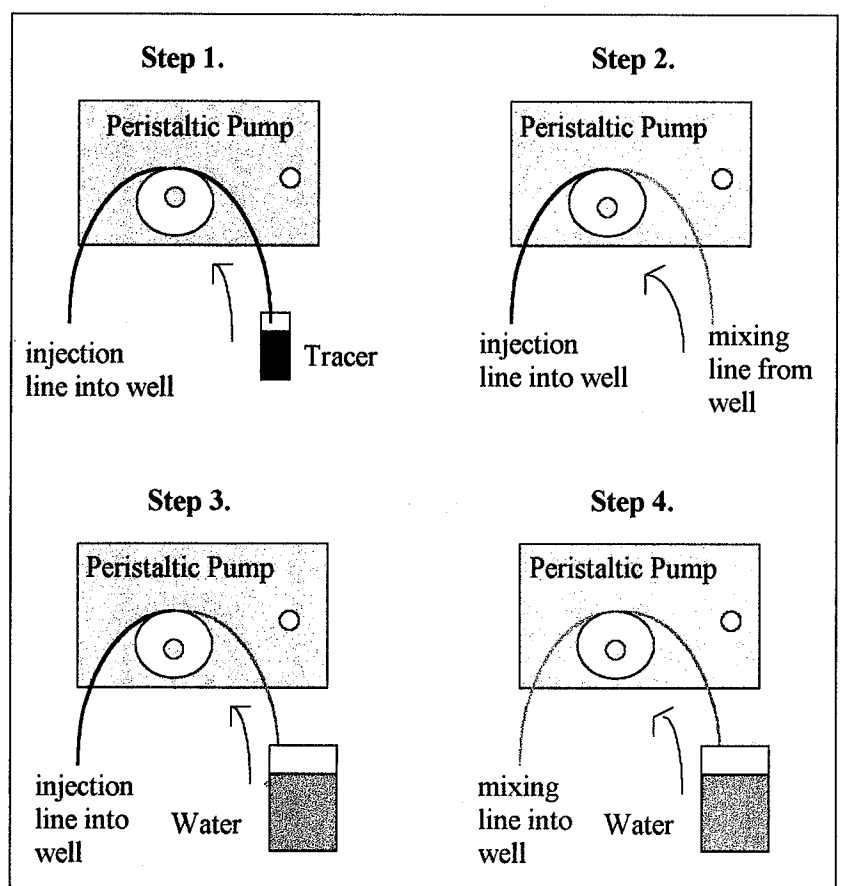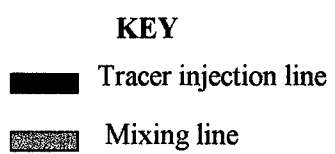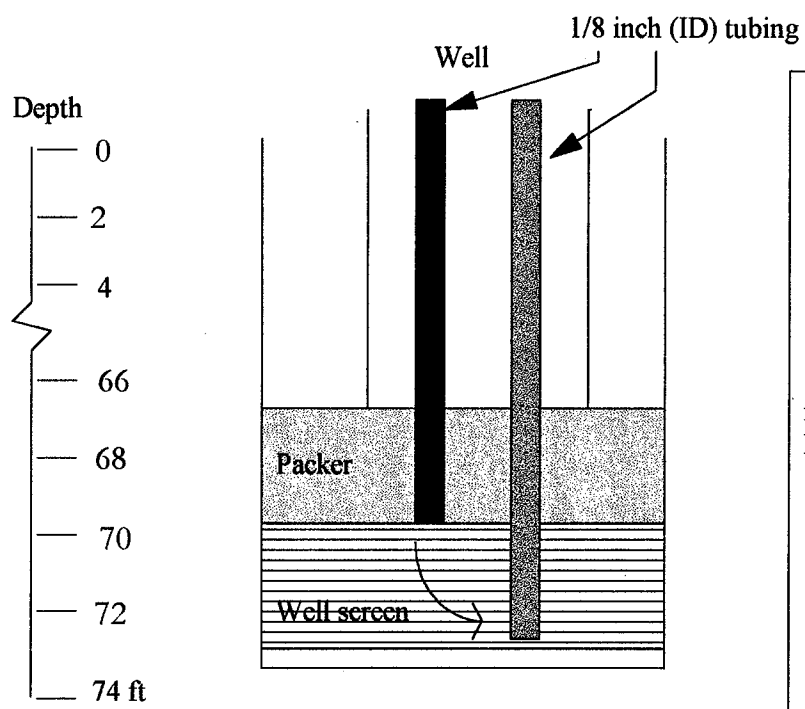
Figure 10. Cross Section of Tracer Injection Well for Tests I-3 and II-4 (Well depths are slightly different than shown in Test I-3) and Steps of Injection.

injection. Peristaltic pumps were used in wells Q16D and T16D for sample collection; they were pumped for one minute prior to collection of each sample to clear the sample line because the pumps were not run continuously. The sampling frequency was about every 10 minutes for Q16D but was about every 20 minutes for well T16D. Well S12D2, completed in the W-fracture, was also monitored to determine if the tracers migrated to this fracture zone. Samples for well S12D2 were collected every 30-60 minutes using a 12V pump; a significant amount of time was necessary for the well to recover after collecting a sample. The 12V pump was pumped for one minute before a sample was collected.

Samples were collected in 500-mL glass jars or 15-mL glass test tubes by hand. Each container was prepared with hydrochloric acid (HCl) to inhibit the degradation of the veratryl alcohol. Four milliliters of 6N HCl was placed in each of the 500-mL sample jars; one drop was placed in each of the 15-mL test tubes. Samples from wells V16D and T16D were collected in 500-mL glass jars. A large amount of sample was necessary for the analysis of the six tracers. The glass jars were chosen because a sufficient number were available for samples from two wells. The samples for well Q16D were collected in 15-mL test tubes because the well yield was low. At low flow rates, a 500-mL sample would take a long period of time to collect. At larger flow rates the hydraulic gradient would change. Test tubes (15 mL) were also used for the sample collection in well S12D2 because an insufficient number of larger sample jars were available. The sample containers were pre-numbered and recorded as to their date and time of collection. Periodically, the samples were brought to a 5°C cold room.

Water levels were measured in wells V16D, T16D, Q16D and Q17D. An electric sounder was used to measure water levels by hand. A pressure transducer was placed in each well and connected to a data logger which was programmed to record measurements on a 15-minute frequency.

No water level measurements were taken in well S12D2 after the start of the test because water levels were largely controlled by operation of the sampling pump. Immediately after the pump was turned on in well S12D2, the water level would fall to the pump intake. The two-inch ID well was too small to allow the electric sounder past the pump. Additional data loggers were unavailable for use in this well.

A problem arose during the experiment requiring a change in the pumping-injection rate. Approximately 90 minutes after the first tracer was injected, it was observed that the injection well was overflowing. The pumping-injection rate was subsequently reduced to 3.1 gpm nine minutes later. Thirteen minutes later the rate was increased to 4.9 gpm because the transducer was not providing readings in the recirculation well. The rate was reduced to 4.2 gpm another 13 minutes later. The rate gradually decreased through the remainder of the test because there wasn't constant rate dole valve. The average discharge rate was 4.7 gpm. Possible explanations of the overflow include leakage past a faulty packer, through the well seals or through a crack in the casing. A borehole television survey of well Q17D following the experiment showed no breaks in the casing.

DESCRIPTION OF CONVERGENT TESTS

Two-well radially convergent tests were successfully conducted in addition to the recirculating tests at the UIGRS. The purpose of these tests was to gain another perspective on the aquifer. Experiments II-2 and II-4 involved using well Q17D as the pumping well and well Q16D as the tracer injection well. These wells were chosen because they are the two closest wells completed within the E-fracture (distance: 20 ft). Well Q17D was utilized as the pumping well because it had a higher well yield than Q16D. Tests II-1 and II-3 were unsuccessful.

Water was pumped from well Q17D and discharged near the creek. A 3.5-inch submersible pump with a one-inch ID steel riser pipe was used in the pumping well. A dole valve was placed within the discharge pipe to maintain a constant flow rate. An inline flow meter was used to measure the discharge rate. A t-connector was placed beyond the flow meter. The stem of the "t" was reduced to a 1/2-inch opening for the tubing which supplied the samples. Well Q17D was pumped at a rate of three gpm. This rate was chosen because a three-gpm dole valve was available and the well produces a maximum of seven to ten gpm. Water levels were measured in wells Q17D and Q16D using both electric sounders and pressure transducers with data loggers.

A problem arose during the experiment requiring a change in the pumping-injection rate. Approximately 90 minutes after the first tracer was injected, it was observed that the injection well was overflowing. The pumping-injection rate was subsequently reduced to 3.1 gpm nine minutes later. Thirteen minutes later the rate was increased to 4.9 gpm because the transducer was not providing readings in the recirculation well. The rate was reduced to 4.2 gpm another 13 minutes later. The rate gradually decreased through the remainder of the test because there wasn't constant rate dole valve. The average discharge rate was 4.7 gpm. Possible explanations of the overflow include leakage past a faulty packer, through the well seals or through a crack in the casing. A borehole television survey of well Q17D following the experiment showed no breaks in the casing.

DESCRIPTION OF CONVERGENT TESTS

Two-well radially convergent tests were successfully conducted in addition to the recirculating tests at the UIGRS. The purpose of these tests was to gain another perspective on the aquifer. Experiments II-2 and II-4 involved using well Q17D as the pumping well and well Q16D as the tracer injection well. These wells were chosen because they are the two closest wells completed within the E-fracture (distance: 20 ft). Well Q17D was utilized as the pumping well because it had a higher well yield than Q16D. Tests II-1 and II-3 were unsuccessful.

Water was pumped from well Q17D and discharged near the creek. A 3.5-inch submersible pump with a one-inch ID steel riser pipe was used in the pumping well. A dole valve was placed within the discharge pipe to maintain a constant flow rate. An inline flow meter was used to measure the discharge rate. A t-connector was placed beyond the flow meter. The stem of the "t" was reduced to a 1/2-inch opening for the tubing which supplied the samples. Well Q17D was pumped at a rate of three gpm. This rate was chosen because a three-gpm dole valve was available and the well produces a maximum of seven to ten gpm. Water levels were measured in wells Q17D and Q16D using both electric sounders and pressure transducers with data loggers.

Test II-2

Test II-2 was conducted to gain more information about the hydrogeology of the site and to test the injection and sampling schemes to be used in Test II-4. Figure 11 is a cross section of the tracer test setup.

The bottom of the packer (Packer Design 1, described in the Field Instrumentation section of this chapter) was placed at the top of the well screen in well Q16D to prevent the tracer from migrating up the well column. The injection line was placed below the packer in the center of the well screen.

Fluorescein was used as the tracer in Test II-2. Fluorescein (268 g) was mixed with sodium hydroxide (NaOH) and deionized water to form a one liter solution. The tracer was injected using a peristaltic pump followed by about 53 liters of water from the pumping well to flush the tracer into the formation. Unlike experiment I-3 the tracer was not recirculated within the well and a sample was not collected in Q16D following the injection. These practices evolved following Test II-2.

Water pumped from well Q17D was discharged toward Paradise Creek with some of the water directed to a fraction collector through a tubing distribution. A t-connector in the discharge pipe was attached to three feet of 1/2-inch ID tubing. At the end of this a reducer was attached to a Y-connector which split into two lines of 1/8-inch ID tubing. One line was used to deliver the water that chased the tracer in well Q16D. The other line was used to deliver the sample to the fraction collector. This line was ultimately reduced to 1/32-inch size tubing to supply the samples to the fraction collector. The smallest ID tubing with the shortest possible length was important in the sample delivery to minimize the amount of sample "sitting" in the tubing. Valves were placed in the lines to regulate flow.

Test II-4

In Test II-4 multiple tracers were used based on the information gained from previous experiments, particularly, II-2. Figure 12 is a cross section of the test setup.

The injection well setup was similar to that of Test I-3. A packer (Packer Design 2, described in the Field Instrumentation section of this chapter) was placed above the screened

B   B'

Depth

— 0

— 10

— 20

— 30

— 40

— 50

— 60

— 70

— 80ft

Discharge is toward
Paradise Creek

Map   N

B Q17D
        T16D
    Q16D   B'
                  V16D

Scale
40ft   0   40ft

E-fracture aquifer

Q17D   Q16D   T16D   V16D

LEGEND

Pump

Water pipe

Discharge valve

Dole valve

Flow meter

Well screen

Packer Design 1

Pressure
transducer

Tracer inj. line

Sample line

Air line

Data logger

Peristaltic pump

Fraction
collector
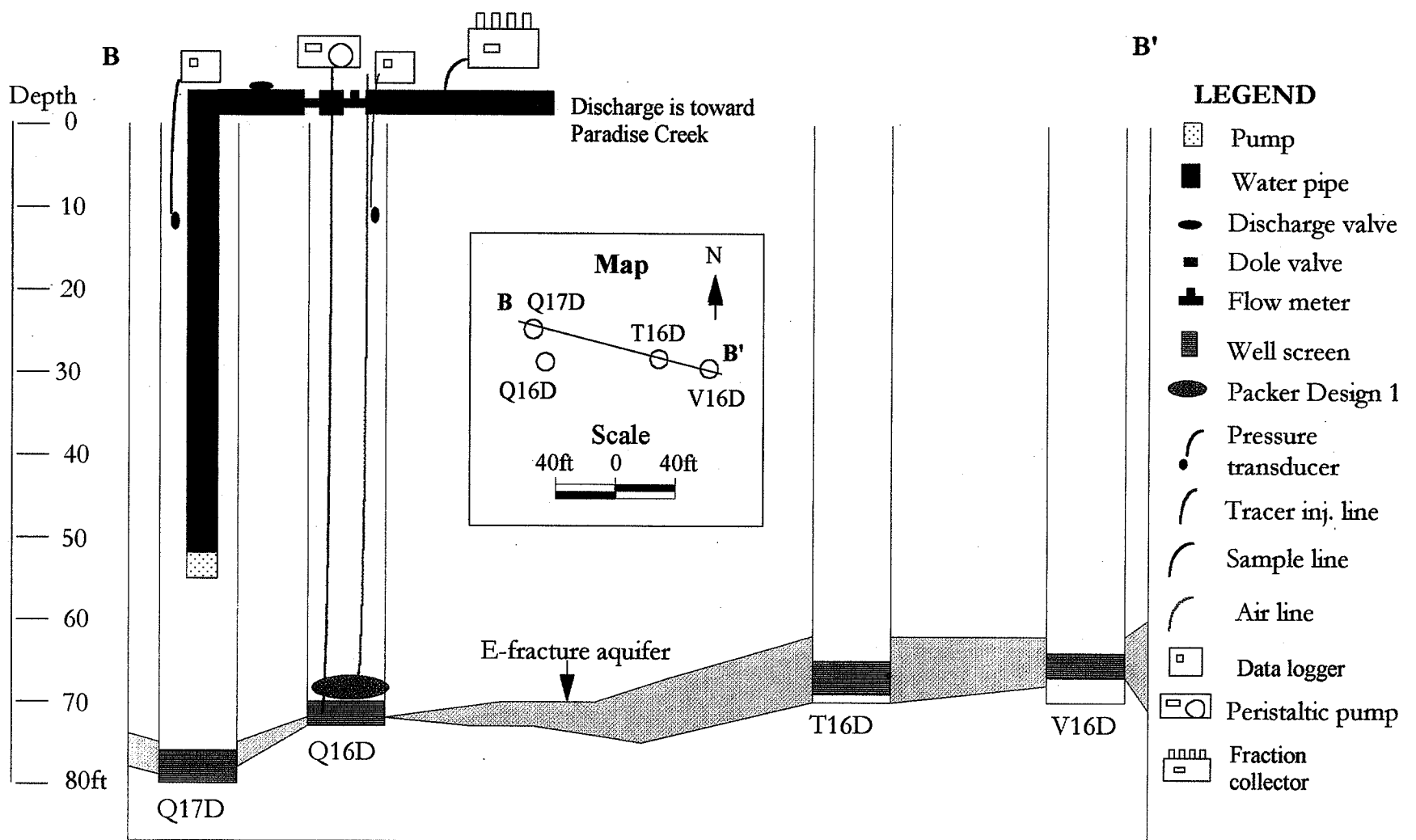
Well diameters and equipment are not to scale.

Figure 11. Cross Section of the E-Fracture During Test II-2.
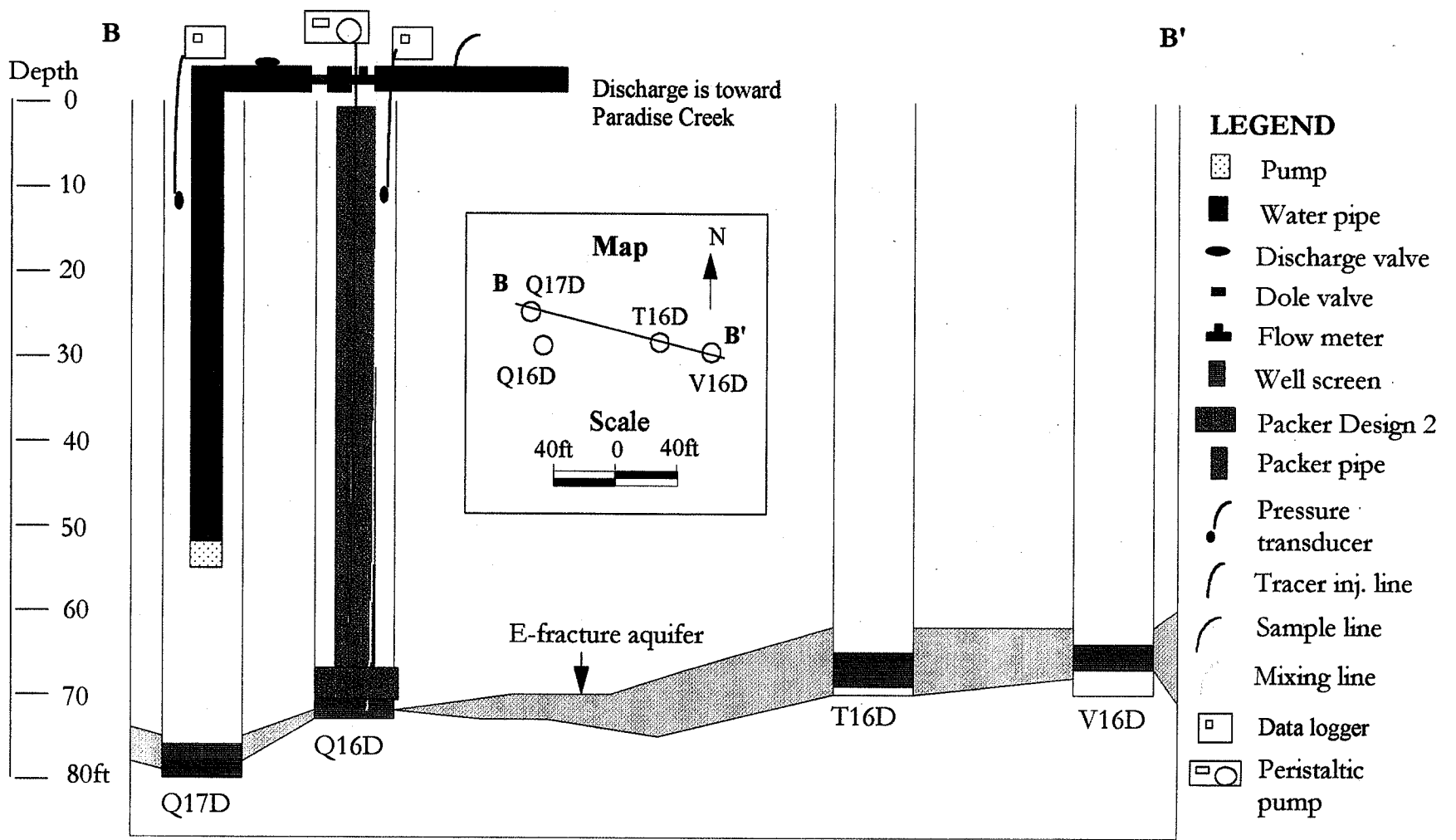
Figure 12. Cross Section of the E-Fracture During Test II-4.

LEGEND

- Pump
- Water pipe
- Discharge valve
- Dole valve
- Flow meter
- Well screen
- Packer Design 2
- Packer pipe
- Pressure transducer
- Tracer inj. line
- Sample line
- Mixing line
- Data logger
- Peristaltic pump

Discharge is toward Paradise Creek

Map

N

B   Q17D
         T16D
    O   B'
Q16D   V16D

Scale
40ft   0   40ft

E-fracture aquifer

Well diameters and equipment are not to scale.

interval in well Q16D. Two tubes passed through the packer. The tracer injection line was placed at the top of the well screen; the mixing line was placed near the bottom of the well.

A number of tracers were employed in Test II-4. These were bromide, fluorescein, veratryl alcohol (VA), benzoic acid (BA), *Bacillus thermoruber* spores (0.5-3 μm) and PC red Polystyrene microbeads (6 μm). The dissolved tracers were injected first followed by the spores and the beads for reasons explained in Test I-3. Bromide was injected first and last for reasons explained later in this chapter.

Bromide was injected the day prior to the actual test, March 26, 1997. This was to be the start of Test II-4 but problems caused the test to be aborted. Two-hundred grams of potassium bromide (KBr) were mixed with deionized water forming a one liter bromide solution. The tracer was injected using a peristaltic pump (see Figure 10). The tracer mixing line was then connected to the pump to mix the tracer within the well. The water within the well was circulated for one minute after which a sample was collected. The packer was also used as a plunger (see the Field Instrumentation section of this chapter for a description). The plunger was then pushed down which took approximately 1.5 minutes. The samples from the pumping well were collected in 15-mL test tubes by hand for approximately three hours. Bromide analysis began on the samples approximately one hour after the injection and no increase in concentration was detected. It was concluded that the plunger was not working properly and should be used only as a packer for the remainder of the tracer injections. The plunger may have pushed the tracer into the bentonite clay which filled the bottom few feet of the well. It was decided to postpone Test II-4 until the following day. The evening of the failed test, well Q16D was pumped for approximately 3.5 hours to remove as much of the bromide as possible because a high concentration may be toxic to the spores which were to be used the following day.

Test II-4 began on March 27, 1997, the day after the bromide test failure, with the tracer injections similar to that in Test I-3. Fluorescein, a cocktail of veratryl alcohol (VA) and benzoic acid (BA), spores and microbeads were injected by a peristaltic pump on March 27th. The fluorescein tracer was mixed within the well screen for four minutes. The BA-VA cocktail was mixed within the well for five minutes. After the spores were injected, mixing within the well continued for 30 minutes after the beads were injected. The long mixing

period of the spores and microbeads was to keep them in suspension. A sample was collected after each tracer was mixed for a few minutes. This was followed by a water flush for one minute to clear each line.

Another dissolved, conservative tracer was desired for this test and thus, bromide was again used. The second bromide injection occurred on March 28, 1997, approximately 1530 minutes after the fluorescein injection. A near super saturation concentration was injected (603 g of KBr in a one liter solution) because bromide was previously injected a higher background was assumed. The solution was heated to dissolve the salt and was slightly warm when injected. Contact with the colder ground water in the well caused the bromide to precipitate in the lines during the circulation of the tracer. Some of the bromide migrated into the formation while some remained in the lines until it was forced out approximately 96 minutes later by a large force of air from an air compressor. The injection of air caused a large surge of water to pour from the injection well.

Five-hundred milliliter *Pyrex* glass jars and 15-mL glass test tubes were used for sample collection in Test II-4. The containers were pre-labeled and recorded as to the date and time of sample collection. Periodically, the boxes of samples and test tubes were brought to a 5°C cold room for storage. The 500-mL glass jars were necessary because a large amount of sample was needed for the analysis of the five tracers injected on day one of the experiment. The 15-mL test tubes were used for the bromide samples because the greater sampling frequency. Plastic bottles were originally going to be used but perfluorocarbons, a candidate at the time of purchase, sorbs to plastic.

Samples were collected from well Q17D at varied intervals. The first sampling schedule for the 500 mL sample bottles consisted of collecting samples at five minute intervals. Sample collection then went to two minute intervals after about 250 minutes, back to five minute intervals after about 370 minutes and ended at 20 minute intervals after about 740 minutes (t=0 at the fluorescein injection). The particle tracers were anticipated to arrive very rapidly which is why the sampling frequency was increased to two minutes. Bromide samples were collected in five minute intervals.

TRACER TEST MECHANICS

Field Instrumentation

Several field instruments were used throughout the tracer experiments including pumps, water level measurement devices and sampling equipment (see Table 9). Four packers were also used in the experiments; three were designed and created for the tracer experiments at the UIGRS and the fourth was a commercially available packer.

A *Berkeley* 1.5 HP 3.5-inch submersible pump was used in the main pumping well in all the experiments. It was connected to 1.25-inch ID steel riser pipes. This pump had a maximum discharge of 38 gpm which was controlled by a valve at the top of the well casing. A power winch raised and lowered the pump that was set between 50 and 60 feet below the top of the casing. Discharge was held constant by a three gpm dole valve in all the tests except I-3. A 30-gpm *Pacific Water Works* flow meter monitored the flow.

Several *Masterflex* peristaltic pumps were used for injection and sampling purposes. In Tests II-2, II-4 and I-3 they were used to inject the tracers. They were also used in Test I-3 to collect samples. The pumps were located above ground and were connected to 1/8-inch ID tubing with an outlet in the screened interval of the well.

Two *EnviroTech* 12 volt pumps were also employed as sampling devices in Tests I-1, I-2 and I-3. Each pump was submersed about 10 feet below the water level in the wells. One-half inch ID intake and outflow tubing was attached to the pump. The intake line was located within the screened interval. The pumps had a maximum discharge rate of three gpm.

Water levels were measured by two methods. 1) By hand using a *Solnist* electric sounder (e-tape) and 2) *Druck* 830 series 0-20 psi pressure transducers connected to *Campbell Scientific* 21X data loggers which recorded the data.

In Tests I-1, I-2 and II-2, vinyl balls were used to fabricate packers (Packer Design 1). Netting was placed around the balls with attached wire and inflation tubing. The packer was placed above the perforations in the injection or sampling wells and inflated prior to the test. The injection or sampling line was sandwiched between the packer and the wall of the well.

In Test II-4 a packer/plunger was fabricated (Packer Design 2). The packer/plunger consisted of a 3.5 foot long two-inch ID PVC pipe with rubber baffles located at the top and bottom of the pipe. The baffles were designed to create a seal within the well. The packer

was attached to 1.5-inch ID PVC pipe leading to the surface. Two 1/4-inch ID tubes passed through the center packer by way of the pipe connection. One was the tracer injection line, the other was the mixing line. Packer Design 2 was initially used to block off the screened interval during the tracer injection; the unit was then used to push the tracer out of the well and into the formation. Problems with using this packer as a plunger forced it to be used only as a packer in the remaining experiments.

In Test I-3, Packer Design 3 was fabricated using two feet of two-inch ID PVC pipe and a motorcycle tire inner-tube. The packers were made by placing a two-inch piece of PVC pipe two feet long inside a motorcycle tire inner-tube. The tube was placed and clamped on the pipe. The inflation line plus the sampling line were routed inside the two-inch PVC pipe.

An *Aardvark* model 34B commercial packer also was used in Test I-3. It was approximately three feet long and three inches in diameter when deflated. One-inch ID pipe was connected to the packer which was raised and lowered using a winch. The inflation line was located on the outside of the packer. Inside were the injection line and the mixing line.

Samples were automatically collected using fraction collectors for Tests I-1, I-2 and II-4. The *Fractomette Alpha* 200 and the *ISCO Golden Retriever* model 328 were used. Each held approximately 100 15-mL test tubes and could be programmed to move on three-second multiple intervals.

Selection of Tracers

Conservative or semi-conservative tracers as well as biological and particle tracers were desired for the tracer experiments at the UIGRS because they were to be used in tracer experiments at the INEEL. Several different tracers were needed for these experiments because multiple tests were to be run in paired wells. Conservative tracers were used to determine parameters such as velocity and dispersivity and to compare the particulate tracers with. Biological tracers and particulate tracers were used to study how microorganisms are transported in the subsurface.

There were several criteria for selecting the tracers used in the experiments. These included the ease of use, ease of tracer solution preparation, cost of the tracer, detection limit, ease and cost of the analysis and information from previous studies. Fluorescein, bromide,

iodide, veratryl alcohol, benzoic acid, *Bacillus thermoruber* spores and Polystyrene fluorescent microbeads (6 micron) were chosen as the tracers for the experiments at the UIGRS. Table 10 lists information about fluorescein and other organic tracers used in the experiments, and Table 11 lists information about the ionic and particulate tracers

	INSTRUMENTATION INFORMATION			
Type of Pump:	3.5" 1.5-HP Submersible Pump	Peristaltic Pump	12V Pump	
Brand:	Berkeley	Masterflex of Cole Parmer	Envirotech	
Model:		7523-20	ES140	
Purpose:	well pump	sampling and tracer injection	sampling	
Riser Pipe/Tubing diameter for pump	steel pipe 1¼ inch	tubing sampling - 1/4 inch tracer inj. - 1/8 inch	tubing 1/2 inch	
Water Level Measurement Devices:	electric sounder	data logger	pressure transducer	
Brand:	Solnist	Campbell Scienticific	Druck	
Model:		21X	830 series (0-20 psi)	
Discharge Measurement Devise:	flow meter			
Brand:	Pacific Water Works			
Model:				
Constant Flow Devise:	3 gpm dole valve			
Packers	Packer Design 1 (round)	Packer Design 2 (plunger)	Packer Design 3 (cylinder)	Aardvark
Model:	fabricated	fabricated	fabricated	34B
Inflation Gas:	air	NA	air	nitrogen
Sampling Equipment (fraction collector) Brand:	Fractomette Alpha	ISCO Golden Retriever		
Model:	200	328		

Table 9. Information About Instrumentation Used in Experiments Conducted at the UIGRS.

used in the experiments. Other tracers were also candidates but ultimately were not chosen.

Fluorescein, a fluorescent dye, was chosen as a tracer for many reasons. Fluorescein is considered to be a fairly conservative tracer (see discussion in Chapter 2). The dye does not occur naturally in the ground water at the UIGRS and could be used as a qualitative tracer numerous times as long as the residual concentrations remained at a low level. It is easily detectable in the field; for example, a yellowish tint can be seen with the unaided eye above 0.1 mg/L. Another reason fluorescein was desirable was the ease of creating the tracer

	FLUORESCEIN	VERATRYL ALCOHOL	BENZOIC ACID
Chemical Composition Used in Experiments:		3,4-dimethoxybenzlalcohol or $(CH_3O)_2C_6H_3CH_2OH$	$C_6H_5CO_2H$
Purchased From:	Aldrich Chemicals in Milwaukee, WI	Sigma in St. Louis, MO	Aldrich Chemicals in Milwaukee, WI
Cost:	500 g for $36.65	100 mL for $57.85	500 g for $27.60
Form:	solid - powder	liquid	solid - crystals
Instrument for Analysis:	FL500 Fluorometer and F4500 *Hitachi* Fluorescence Spectrophotometer 2504060-04	gas chromatograph and HPLC	gas chromatograph
Detection Limit:	fluorometer: 0.2 ppb fluorescence spectrometer: 5 ppb	~1.0 mg/L	~1.0 mg/L

Table 10. Information About Organic and Dye Tracers Used in Experiments Conducted at the UIGRS.

	BROMIDE	IODIDE	*BACILLUS THERMORUBER* SPORES	MICROBEADS (YELLOW-GREEN)	MICROBEADS (PC RED)
Chemical Composition Used in Experiments:	KBr	KI	NA		
Purchased From:	*Aldrich* Chemicals in Milwaukee, WI	*Aldrich* Chemicals in Milwaukee, WI		*Polysciences* in Warrington, PA	*Polysciences* in Warrington, PA
Cost:	500 g for $32.05			$111.30 for 2 mL	$132.70 for 2 mL
Form:	solid - crystals	solid - crystals	solid	solid spheres	solid spheres
Instrument for Analysis:	HPLC and *Corning* ion selective electrode	*Orion* ion selective electrode	plate counts	Electron microscope	Electron microscope
Detection Limit:	HPLC: 4 mg/L ISE: 2.0 mg/L	ISE: 0.5 mg/L			

Table 11. Information About Ionic and Particulate Tracers Used in Experiments Conducted at the UIGRS.

solution. Sodium hydroxide (NaOH) is added to the fluorescein and water mixture to dissolve the solid fluorescein. Finally, fluorescein is inexpensive and the analysis instruments were readily available on the UI campus.

Bromide and iodide were chosen as ionic tracers for several reasons. They are conservative tracers and both had low background concentrations at the site. Bromide is the most common tracer and thus much is known about its behavior. It is easily prepared into a solution, is biologically stable and generally does not sorb (Davis et al., 1985). Iodide also is easily prepared but has been shown to be biologically unstable and may sorb more than bromide. Both are inexpensive and fairly easy to analyze.

Veratryl alcohol (VA) and benzoic acid (BA) were chosen as organic tracers because of their desirable qualities. They are fairly soluble, should not sorb and are inexpensive. However, veratryl alcohol oxidizes to veratraldehyde within hours and is biodegradable under normal conditions (non-acidic conditions). Benzoic acid also biodegrades rapidly. Analysis can be costly, time consuming and require solvents in the analyses using a gas chromatograph. Benzoic acid is not pergeable. However, veratryl alcohol is easily analyzed by the HPLC (*Hewlett-Packard* Liquid Chromatograph).

Spores of *Bacillus thermoruber*, a red-pigmented Thermophilic bacterium, were chosen as the biological tracer for several reasons. This spore is easily identified as dark red/brown colonies. They do not sporelate at the temperature of the ground water at the UIGRS; in order for their rejuvenation they need to be heat shocked at 80°C for ten minutes. Spores are easily grown in a laboratory and fairly simple to analyze; however, filtration is necessary when their numbers are small, and this process is very time consuming.

Fluoresbrite™ Plain Microspheres (fluorescent labeled polystyrene 2.5% solids latex microbeads (6 μm)) were chosen as the particle tracer. They are relatively new and previous studies have shown them to be successful ground water tracers. They are easily identifiable under an electron microscope by their spherical shape and bright fluorescent color. The six micron diameter size was selected to compliment the spores (about three micron) in the particle transport experiments. Yellow-green beads and PC red beads were used in different tests. A disadvantage of the microbeads is their high cost. Also, their analysis is time consuming.

Chloride and perfluorocarbons were tracer candidates but were not chosen for the experiments at the UIGRS for many reasons. Chloride has similar qualities to bromide but was not chosen due to the high background concentration of about 24 mg/L. Perfluorocarbons have been used as tracers in experiments in the literature but their analysis produces undesirable byproducts.

Method of Analysis

The following section is a discussion of the methods of analysis for the tracers used in the field experiments. Tables 10 and 11 summarize the tracers used with their analysis instruments and detection limits.

Fluorescein samples from Tests I-1, I-2, II-2 and II-4 were analyzed using a FL500 Fluorometer in a laboratory on campus. An excitation of 485 and an emission of 530 was used for the fluorescein analysis. Two-tenths of a milliliter of sample was placed in one of 96 slots in a plastic *Corning* cartridge. Each sample was analyzed in triplicate and at least two known standards were placed in each cartridge. The fluorometer provided light readings for each sample which were then calculated into concentrations by the standard curve.

Fluorescein samples from Test I-3 were analyzed by the F4500 *Hitachi* Fluorescence Spectrophotometer 2504060-04. A standard curve was constructed prior to any sample analysis at the start of the day. Each sample was buffered to increase the pH to slightly above neutral. The samples were acidic (pH of 2) because 4 mL of 6N HCL was added to each of the 500 mL sample jars to preserve the veratryl alcohol. Two milliliters of sample were placed in a plastic cuvette and placed in the machine to be analyzed. Fluorescence readings were provided for each sample and concentrations were calculated from the standard curve.

The bromide analysis was conducted initially by a *Cole Parmer* ion selective electrode (ISE). Four milliliters of sample were placed in a small plastic cup on a stir plate with a flea (small stir bar) to maintain a homogeneous sample. Two-hundredths of a milliliter of 5M $NaNO_3$ was added for a quicker reading stabilization. The electrode was placed in the cup and after three minutes a reading was taken. Standard curves were created prior to the sample analysis and frequently during the bromide analysis because probe drifting occurred.

Problems with drifting of the bromide probe caused the data generated by the ISE to be questioned; therefore, a different method was employed. The HPLC (*Hewlett Packard Liquid Chromatograph*) was chosen for the analysis because it has a high degree of accuracy was readily available. This machine required one mM phthalate buffer with a pH of 6 and nanopure water. One milliliter of sample was filtered and placed in a small glass HPLC container. One-hundred samples could be loaded into the machine and allowed to run. Again, a number of standards were analyzed at the beginning of a large sample run to generate the standard curve. Concentrations were calculated based on the standard curve.

Iodide analysis was conducted using an *Orion* combination iodide selective electrode. The procedure was similar to the bromide analysis by the ISE except 5 mL of sample were used and a reading was taken after one minute.

Veratryl alcohol and benzoic acid were analyzed in Test II-4 by a gas chromatograph (GC) by purge and trap using an extraction method. In Test I-3 the veratryl alcohol was analyzed using an HPLC in a similar fashion to the bromide analysis.

The spores were analyzed by plate counts in a laboratory. For Test II-4, 5 mL of each sample were removed from the shaken sample jar and placed in a test tube. The samples were then heat shocked at approximately 80°C for 10 minutes in a water bath. Under a laboratory hood the 5 mL of sample were vortexed and 100 μL plated on prepared GYE media in pre-labeled petri dishes. The petri dishes were then placed in a 45°C incubator for up to five days. The deep red colonies were then counted; 30 to 300 colonies are necessary to be statistically accurate. In Test I-3, this same method was used but did not produce results. Instead of heat shocking 5 mL of sample, approximately 400 mL of sample was heat shocked and filtered through sterile *MicronSep* mixed esters of cellulose filters with a pore size of 0.22 μm. This was to increase the spore population. Vigorous mixing of the samples was done prior to filtration. The filters were then placed on the GYE media and allowed to incubate as previously described. Sterile water was used to rinse the sides of the filtration column after each sample to wash down any spores remaining on the sides of the filter column. Ethanol was used to clean the column.

The microbeads were filtered and the microbeads on the entire filter were counted under a microscope with a magnification of 10x. In Test II-4, 15 mL of each sample was

filtered through a *Poretics Products* membrane filter with a pore size of 0.22 µm. De-ionized water was used to rinse the sides of the filter column to flush any beads sticking to the sides of the glass. After the water wash, the column was cleaned using ethanol. Each filter was placed on a microscope slide with a cover slip over the filter. The cover slip was sealed to the slide with clear nail polish to preserve the sample for future analysis. In Test I-3, 100 mL of each sample were filtered in order to obtain results. The first 20 samples for well V16D were filtered using a 0.22 µm pore size filter but the remaining samples used a pore size filter of 0.45 µm to speed up the filtration process.

CHAPTER 5
METHODS OF ANALYSIS

INTRODUCTION

Tracer test results may be analyzed by using either analytical or numerical methods. Analytical methods are used to solve transport equations using a number of equations or spreadsheet applications which include the matching of field data to generated type curves. Numerical methods involve the use of computer models to represent solute transport in simple to complex hydrogeologic environments. The application of numerical models require numerous inputs including aquifer parameters and source transport parameters. Analytical methods often are utilized to estimate these input parameters. Thus analytical analysis often is the first step in an investigation followed by numerical modeling. Analytical models are applied in the analysis of the tracer tests conducted at the UIGRS. Construction of a numerical model was beyond the scope of this study.

This chapter describes the analytical methods used for analysis of the tracer test results. The tracer breakthrough curves are described in Chapter 6. Simple equations are used to solve for the average tracer velocity, average hydraulic gradient and the mass balance results. In Chapter 7 the tracer data are matched to generated type curves. Discussions of the findings are provided in Chapter 8.

BASIC ANALYTICAL METHODS

A qualitative description of the tracer test results is given based upon graphs of concentration versus time (minutes) and relative concentration (C/Co) versus time for each well. Concentration (C) is given in mg/L (ppm) for the dissolved tracers, and the number of particles per $\underline{x}$ number of mL for the particulate tracers. The initial concentration (Co) is the mass of the dissolved tracer injected divided by the volume of water in which it is mixed. The water volume includes that used to makeup the tracer solution plus the water within the screened or packed off interval of the test well. For the particulate tracers Co is the actual number of particulates injected.

The test data are entered into mathematical equations to estimate the average tracer velocity, average hydraulic gradient and the mass of the tracer recovered. The average tracer velocity is calculated by dividing the distance between the pumping and injection wells by the peak breakthrough time of the tracer. The average hydraulic gradient is calculated by dividing the difference in hydraulic head by the distance between the wells. The mass recovery of the tracers is calculated by multiplying the discharge rate by the time interval between two data points which is then multiplied by the concentration for each data point. The mass recovered per interval is then summed for all the intervals. Thus, the recovery is dependent upon the length of the experiment. In addition, some of the tracer is recycled during recirculating tests, providing an over estimation of the tracer recovery.

CURVE MATCHING METHODS

Curve matching techniques are applied to the tracer test data in Chapter 7. The purposes of these methods are to determine a Peclet number, dispersivity value and dispersion coefficient.

Two curve matching methodologies are applied to the tracer test data. The first method is from Sauty (1980). Sauty's equations are applicable to nonrecirculating tests and for the nonrecirculating well pairs in the recirculating tests. The Brenner solution of Brenner (1962), modified by Grove and Beetem (1971), is used to analyze data from the pumping-recharging well pair in a recirculation experiment. In both methods the field data are matched to generated type curves, each with a different Peclet number. Ideally, all the experimental data points fall on a type curve; however, the breakthrough curve tail often falls above the type curves because of hydrologic processes not considered in the methods. A Peclet number is determined from the best fit between the experimental data and a type curve. Dispersivity and dispersion can then be calculated using these equations (Sauty, 1980):

$$P = \frac{R}{\alpha}$$

and

$$P = \frac{vL}{D_L}$$

where P = Peclet number
  R = distance between wells [L]
  α = dispersivity [L]
  v = average linear velocity [L/t]
  L = characteristic flow length [L]
  D_L = mechanical dispersion coefficient [L²/t]

Effective porosity may also be determined by curve matching using the Brenner solution as discussed later in this section. Homogeneous and isotropic conditions are assumptions of both methods. Their application to tracer tests in a heterogeneous fractured rock system is evaluated later in the paper. No specific analytical methods for transport in fractured rock were found.

The type curves applied to data from a nonrecirculating well pair are generated from equations in Sauty (1980). These equations are for a slug (pulse) injection in a uniform one-dimensional flow field. However based on a comparison to numerical solutions, these equations are applicable for radial converging flow if the curve match generates a Peclet number greater than three (Sauty, 1980). An analytical solution was not found specifically for radial convergent flow. The equations used to generate the type curves from Sauty (1980) are:

$$C_R = \frac{K'}{t_R^{1.5}} \exp\left(-\frac{P}{4t_R}\left(1-t_R\right)^2\right)$$

where

$$K' = t_{R\max}^{1.5} \exp\left(\frac{P}{4t_{R\max}}\left(1-t_{R\max}\right)^2\right)$$

$$t_{R\max} = \left(1+9P^{-2}\right)^{0.5} - 3P^{-1}$$

$$t_R = \frac{vt}{R}$$

and t_R = dimensionless time
  t_{Rmax} = dimensionless time at maximum peak
  t = time [T]
  C_R = dimensionless concentration
  P = Peclet number
  R = distance between wells [L]
  v = effective velocity [L/T]

The type curves are generated by plotting dimensionless concentration (C_R) versus dimensionless time (t_R) on semi-log graph paper. Each type curve is generated for a different Peclet number. On another sheet of semi-log graph paper the experimental data are plotted as C/C_{max} versus dimensionless time where C is the tracer concentration and C_{max} is the maximum concentration detected in the monitoring well during the tracer test. The field data are plotted on semi-log paper with the same scale as the type curves. The field data BTCs (breakthrough curves) are placed over the type curves. The graphs are then shifted along the horizontal axis until a best-fit is found based on the shape of the curves. This procedure was conducted using a computer program, SigmaPlot of *Jandeel Corporation*.

The Brenner solution type curves are used to analyze data from a recharging-discharging well pair. The basis of the solution is that water travels along a number of streamlines between two wells creating a flow field. Each streamline is referred to as a crescent. A total of 70 crescents is arbitrarily incorporated into a flow field in the solutions for the experiments conducted at the UIGRS. Thus, there are 70 breakthrough curves, that when summed, form a composite breakthrough curve. The equations used to generate these curves are modified from Brenner (1962) by Grove and Beetem (1971) and are:

$$\frac{C}{Co} = 1 - \exp\left[P(2 - t')\right] \sum_{k=1}^{\infty} \frac{\lambda_k \sin(2\lambda_k)}{\left(\lambda_k^2 + P^2 + P\right)} \exp\left(-\lambda_k^2 t'/P\right)$$

$$L = \frac{2a\alpha}{\sin \alpha}$$

$$t = \frac{4\pi\theta a^2}{q \sin^2 \alpha}(\alpha \cot \alpha - 1)$$

$$t' = \frac{T}{t}$$

where: C/Co = relative concentration of tracer
L = arc length of a streamline [L]
a = half the distance between the wells [L]
q = pumping rate per aquifer thickness [L^3/t/L]
β' = streamline angle
$\alpha = \beta' + \pi$
θ = porosity

λ_k = number of flow lines
t = time for plug flow through the arc [T]
t' = dimensionless time
T = time since slug injection began [T]

Brenner (1962) provides tabulated solutions to the C/Co equation above for each dimensionless time step. The type curves are plotted as C/Co (sum of the 70 crescents) versus time. Again, each type curve has a different Peclet number. On the same graph, the experimental data are plotted as relative concentration (C/Co) versus time, where C is the tracer concentration and Co is the initial tracer concentration. By increasing the effective porosity, the type curves shift to the right and increase in peak intensity. However the effective porosity is based upon a chosen aquifer thickness which may not necessarily be known. The curve match is selected based on the similar timing of the peaks as well as matching the shape of the curves. In the following analyses the rise and peaks of the breakthrough curves are matched. This is because it is the early time transport data that are affected by dispersion (Grove and Beetem, 1971). Most breakthrough curve tails do not match the predicted type curves because of several hydrologic processes including well bore storage, rough fracture effects, desorption, increasing dispersivity with time (Gelhar et al., 1992) and matrix diffusion.

CHAPTER 6
ANALYTICAL ANALYSIS OF TRACER TEST RESULTS

INTRODUCTION

This chapter describes the results of the recirculation and nonrecirculation tracer tests by basic analytical methods. A qualitative description of the breakthrough curves is provided in addition to calculations of aquifer and tracer parameters. A map of the study site and a cross section of the E-fracture wells is shown in Figure 13.

RECIRCULATION TESTS

Test I-1

Results for well V16D are discussed for Test I-1. Samples were collected solely from this well because the pumps failed in wells Q16D and T16D prior to sample collection.

Well V16D data for Test I-1 are plotted as fluorescein concentration versus time and relative concentration versus time (Figures 14 and 15). A rapid increase in concentration begins at approximately t=120 minutes (t=0 at time of injection) which peaks at a concentration near 0.30 mg/L and a C/Co of 1.40×10^{-4} at t=205 minutes. Following the peak of the breakthrough curve there is a small fluctuation then a rapid decrease in concentration with the tail retreating to near detection limits. This fall in concentration was probably due to the end the recirculation portion of the test at t=294 minutes caused by an alteration of the flow line regime and significant gradient change. Fewer flow lines from the injection well converge at the pumping well resulting in less tracer delivered to well V16D. Decreasing the hydraulic gradient decreases the velocity as well. It is therefore difficult to make conclusions about the tail of the breakthrough curve after this time because the system was altered.

Parameters of the tracer test, aquifer and tracers calculated from the test results for well V16D in Test I-1 are presented in Table 12. The parameters include the average discharge, average hydraulic gradient, average tracer velocity and mass balance results. This table also includes the information necessary to solve the equations such as the distance between the wells. Only 3.71% (after 1419 minutes) of the fluorescein was recovered.
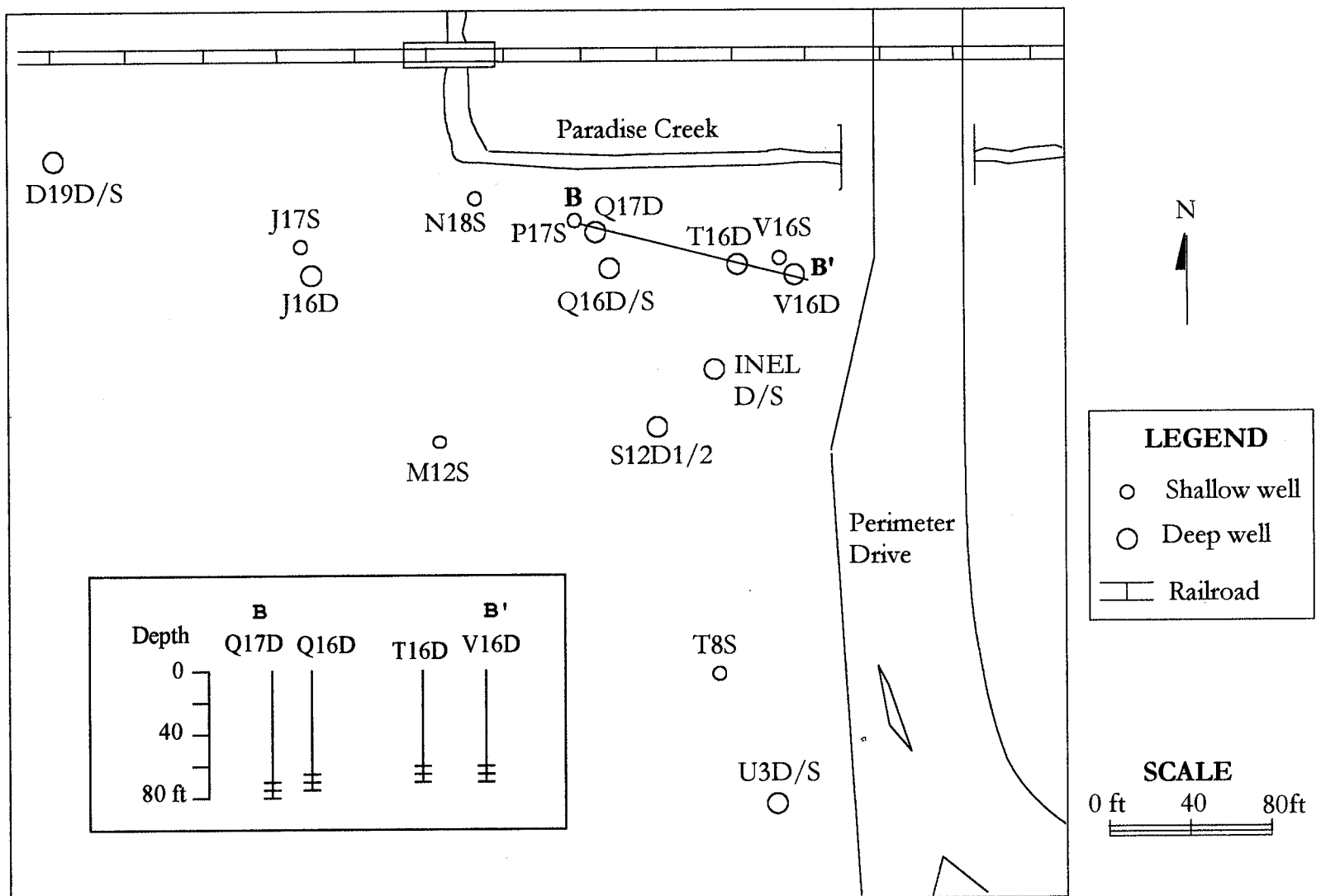
Figure 13. Map of the University of Idaho Groundwater Research Site (UIGRS) and Cross
Section of E-Fracture Wells from B-B'.
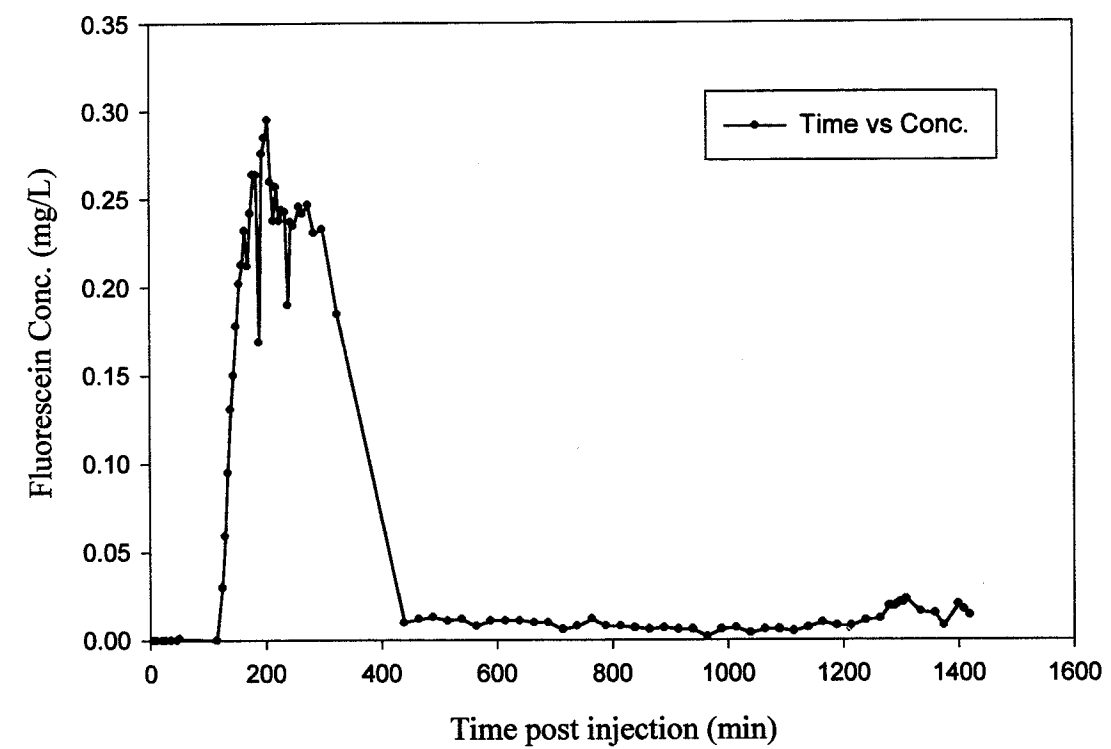
Figure 14. Fluorescein Concentration vs Time for Well V16D in Test I-1.
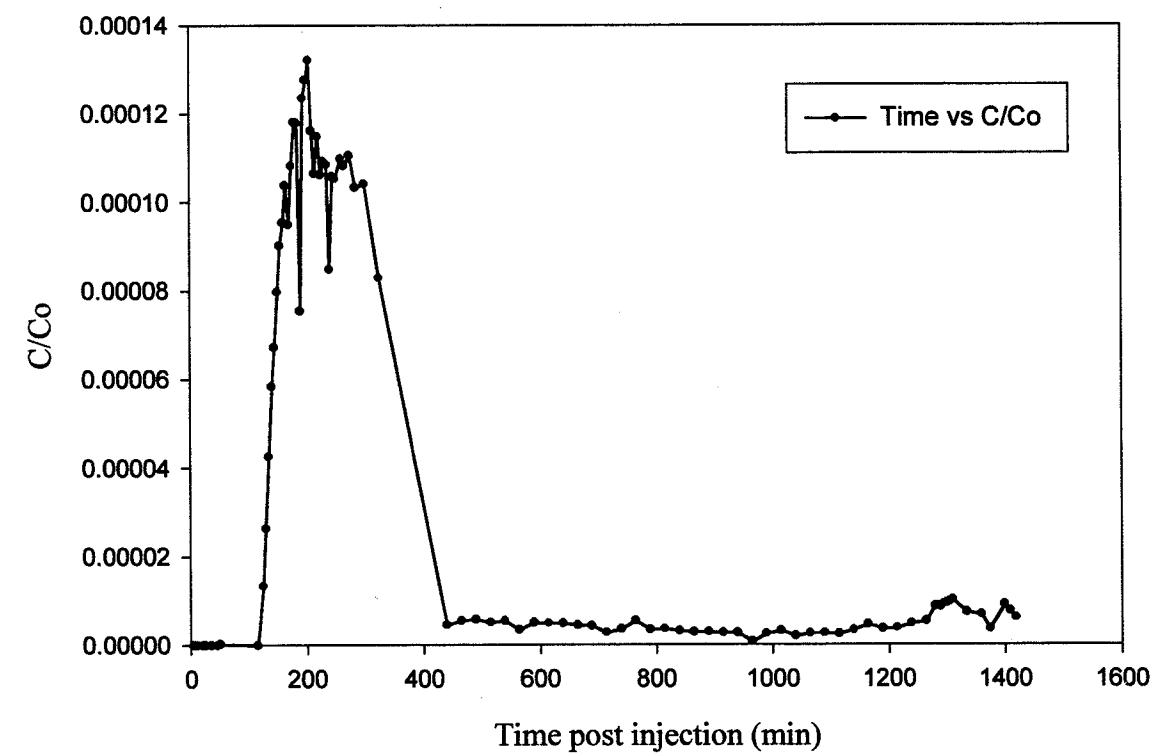
Figure 15. Relative Fluorescein Concentration vs Time for Well V16D in Test I-1.

	V16D
Distance from injection well (ft)	100
Ave. discharge (ft³/min)	0.40
Average hydraulic gradient (initial)	0.061
(after recirc. stopped)	0.003
Fluorescein Peak breakthrough time (min)	204
Ave. velocity (ft/min)	0.49
Tracer injected (g)	16.7
Tracer recovered (g)	0.62
Total percent recovered (after 1419 min.)	3.71

Table 12. Test, Tracer and Aquifer Parameters Calculated For Well V16D in Test I-1.

Test I-2

Results for wells V16D and Q16D are described for Test I-2. Samples were collected only from these wells because the pump in well T16D failed. Water levels were measured in well Q16D above the packer. There was a water level change after the pump was turned on indicating the packer leaked. High pressure transducers were not available to place below the packer.

The fluorescein data for Test I-2 are plotted as concentration versus time for well V16D (Figure 16). A rapid increase in concentration began approximately 85 minutes into the test. The data peaked at a concentration of 0.17 mg/L at t=125 minutes (t=0 at time of injection). The peak is very well defined with a fairly long tail that continues for nearly 400 minutes. At approximately t=468 minutes the concentration drops from 0.0280 to 0.0034 mg/L. The fall in concentration is likely due to a problem with the sample analysis. Recirculation ceased about 120 minutes after the tracer injection, which coincides with the timing of the peak breakthrough. The flow lines were altered and the hydraulic gradient changed as a result which affected the breakthrough curve tail.

Fluorescein data are plotted for well Q16D as concentration of versus time for Test I-2 (Figure 17). A rapid increase in concentration began at t=73 minutes. There are two peaks to this breakthrough curve. The first occurs at t=120 minutes and the second occurs at t=175 minutes. At t=120 minutes recirculation ceased which coincides with the timing of the first peak. The first peak had a slightly higher concentration, 19.3 mg/L, and is very sharp with a rapid rise and a rapid fall. The curve then has a rapid increase to the second peak at 18.3 mg/L. The second peak may be the result of altered flow lines capturing more of the tracer following the end of the recirculation portion of the experiment. The concentration decreases after the second peak to a level between 11 and 13 mg/L for the remainder of the test. There is a change in slope of the tail at approximately t=400 minutes which may be caused by the fracture network pattern. The concentration in Q16D is nearly 100 times higher than in well V16D because it is closer to the injection well. The peak may have occurred at a later time and at a higher concentration had recirculation continued. Therefore, as in well V16D, no major conclusions are made about the breakthrough curve tail.

The fluorescein data for wells V16D and Q16D are also plotted as relative concentration versus time (Figures 18 and 19). The C/Co peak for V16D is 7.67×10^{-5}. The C/Co peak for Q16D is 8.60×10^{-3}.

Parameters such as the average discharge, average hydraulic gradient, average tracer velocity and mass balance results for wells V16D and Q16D in Test I-2 are provided in Table 13 in addition to the information necessary to solve for them. Because the gradient changed between wells Q16D and V16D, two values are listed. The first number represents the first 120 minutes of the test while the second number represents the remainder of the test. The velocity between the injection well and V16D is much higher than between the injection well and Q16D which has twice the gradient.

The fluorescein recovery for this test is very different for wells Q16D and V16D. The total recovery for fluorescein from well V16D is 1.54% and for Q16D it is 187%. The calculated amount recovered after 500 minutes for well V16D is 1.53% and for well Q16D is 139%. The amount recovered from well Q16D is impossible, even if some of the fluorescein is residual from the previous test and some from recirculated tracer. Explanations for the high recovery in well Q16D include analysis error or more likely, quenching, because the samples
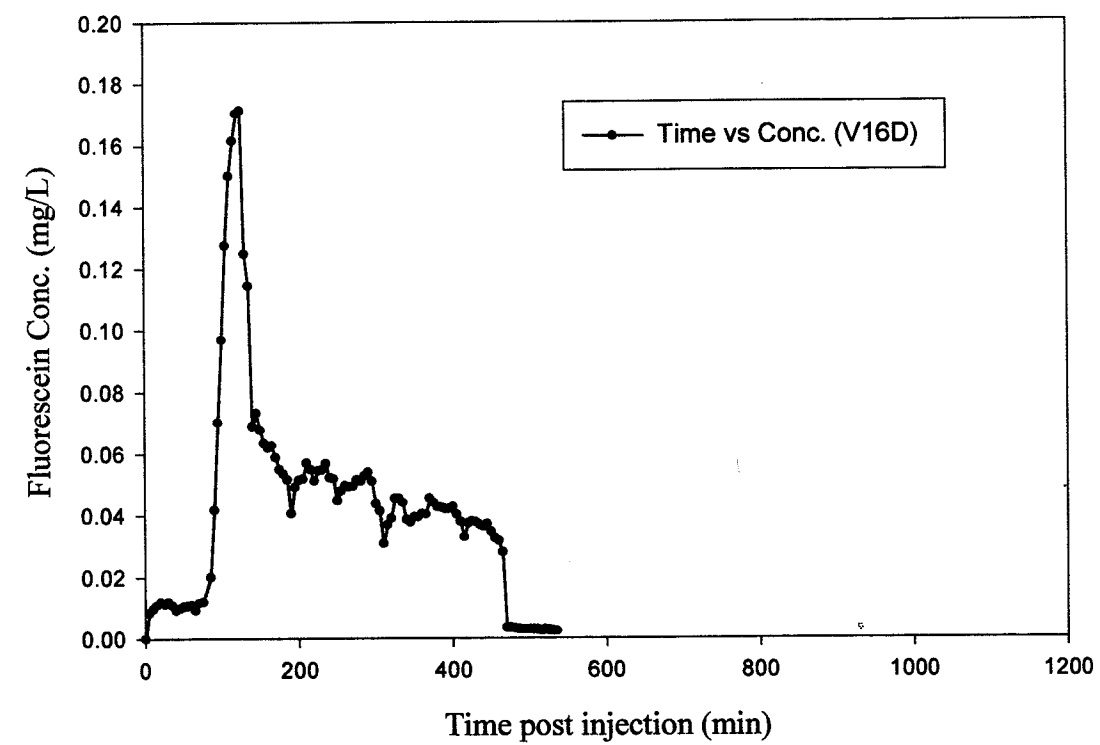
Figure 16. Fluorescein Concentration vs Time for Well V16D in Test I-2.
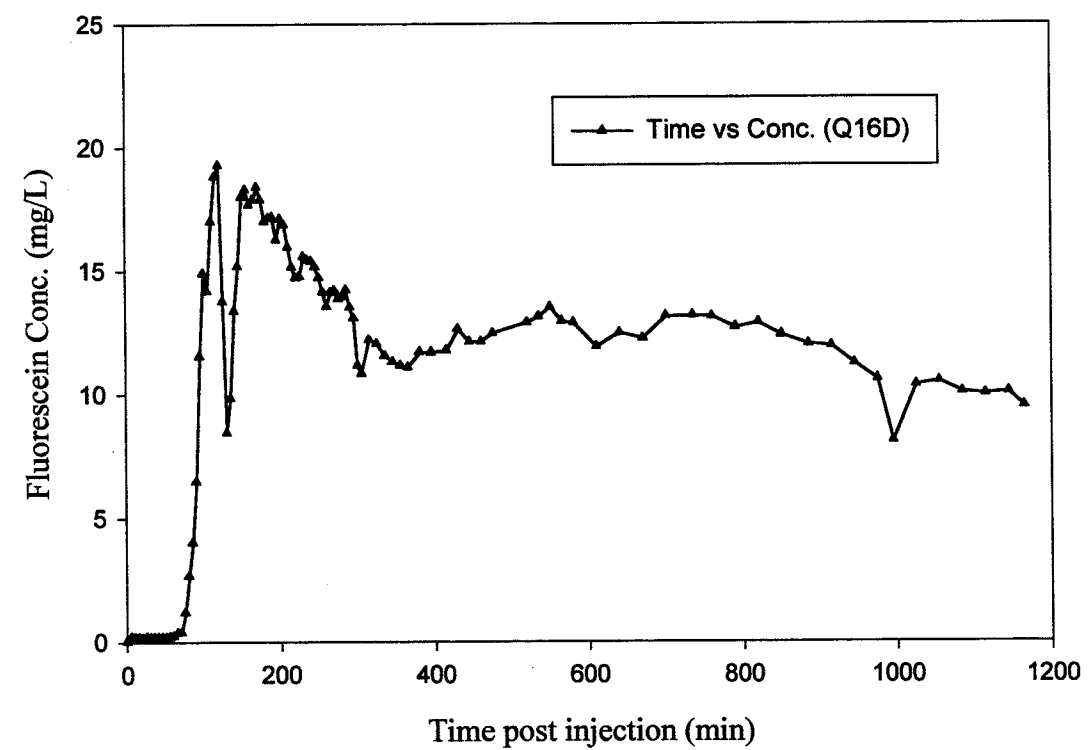
Figure 17. Fluorescein Concentration vs. Time for Well Q16D in Test I-2.
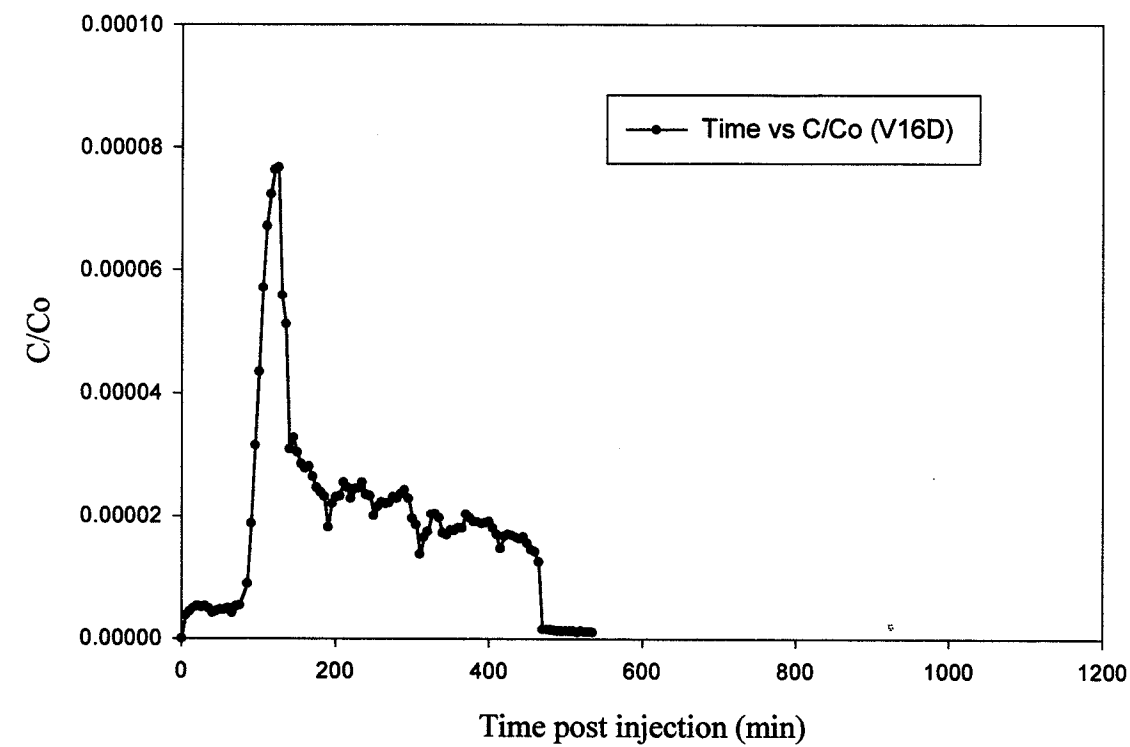
Figure 18. Relative Fluorescein Concentration vs. Time for Well V16D in Test I-2.
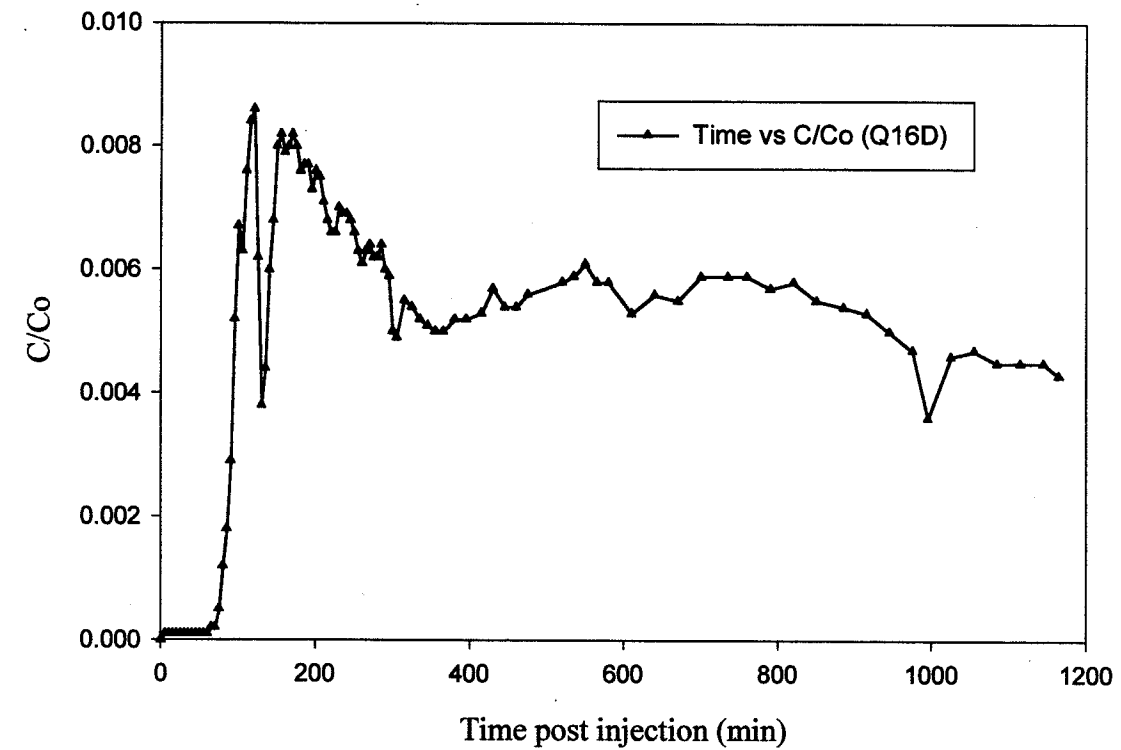
Figure 19. Relative Fluorescein Concentration vs. Time for Well Q16D in Test I-2.

have a high intensity of the fluorescein color. Quenching is described in Chapter 2 of this thesis. The shape of the breakthrough curve is accurate but the concentrations are probably incorrect if quenching is the problem. Therefore, the timing of the peak is believable but the magnitude is not. Well Q16D has very high concentrations of fluorescein, probably because it is located much closer to the tracer injection well and has a much higher gradient in the direction of the injection well than does well V16D.

	V16D	Q16D
Distance from injection well (ft)	100	20
Ave. discharge (ft^3/min)	0.40	0.20
Average hydraulic gradient (initial)	0.072	0.14/
(after recirc. stopped)	0.005	0.014
Fluorescein Peak breakthrough time (min)	125	120
Ave. velocity (ft/min)	0.80	0.17
Tracer injected (g)	16.7	16.7
Total tracer recovered (g)	0.26	31.35
Time for total tracer recovered (min)	535	1145
Total percent recovered	1.54	187
Percent recovered after 500 minutes	1.53	139

Table 13. Test, Tracer and Aquifer Parameters Calculated for Wells V16D and Q16D in Test I-2.

Test I-3

Samples were collected from wells V16D, T16D, Q16D and S12D2. Tracers were found in all the wells except S12D2; although, very few samples were collected because the drawdown caused by the collection of a sample was great enough that a period of about 0.5 hour or more was necessary to recharge the well. Well S12D2 is located 100 feet from the injection well and is completed in a fracture zone with a limited hydraulic connection to the E-fracture zone. For these reasons it is not surprising the tracers were not detected.

Breakthrough Curve Analysis

The tracer results for well V16D in Test I-3 are graphed as concentration and particulate counts versus time (Figure 20). The breakthrough curves shown are fluorescein, iodide, veratryl alcohol (VA) and microbeads. Spores were not detected in any of the samples.

The dissolved tracer breakthrough curves for well V16D resemble one another quite well, each having at least two main peaks, one clearly greater than the other. The curves have similar peaks and troughs. Table 14 lists the breakthrough curve peaks for each tracer and the corresponding times. The second peak is greater for fluorescein and veratryl alcohol (VA); both peaks occur at very similar times. The first peak is greater for iodide and occurs at nearly the same time as the first peak for the other two dissolved tracers. The second peak for iodide matches very closely with the second peak for fluorescein. All three tracer breakthrough curves have long tails with similar slopes. Because the breakthrough curves for fluorescein and VA follow a similar pattern with iodide, a conservative tracer, it is concluded they too act as conservative tracers. Fluorescein is the only tracer with a slight residual because it was used in previous experiments.

The microbead breakthrough curve for well V16D has two peaks greater than 1 bead /100 mL. The bead counts and times are listed in Table 14. The initial peak breakthrough occurs prior to the conservative tracers in well V16D. This is expected due to the preferential flow path theory and porosity exclusion effects. The initial peak at a count of 3 beads/100 mL occurred at t=44 minutes (t=0 at time of injection). The first peak for the conservative tracers arrived about 22 minutes later. The second bead peak of 22 beads/100 mL occurred at t=169 minutes. The discharge rate was decreased by approximately 0.5 gpm preceding the microbead injection, possibly giving rise to later than expected particle peak when compared to the dissolved tracer peaks.

There are several possibilities for the two microbead peaks. The second peak may be the result of recirculated beads, or more likely, it may also be the result of a longer pathway. Another hypothesis is a result of a "bead dam". During the bead analysis numerous fluorescing fragments were found in this sample which is uncharacteristic of most of the other samples. These fragments may be pieces of beads that were scraped off by the rough fracture
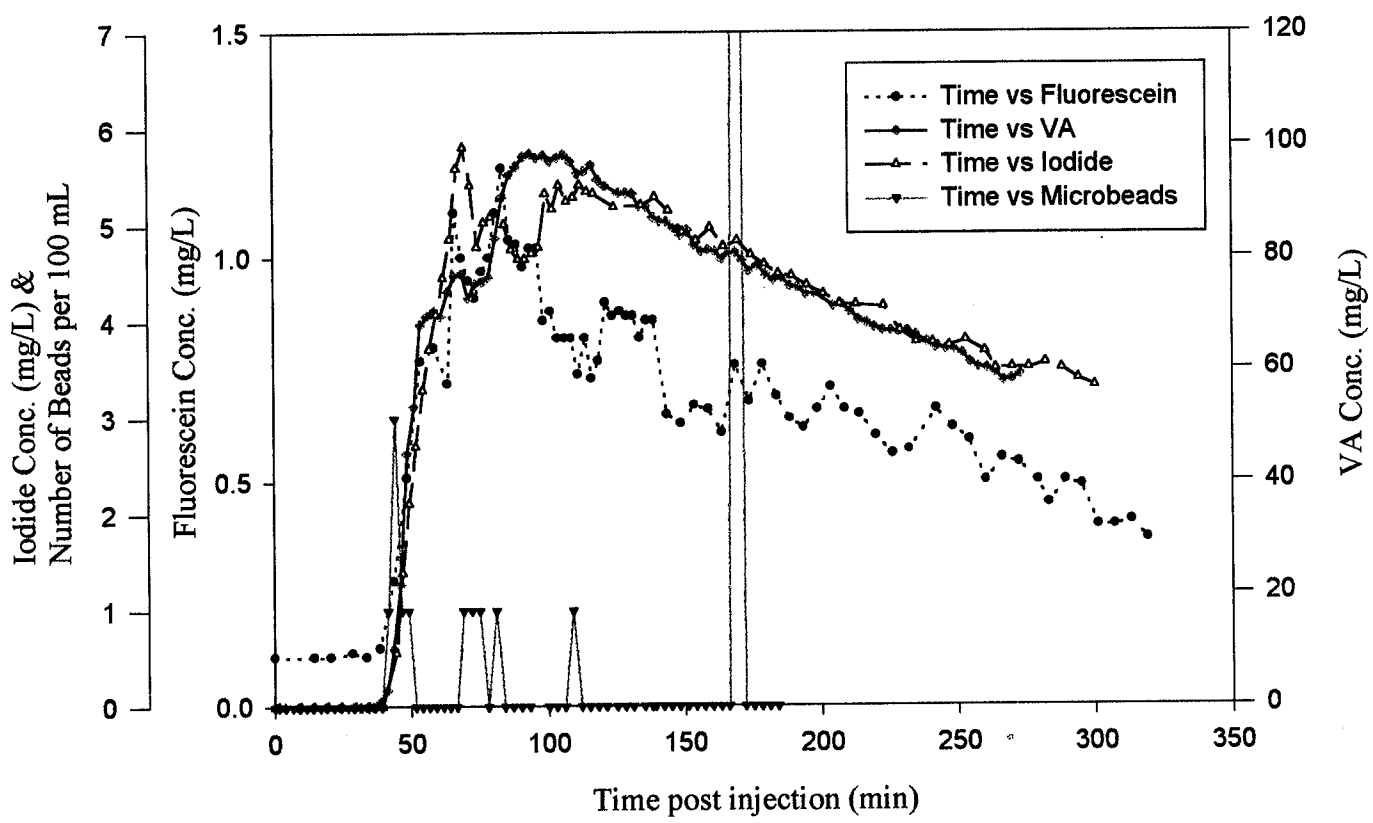
Figure 20. Concentration vs. Time for All Tracers in Well V16D in Test I-3.

	FLUORESCEIN			IODIDE			VA			MICROBEADS		
	Time (min)	Conc. (mg/L)	C/Co	Time (min)	Conc. (mg/L)	C/Co	Time (min)	Conc. (mg/L)	C/Co	Time (min)	# beads/ 100 mL	C/Co
Peak 1	65.9	1.10	1.90E-4	69.3	5.81	1.72E-4	68.5	77.15	1.54E-3	44.0	3	8.88E-10
Peak 2	83.4	1.20	2.09E-4	79.3	5.09	1.51E-4	93.67	98.52	1.97E-3	169	22	6.51E-9
Peak 3	NA	NA	NA	104.3/ 111.8	5.42	1.60E-4	NA	NA	NA	NA	NA	NA

Table 14. Timing and Concentration Values of Various Peaks for Tracers from Well V16D in Test I-3.

surface during a burst "bead dam". Filtration is the mechanism that creates these dams. The surge of beads from the broken dam would therefore not constitute the actual peak breakthrough.

The relative tracer concentrations and particulate counts are graphed versus time for well V16D in Test I-3 (Figure 21). There is little distinction between the graph of regular concentration data in Figure 20 except the axes of the tracers have changed. The residual concentration of fluorescein is subtracted from each sample and is represented by C-res (concentration minus residual) instead of C (concentration). The C/Co peaks and corresponding times for each tracer is listed in Table 14. The VA relative concentrations are one order of magnitude higher then those of fluorescein and iodide.

The results for well T16D are graphed as concentration and particulate counts versus time for Test I-3 (Figure 22). Again, breakthrough curves of fluorescein, iodide, veratryl alcohol (VA) and microbeads are depicted. No spores were detected. Similar to well V16D, the microbead breakthrough peak arrived at least 100 minutes prior to the dissolved tracers' peaks. A microbead peak count of 3 beads/100 mL of sample occurred after 34 minutes. The shape of the conservative tracer breakthrough curves are very similar to one another with the fluorescein and iodide curves more closely related in part by the way they are plotted. The initial rise of the breakthrough curves began with the microbeads, followed by VA, iodide and finally fluorescein. All three of the dissolved tracers have broad highs and therefore the timing of their peak concentrations are difficult to identify. The VA peak followed the bead's at t=178 minutes (t=0 at each tracer injection) with a concentration of 26.3 mg/L, next is iodide with 16.1 mg/L at t=192 minutes, and lastly, fluorescein with 1.98 mg/L at t=211 minutes. Had the test been conducted for a longer period of time it may have been easier to identify the peak and the tail. It is interesting to note higher concentrations of iodide and fluorescein are found in this well compared to V16D. Fluorescein is the only tracer with a slight residual.

The relative concentration data and particulate counts for well T16D are graphed versus time in Figure 23. This graph looks somewhat different from the concentration and particulate counts graph in Figure 22 because of changes in scales. The dissolved tracers are located on the left axis and the microbeads are on the right axis. The initial rise of the breakthrough curves begins with the beads, followed by VA, iodide and finally fluorescein
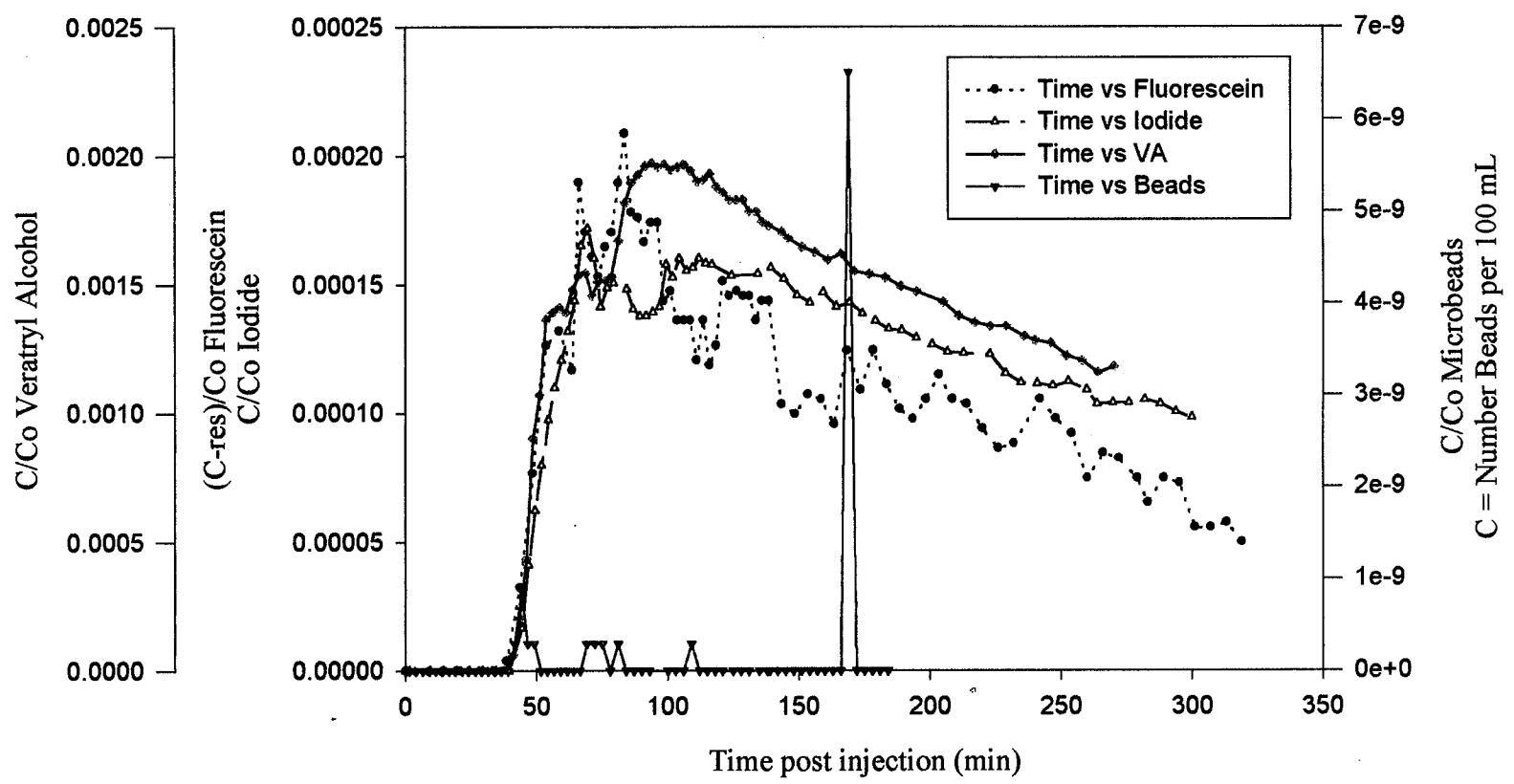
Figure 21. Relative Concentration vs Time for All Tracers in Well V16D in Test I-3.
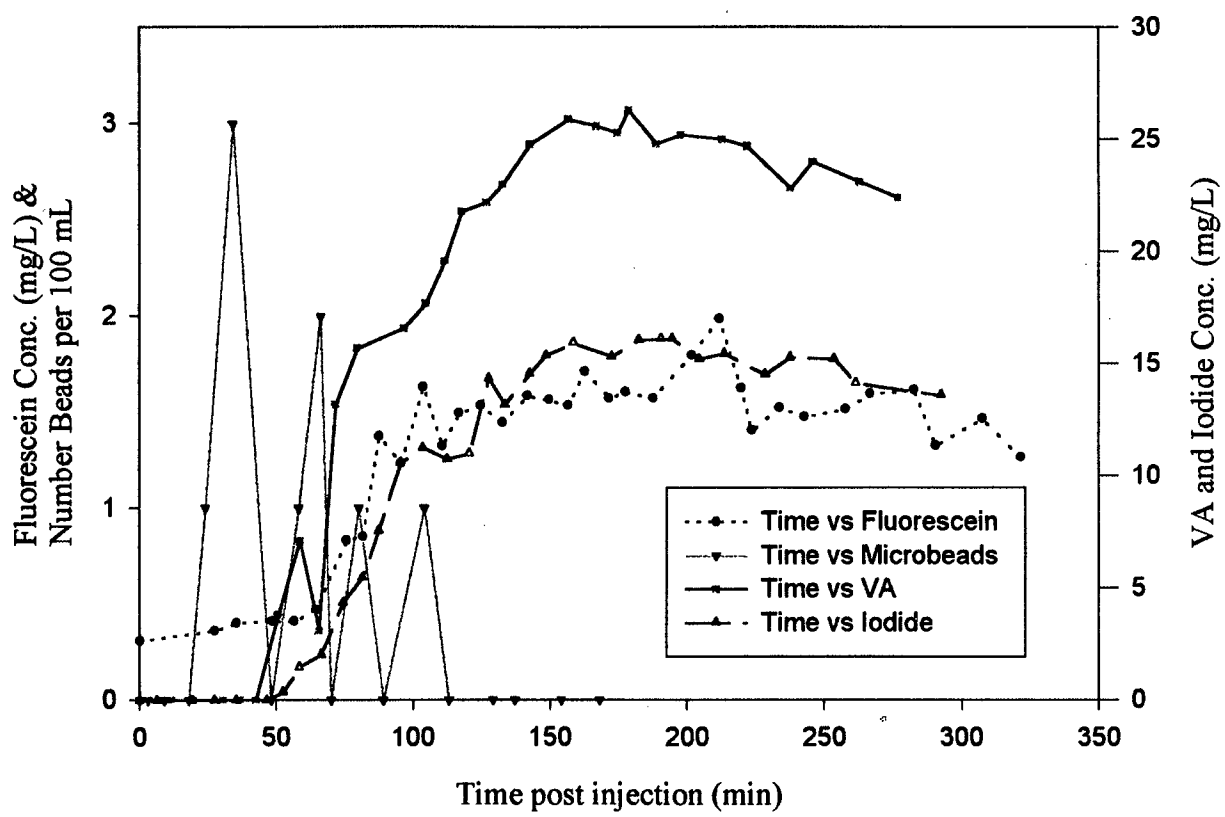
Figure 22. Concentration vs Time for All Tracers in Well T16D in Test I-3
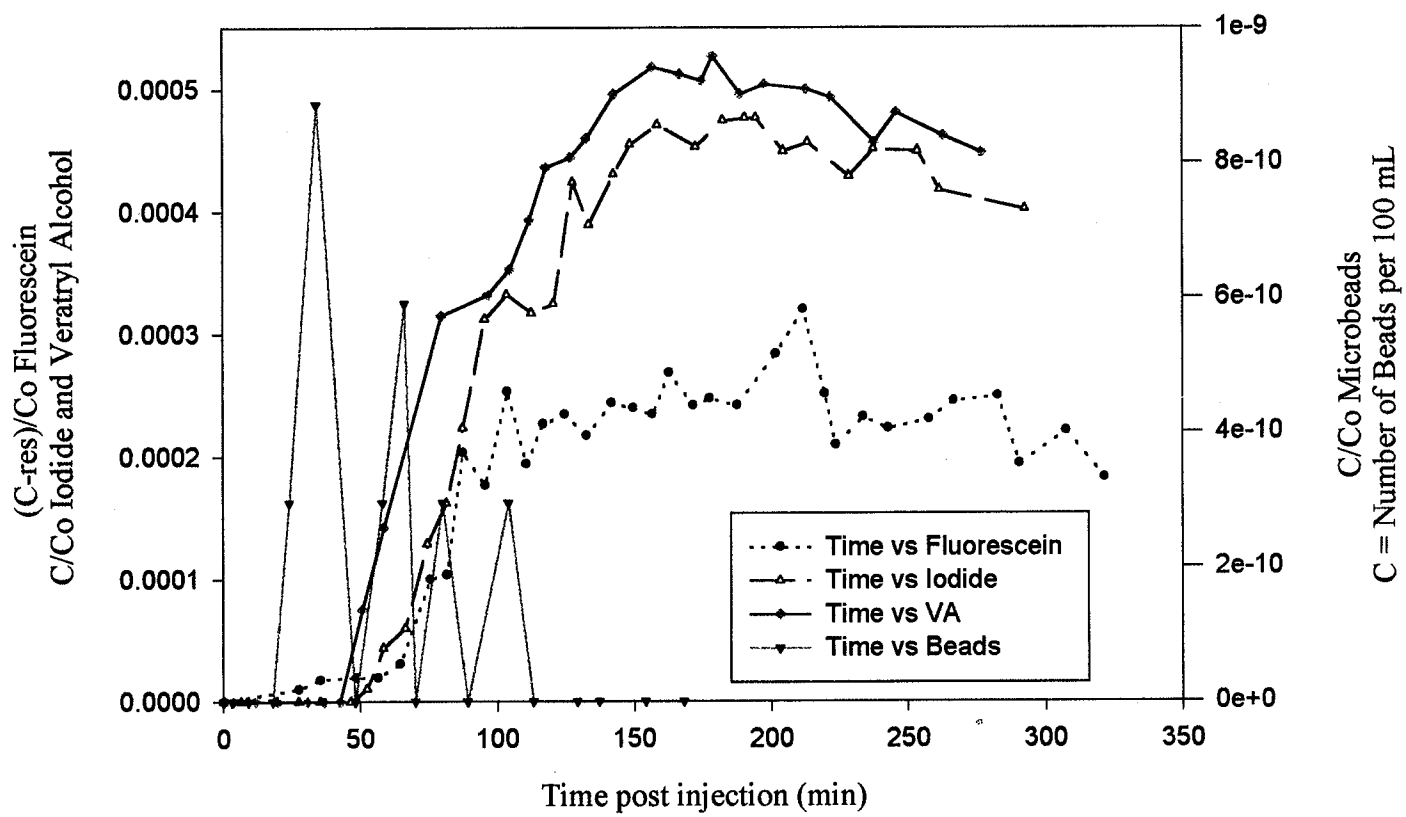
Figure 23. Relative Concentration vs Time for All Tracers in Well T16D in Test I-3.

with the latest rise. This is the same sequence with respect to relative concentration and particulate count peaks. The early rise of the iodide and fluorescein breakthrough curves is very similar but after they deviate the iodide and VA curves resemble one another. The beads peaked at a relative count (C/Co) of 8.88×10^{-10} at t=34 minutes, VA with a C/Co of 5.27×10^{-4} at t=178 minutes, iodide with a C/Co of 4.76×10^{-4} at t=192 minutes and fluorescein with a C/Co of 3.20×10^{-4} at t=211 minutes. The residual concentration for fluorescein is subtracted and is represented in the graph by C-res (concentration minus residual concentration) instead of C (concentration).

The concentrations versus time for well Q16D are graphed in Figure 24 for Test I-3. Analysis was conducted only for iodide and VA. Analysis of fluorescein and spores was not conducted because they were previously injected into this well and their residual concentrations are likely to be very high. VA was also previously injected but was thought to have been degraded by the time Test I-3 was run based on the rapid decay rate shown in Test II-4. There was a significant amount of unidentified precipitate in each sample which clogged the membranes used to filter the microbeads; therefore, no samples could be analyzed for the microbeads. Both tracers began to increase at very similar times, following each other very closely. The length of sampling was inadequate to properly define the breakthrough peaks. The actual breakthrough peak is not determinable from the available data; therefore, the last data points represent the highest measured concentrations since the curves maintain an upward trend. These values are only used for comparisons with the other wells in this test. The peak concentration of VA was measured at t=287 minutes with a concentration of 30.8 mg/L. The peak concentration of iodide occurred at t=292 minutes with a concentration of 8.60 mg/L. Residual VA from a previous test may be a lingering impact causing the heightened baseline concentration.

Lastly, the relative concentrations of VA and iodide are graphed versus time for well Q16D (Figure 25). This graph appears much different than the regular concentration graph (Figure 24). Both tracers are on the left horizontal axis. There is a residual level of VA which was difficult to subtract and is why some of the data points fall below zero. These curves do not correspond as well as when graphed as their regular concentrations. The breakthrough curves begin to ascend at similar times but the VA curve rises much faster than iodide. The
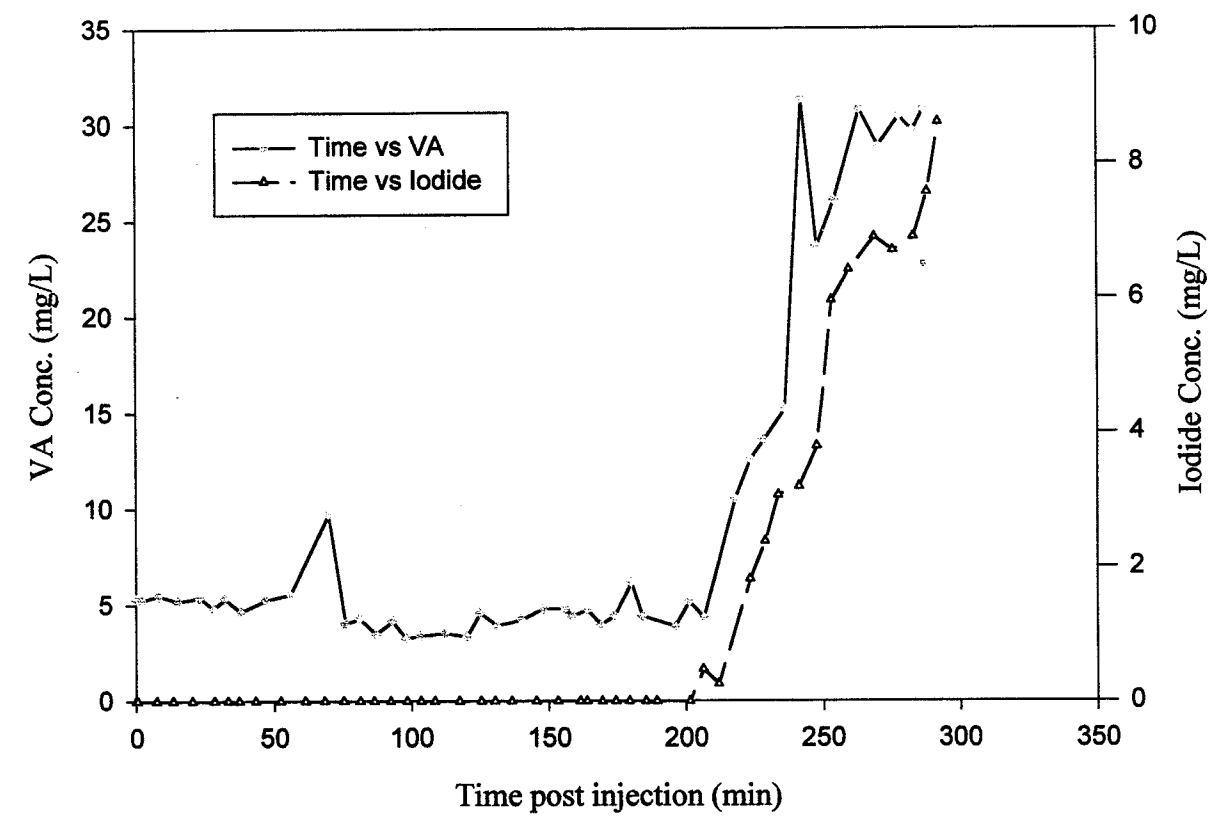
Figure 24. Concentration vs Time for Tracers in Well Q16D in Test I-3.
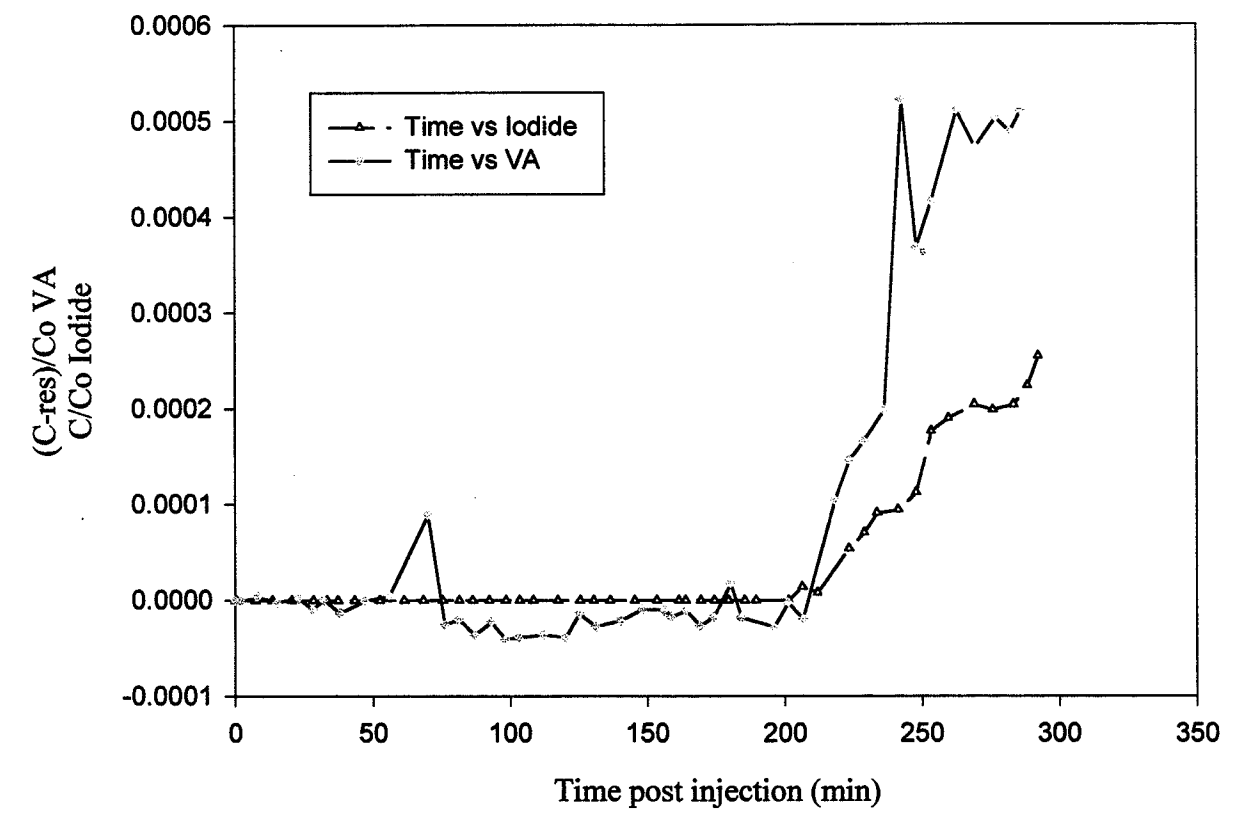
Figure 25. Relative Concentration vs Time for Tracers in Well Q16D in Test I-3.

highest measured C/Co for iodide is 2.55×10^{-4} and for VA C/Co is 5.10×10^{-4}. Residual VA is subtracted from the concentration and is represented in the graph by C-res (concentration minus residual concentration) instead of C (concentration).

Comparison of Tracer Breakthrough Curves Among Wells

The breakthrough curves for the different tracers are compared among the various wells. Figures 26 and 27 are fluorescein concentration versus time and relative concentration versus time graphs for wells V16D and T16D, respectfully. The first appearance of fluorescein is in well T16D. This well also has a higher concentration throughout most of the test. The peak concentration in well V16D occurs before the T16D peak. Figures 28 and 29 show graphs of iodide concentration versus time and relative concentration versus time, respectfully. The first arrival and highest peak concentration for iodide occur in well V16D, second in T16D and last in Q16D. Well T16D again has the higher concentrations. Figures 30 and 31 are graphs of VA concentration versus time and relative concentration versus time, respectfully. Similar to the breakthrough curves for iodide, the first arrival and peak concentration for VA begin with V16D, then T16D and finally Q16D. The difference is that well V16D has the highest concentration followed by Q16D (at the peak) ending with T16D. In each graph of the dissolved tracers the breakthrough peak occurs first in well V16D, second in T16D and last in Q16D. However, the particulate tracer breakthrough peak arrives first in well T16D and last in V16D as seen in Figures 32 and 33. The initial rise of the breakthrough curve is first in well T16D and last in V16D. The same amount of beads for the peak concentration is found in both wells V16D and T16D.

Parameter Calculations

The average hydraulic gradient, peak breakthrough times and average velocity for each tracer in the three monitoring wells are presented in Table 15. Based on the hydraulic gradients and distances between wells the tracer peak breakthrough times should be smallest for well Q16D followed by T16D and lastly by V16D. Interestingly, just the opposite is seen. Also, different patterns of tracer velocities in the various wells apparent. In well V16D the beads are the first to arrive, followed by iodide, fluorescein and finally VA. In well T16D the
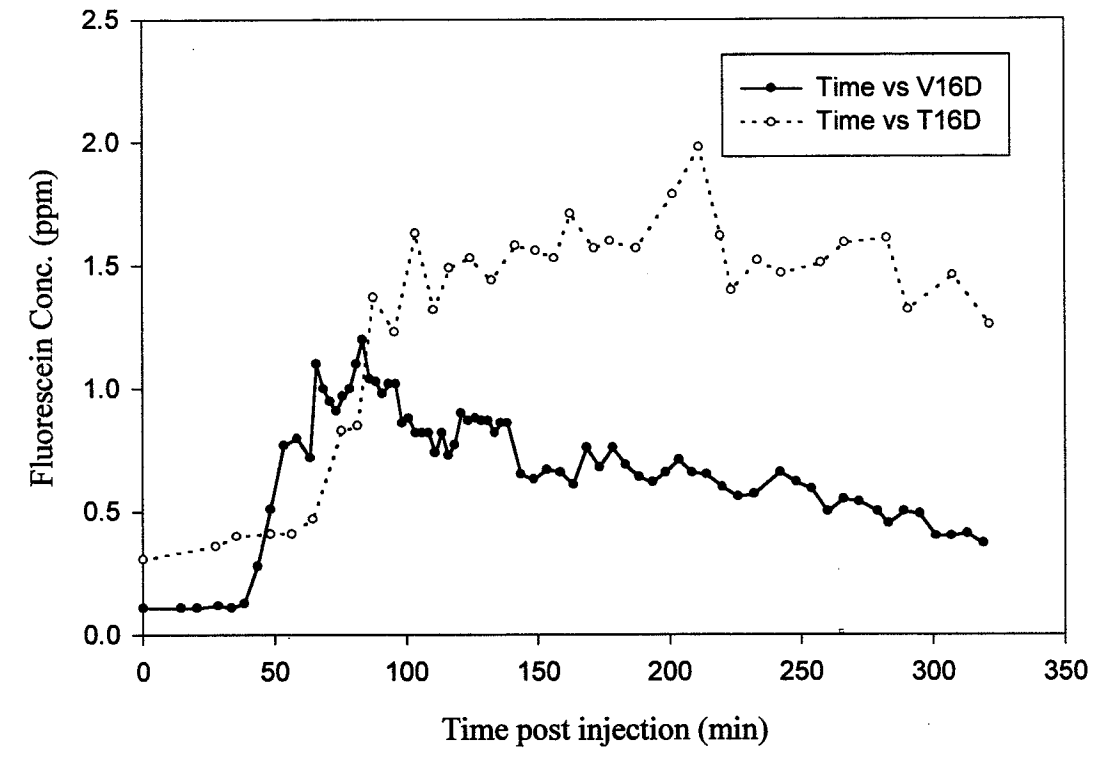
Figure 26. Fluorescein Concentrations in Wells V16D and T16D in Test I-3.
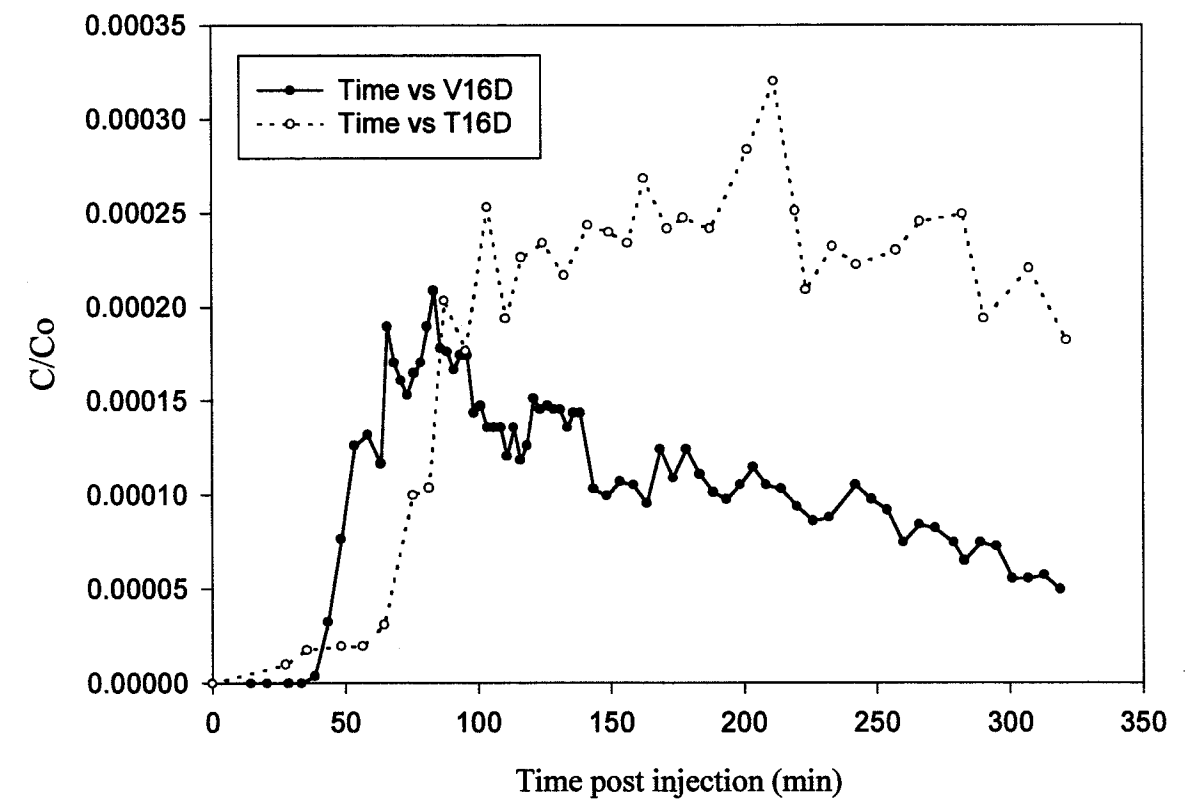
Figure 27. Relative Fluorescein Concentration in Wells V16D and T16D in Test I-3.
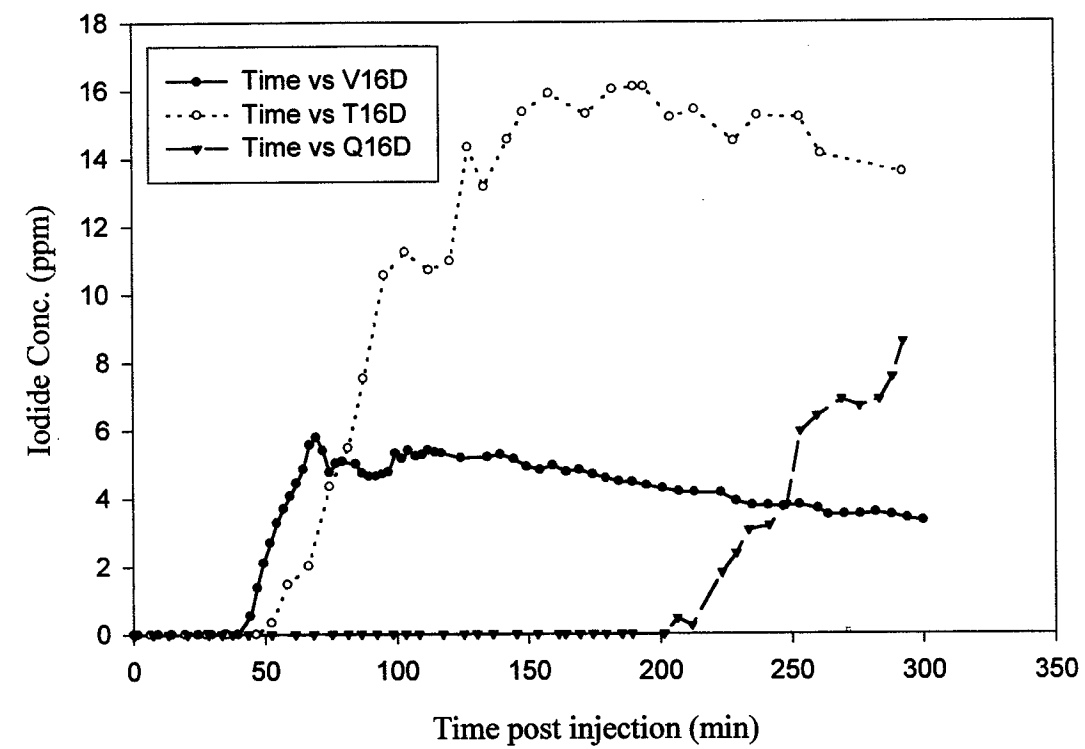
Figure 28. Iodide Concentrations in Wells V16D, T16D and Q16D in Test I-3.
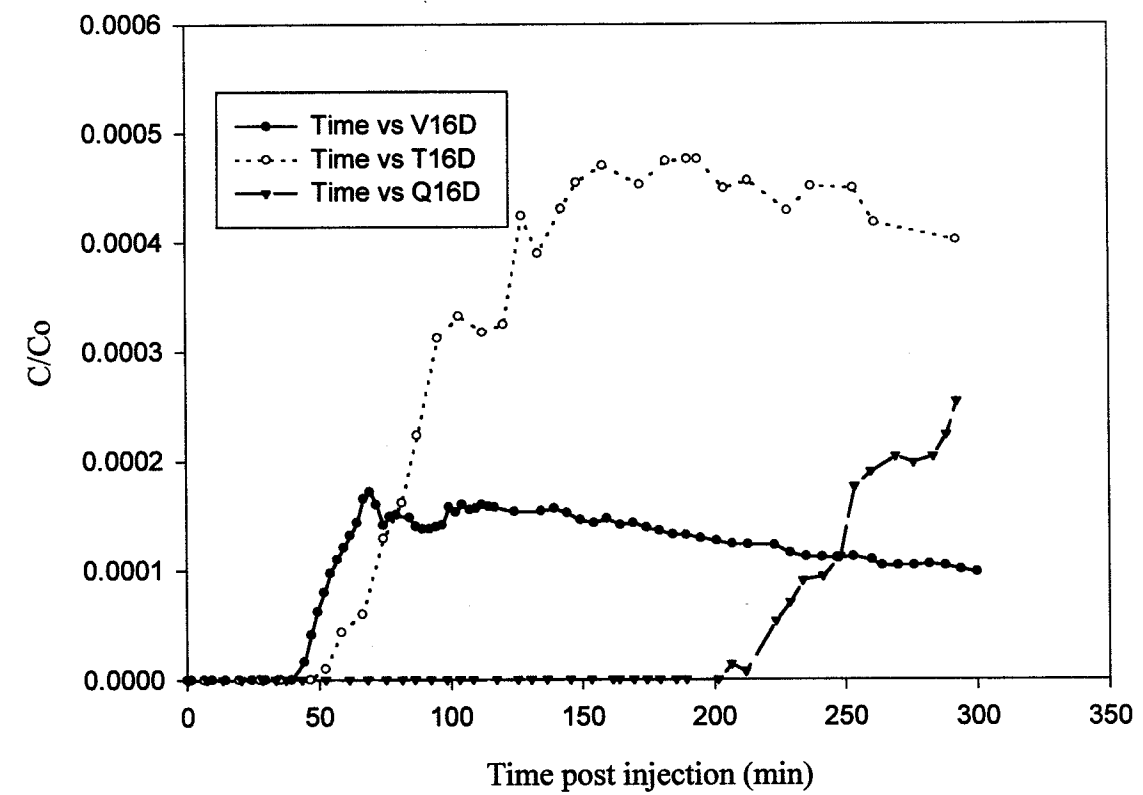
Figure 29. Relative Iodide Concentrations in Wells V16D, T16D and Q16D in Test I-3.
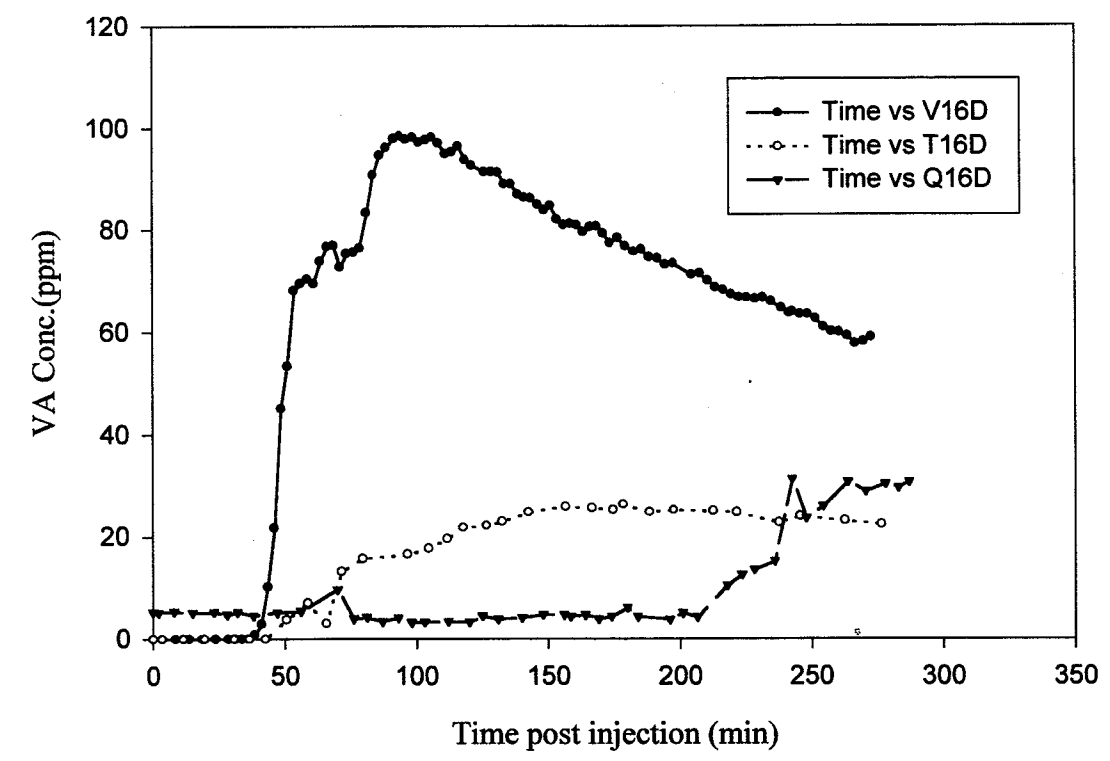
Figure 30. Veratryl Alcohol Concentrations in Wells V16D, T16D and Q16D in Test I-3.
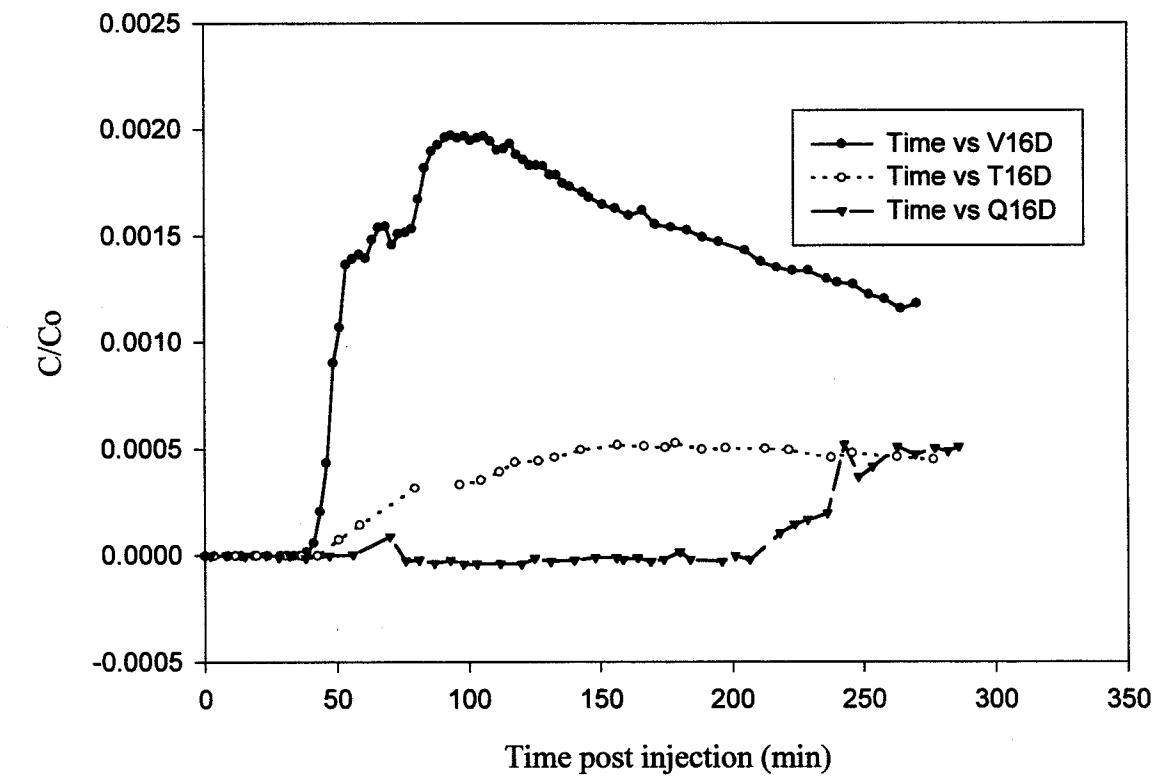
Figure 31. Relative VA Concentrations in Wells V16D, T16D and Q16D in Test I-3.
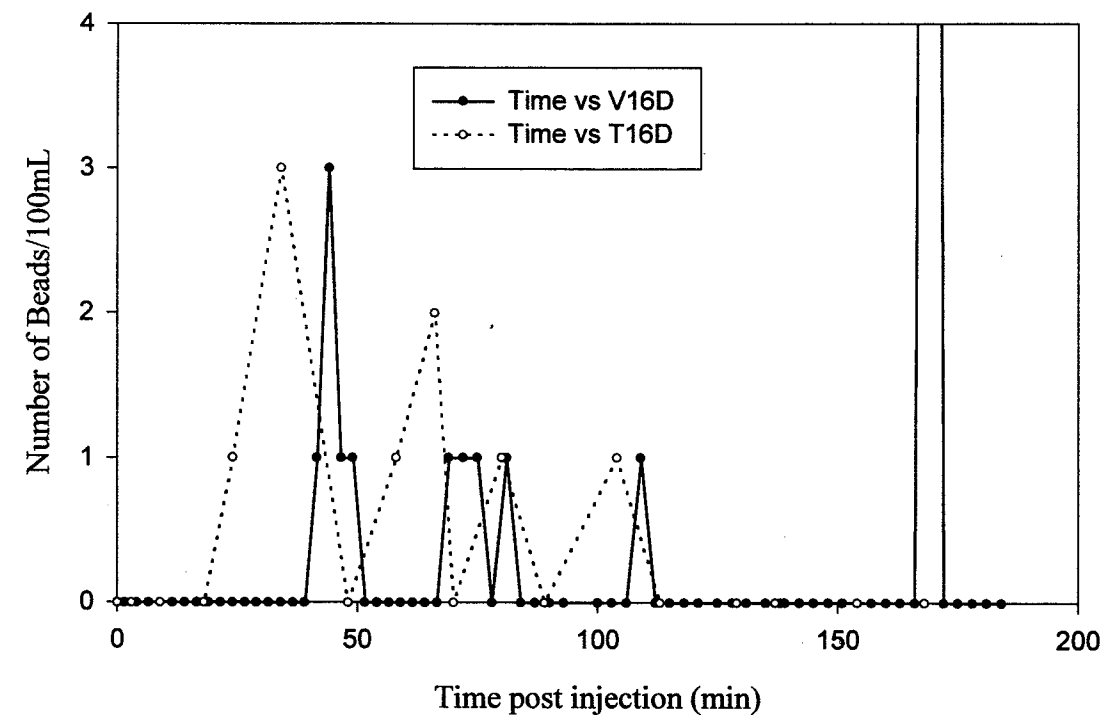
Figure 32. Microbead Count in Wells V16D and T16D in Test I-3.
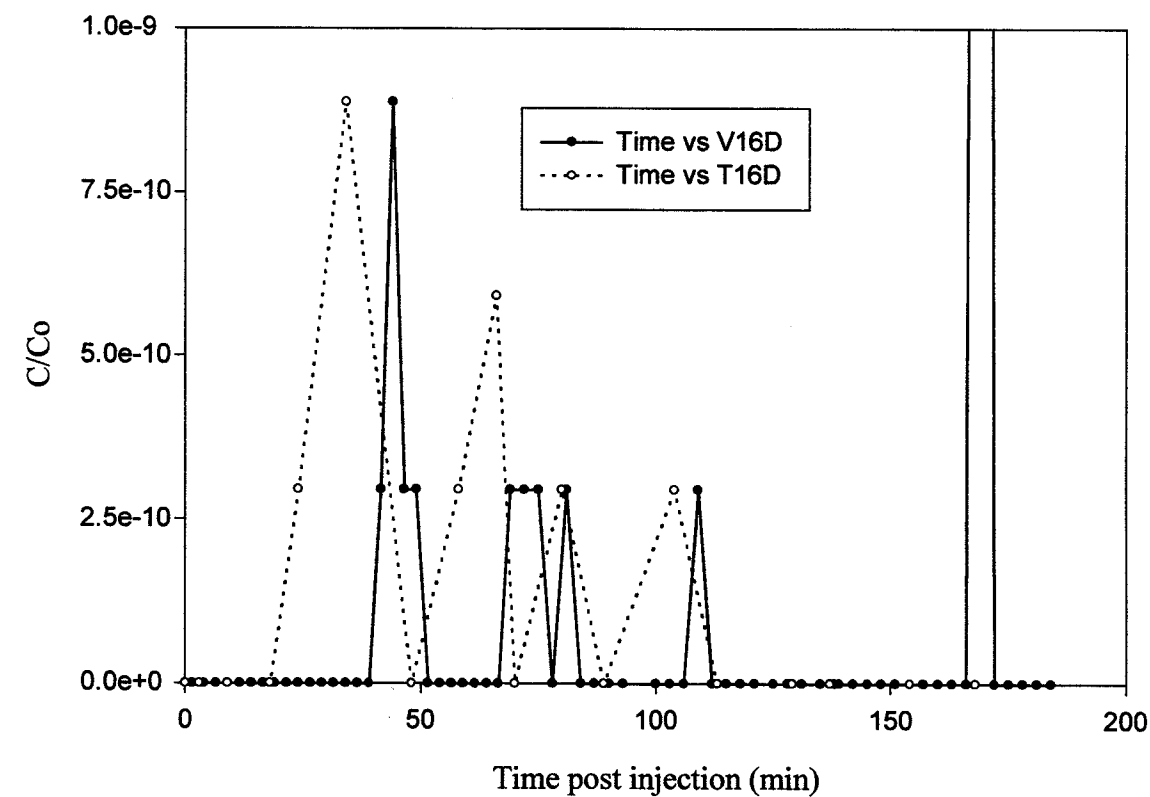
Figure 33. Relative Microbead Count in Wells V16D and T16D in Test I-3.

beads are the first to arrive again, but are followed by VA, iodide and finally fluorescein. The velocities for well T16D are more alike than those for well V16D.

	V16D	T16D	Q16D
Distance from injection well (ft) - Q17D	100	70	20
Average gradient	0.16	0.19	0.48
Fluorescein PBT (min)	83	211	NA
Iodide PBT (min)	69	192	>292
Veratryl alcohol PBT (min)	106	178	>287
Microbead PBT (min)	44	34	NA
Ave. fluorescein velocity (ft/min)	1.20	0.33	NA
Ave. iodide velocity (ft/min)	1.45	0.36	<0.69
Ave. VA velocity (ft/min)	0.94	0.39	<0.70
Ave. microbead velocity (ft/min)	2.27	2.06	NA

NA = not applicable   PBT = peak breakthrough time

Table 15. Background Data, Average Gradient, Peak Breakthrough Times and Average Tracer Velocities for Wells in Test I-3.

Mass balance results for the various tracers for wells V16D in Test I-3 are given in. Table 16. For comparison purposes the percent recovery after 286 minutes is calculated for the dissolved tracers. Fluorescein and iodide have similar percentages, 6.1 and 6.3, respectfully. However, for VA the recovery is 67.0%. This is more than ten times higher than the other two dissolved tracers. This was also seen in the relative concentration graph in Figure 18 and discussed in the corresponding section. The microbeads have a very low recovery rate, much less than one percent.

Mass balance results for wells T16D and Q16D are also calculated. The pumps in these wells were not run continuously, consequently, the amount of tracer recovered is very small for all the tracers.

	V16D	T16D	Q16D
Fluorescein Tracer injected (g)	40		
Tracer recovered (g)	2.58	3.33×10^{-2}	NA
Percent recovered after 286 minutes	6.08	7.71×10^{-5}	NA
Total percent recovered (319 min)	6.44	8.34×10^{-5}	NA
Iodide Tracer injected (g)	267.4*		
Tracer recovered (g)	17.49	2.33×10^{-1}	9.36×10^{-3}
Percent recovered after 286 minutes	6.29	8.52×10^{-5}	3.00×10^{-6}
Total percent recovered (300 min)	6.54	8.70×10^{-5}	3.50×10^{-6}
Veratryl Alcohol Tracer injected (g)	400		
Tracer recovered (g)	268	3.94×10^{-1}	1.38×10^{-1}
Percent recovered after 286 minutes	67.0	9.85×10^{-5}	3.45×10^{-5}
Total percent recovered (286 min)	67.0	9.85×10^{-5}	3.45×10^{-5}
Microbeads Tracer injected (number)	3.38×10^{9}		
Tracer recovered (number)	33	9	NA
Total percent recovered (168 min)	9.76×10^{-7}	2.66×10^{-9}	NA

* actual I^- not KI

Table 16. Mass Balance Results of Tracers for Monitoring Wells in Test I-3.

NONRECIRCULATION TESTS

Test II-2

Fluorescein concentrations versus time and relative concentrations versus time are graphed for well Q17D in Test II-2 (Figures 34 and 35). Fluorescein was detected in the samples after approximately one hour. The peak concentration of fluorescein was 9.2 mg/L with a C/Co of 2.91×10^{-4} which occurred after 120 minutes. After approximately t= 650 minutes the slope of the tail in the breakthrough curve is much flatter. The breakthrough

curve does not return to a concentration near residual level, instead it levels off midway between the peak and residual concentration.

Tracer test, tracer and aquifer parameters for well Q17D in Test II-2 are listed in Table 17. The tracer velocity coincides with those from previous tests of the same pumping rate. The hydraulic gradient is similar to other experiments. The total mass of fluorescein recovered is 53% after 2255 minutes.

	Q17D
Distance from injection well (ft) - Q16D	20
Ave. discharge rate (ft^3/min)	0.40
Ave. hydraulic gradient	0.121
Fluorescein Peak breakthrough time (min)	120
Ave. velocity (ft/min)	0.17
Tracer injected (g)	267
Tracer recovered (g)	142
Total percent recovered (after 2255 min.)	53.2

Table 17. Test, Tracer and Aquifer Parameters Calculated for Well Q17D in Test II-2.

Test II-4

Concentrations of fluorescein and bromide in addition to spore and microbead counts are graphed versus time for well Q17D in Test II-4 (Figure 36). Figure 37 is the first 300 minutes of the breakthrough curve in Figure 36. Benzoic acid (BA) and veratryl alcohol (VA) were not detected in any of the samples. These two tracers are easily biodegradable at non-acidic pH's in a short period of time. The microbeads and fluorescein appeared at nearly the same time with bromide following closely behind. The beads were the first to peak with 4 beads/15 mL at t=58 minutes and 68 minutes (t=0 at the time of each injection); the timing of the peak, for velocity purposes, is averaged at t=63 minutes. Spores were found in only one sample at t=56 minutes. The spore data are suspect because there is only a single data point. Fluorescein peaked at a concentration of 2.35 mg/L at t=259 minutes. The fluorescein

Figure 34. Fluorescein Concentration vs Time for Well Q17D in Test II-2.
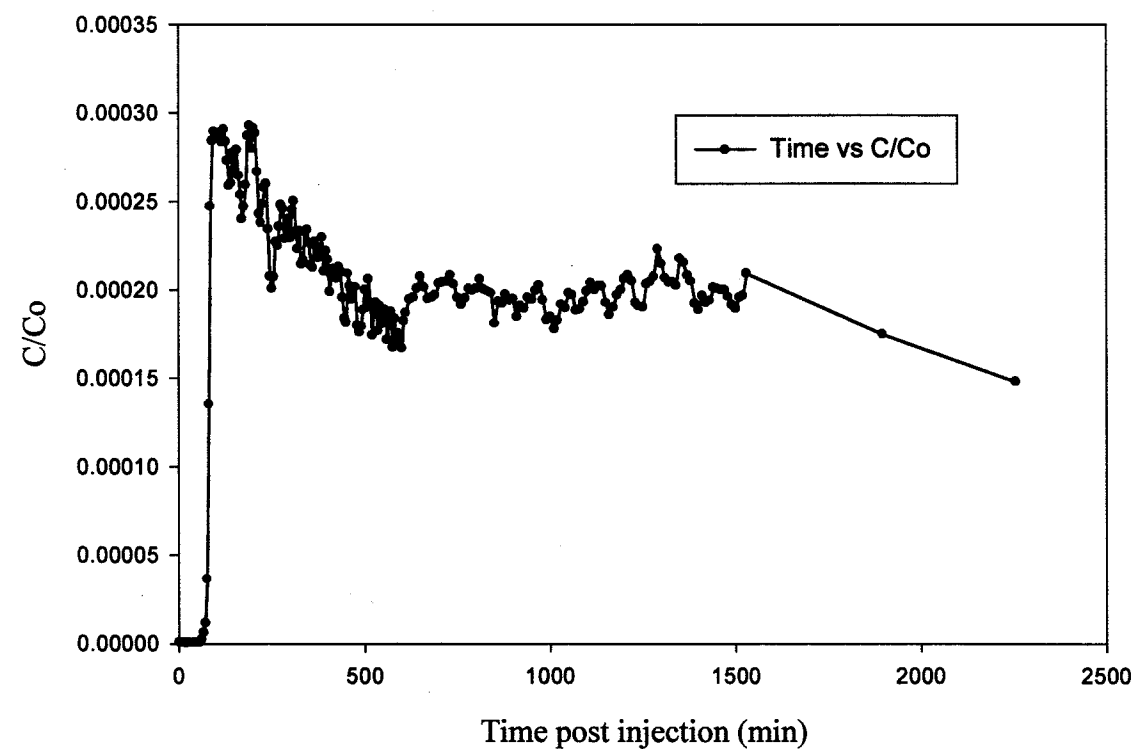
Figure 35. Relative Fluorescein Concentration vs Time for Well Q17D in Test II-2.

curve does not return to a concentration near residual level, instead it levels off midway between the peak and residual concentration.

Tracer test, tracer and aquifer parameters for well Q17D in Test II-2 are listed in Table 17. The tracer velocity coincides with those from previous tests of the same pumping rate. The hydraulic gradient is similar to other experiments. The total mass of fluorescein recovered is 53% after 2255 minutes.

	Q17D
Distance from injection well (ft) - Q16D	20
Ave. discharge rate (ft^3/min)	0.40
Ave. hydraulic gradient	0.121
Fluorescein Peak breakthrough time (min)	120
Ave. velocity (ft/min)	0.17
Tracer injected (g)	267
Tracer recovered (g)	142
Total percent recovered (after 2255 min.)	53.2

Table 17. Test, Tracer and Aquifer Parameters Calculated for Well Q17D in Test II-2.

Test II-4

Concentrations of fluorescein and bromide in addition to spore and microbead counts are graphed versus time for well Q17D in Test II-4 (Figure 36). Figure 37 is the first 300 minutes of the breakthrough curve in Figure 36. Benzoic acid (BA) and veratryl alcohol (VA) were not detected in any of the samples. These two tracers are easily biodegradable at non-acidic pH's in a short period of time. The microbeads and fluorescein appeared at nearly the same time with bromide following closely behind. The beads were the first to peak with 4 beads/15 mL at t=58 minutes and 68 minutes (t=0 at the time of each injection); the timing of the peak, for velocity purposes, is averaged at t=63 minutes. Spores were found in only one sample at t=56 minutes. The spore data are suspect because there is only a single data point. Fluorescein peaked at a concentration of 2.35 mg/L at t=259 minutes. The fluorescein

Figure 36. Concentration vs Time for All Tracers in Well Q17D in Test II-4.
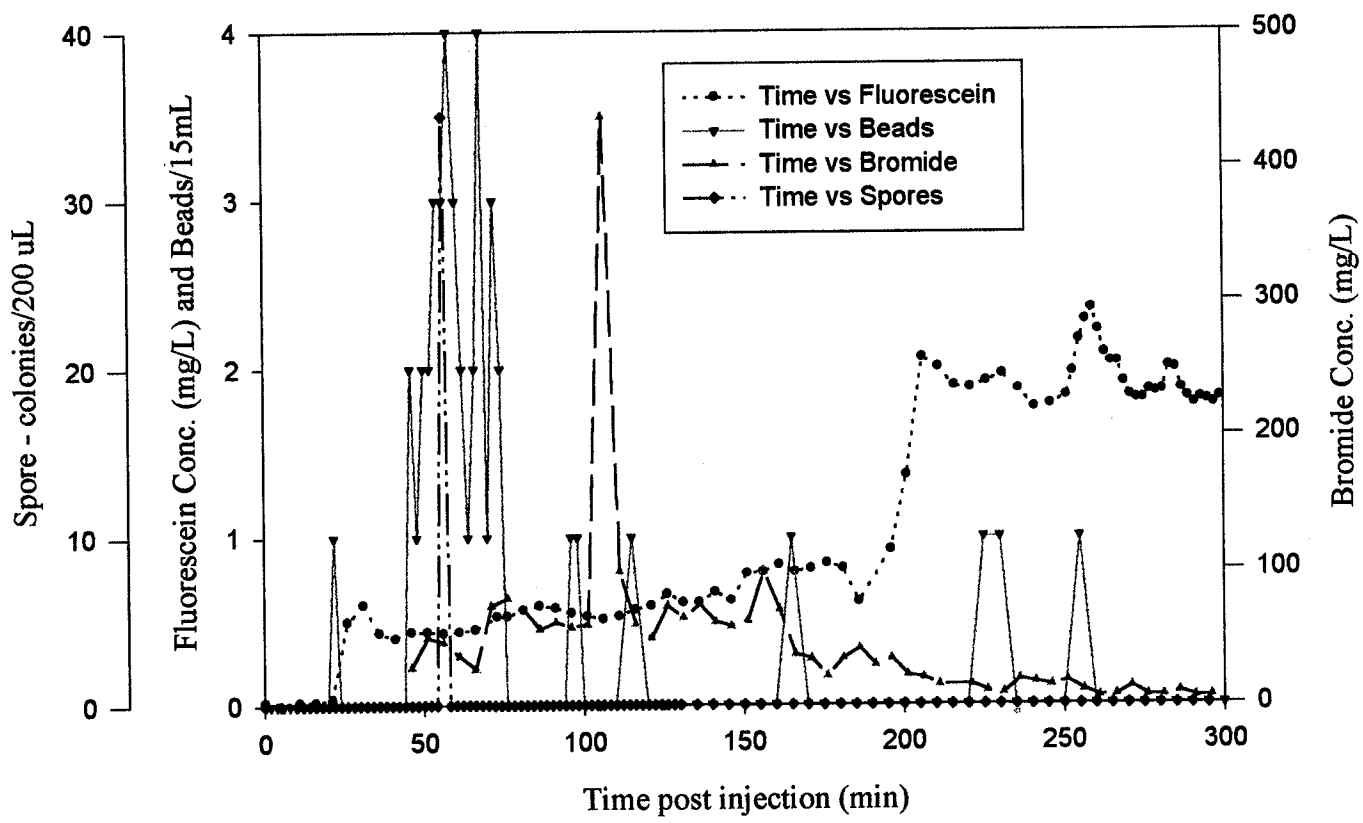
Figure 37. Concentration vs. Time (first 300 minutes) for All Tracers for Well Q17D in Test II-4.

breakthrough curve has several fluctuations and a fairly lengthy tail which drops abruptly between 1686 and 1706 minutes. The bromide breakthrough curve has two peaks, the first at a concentration of 437 mg/L at t=106 minutes and the second peak at a concentration of 815 mg/L at t= 326 minutes. This concentration is very high, although possible. Because there are two bromide peaks it is difficult to determine which one is the "correct" one. The first peak has a bell shape which is unusual for the experiment based upon previous tests and the heterogeneous fractured rock environment. The second peak is very high with limited data. There is essentially no tail for the bromide curve.

The relative concentrations and counts are plotted versus time for the tracers in Test II-4 (Figure 38). C/Co values for fluorescein and bromide are plotted on the same scale. The microbead breakthrough curve peaked at a C/Co of 2.38×10^{-9} and fluorescein peaked at a C/Co of 3.79×10^{-3} (t=350 minutes). The first bromide peak crested at a C/Co of 6.08×10^{-3} and the second peak of bromide crested at a C/Co of 0.011. The C/Co for spores is too small to mention.

The spore recovery was very low, with only one sample exhibiting spore growth. Only 30-40 colonies/200 μL grew on the media; however, they do not appear exactly like the colonies from the stock solution. This low response may be due to a variety of reasons. The spore counts of the stock solution were lower than initially thought. Also, when examining them under a microscope, they were football shaped and had tails. This changed their anticipated size to 2-4 μm in diameter instead of the anticipated 0.5-2 μm size. They were very close to the same size as the beads. Their larger size could cause greater straining and therefore less spore recovery. Other reasons are the same as those listed for Test I-3.

The peak breakthroughs for bromide and fluorescein are unclear. There are several possible explanations due to the previously explained circumstances in Chapter 4 (i.e. pumping of the injection well the evening prior to the test and the air injection/explosion). The fluorescein breakthrough curve peak should occur at a similar time to bromide breakthrough curve peak if it behaves as a conservative tracer.

One interpretation of the data involves accepting that the main fluorescein peak which occurs at approximately t=350 minutes. Fluorescein was used in several previous experiments and the effects of residual concentrations are likely to be the cause of the breakthrough curve
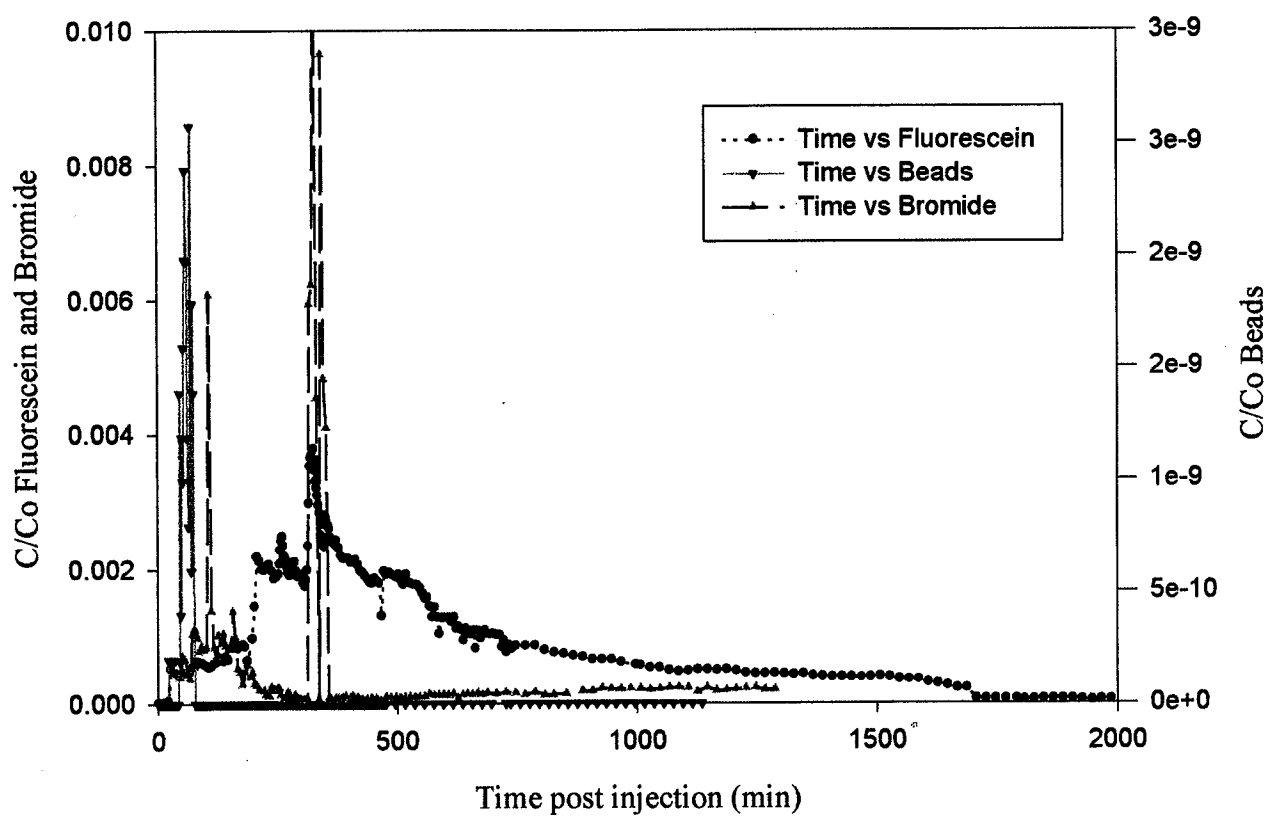
Figure 38. Relative Concentration vs. Time for All Tracers (except spores) in Well Q17D in Test II-4.

shape. The fluorescein recovery is more than 100%; indicating some of the fluorescein was recovered from previous experiments. Diffusion from fluorescein in the rock matrix, pore spaces and fractures back into the moving water may cause an increase in concentration. This may explain the shoulders (fluctuations) leading to the rise of the main fluorescein peak.

The second interpretation of the data is based on accepting the first combined fluorescein peak at about t=176 minutes and for the bromide peak at about t=106 minutes. This breakthrough time coincides with the fluorescein peak for Test II-2. The early relative data (Figure 38) are similar for fluorescein and bromide. The large fluorescein peak at t=350 minutes may then be caused by fluorescein from previous experiments. Fifteen times less fluorescein was injected in Test II-4 in comparison with Test II-2, but the peak concentration was only 1/3 that of Test II-2.

The air injection caused explosion of water from the injection well occurred approximately 1700 minutes after the fluorescein injection. Its effect is seen by an immediate drop in the fluorescein and bromide concentrations (see Figure 38). The explosion occurred at the same time as the first bromide peak; therefore, the second bromide peak may be the breakthrough curve peak of the precipitated bromide in the line that was re-dissolved as a result of the air injection forcing it into the formation or mobilization caused by the air surge. This suggests the first bromide peak may have occurred at a later time and at a higher concentration but was stopped by the air injection. The bromide breakthrough curve may have had a much different shape as well.

Only the hydraulic gradient and the dissolved tracer data are calculated for Test II-4 (Table 18). The hydraulic gradient between the pumping and injection well was 0.13. The tracer velocity results of the dissolved tracers are meaningless due to the problems of the test. Based on the breakthrough curves it is obvious that the particle tracers have a faster velocity than the dissolved tracers.

The mass balances of the tracers in Test II-4 are calculated and listed in Table 19. The percent recoveries for the conservative tracers are quite high. The total amount of fluorescein recovered is 111%. Some of the fluorescein may have come from the previous tests or erroneously quantified due to quenching. The total amount of bromide recovered is 71%.

	Q17D
Distance from injection well (ft) - Q16D	20
Ave. discharge rate (ft^3/min)	0.40
Ave. hydraulic gradient	0.13
Microbeads Breakthrough (min)	63
Ave. velocity (ft/min)	0.32
Spores Breakthrough (min)	56
Ave. velocity (ft/min)	0.36

Table 18. Average Hydraulic Gradient, Peak Breakthrough Times and Tracer Velocities for the Particulate Tracers in Well Q17D for Test II-4.

The smallest percentage of recovery are the particulate tracers, each is much less than 1%. The amount of recovered microbeads is based on the total bead count including the samples analyzed in triplicate. The amount of fluorescein and bromide recovered after 1286 minutes is provided for comparison, 97% for fluorescein and 71% for bromide. Both values are very high.

SUMMARY OF TESTS

A summary of the results for the recirculation and nonrecirculation experiments is listed in Table 20.

	Q17D
Fluorescein	
Tracer injection (g)	15.0
Tracer recovered (g)	16.8
Percent recovered after 1286 minutes	97.1
Total percent recovered (3346 min)	111
Bromide	
Tracer injected (g)	605
Tracer recovered (g)	429.4
Percent recovered after 1286 minutes	71.0
Total percent recovered (1286 min)	71.0
Spores	
Tracer injected (number)	10^8/mL
Tracer recovered (# colonies/200 µl)	35
Total percent recovered (3000 min)	<1
Microbeads	
Tracer injected (number)	1.69×10^9
Tracer recovered (number)	122
Total percent recovered (1135 min)	<1

Table 19. Mass Balance Results in Well Q17D for Test II-4.

TEST	RECIRCULATING						NONRECIRCULATING	
	TEST I-1	TEST I-2		TEST I-3			TEST II-2	TEST II-4
Start date of test	9-12-96	9-20-96		10-17-97			10-10-96	3-27-97
Observation wells	V16D	V16D	Q16D	V16D	T16D	Q16D	Q17D	Q17D
Distance from inj. well (ft)	100	100	20	100	70	20	20	20
Ave. gradient (initial) After recirc. stopped	0.061/ 0.003	0.072/ 0.005	0.14/ 0.014	0.16	0.19	0.48	0.12	0.13
Fluorescein PBT (min)	205	125	120	83	211	NA	120	NA
Bromide PBT (min)								NA
Iodide PBT (min)				69	192	>292		
VA PBT (min)				106	178	>287		ND
BA PBT (min)								ND
Spore PBT (min)				ND	ND	ND		56
Bead PBT (min)				44	34	NA		63
Ave. fluorescein velocity (ft/min)	0.49	0.80	0.17	1.20	0.33	NA	0.17	NA
Ave. bromide velocity (ft/min)								NA
Ave. iodide velocity (ft/min)				1.45	0.36	<0.69		
Ave. VA velocity (ft/min)				0.94	0.39	<0.70		NA
Ave. BA velocity (ft/min)								NA
Ave. spore velocity (ft/min)				NA	NA	NA		0.36
Ave. bead velocity (ft/min)				2.27	2.06	NA		0.32

ND = non-detect   NA = not applicable   PBT = peak breakthrough time

Table 20. A Summary of Tracer and Aquifer Parameter Calculations For All Tests.

CHAPTER 7
ANALYSIS OF TRACER TEST DATA BY CURVE MATCHING

INTRODUCTION

In this chapter, the field results are compared to response curves generated by analytical models. The experimental tracer test data from the recirculation and nonrecirculation tests are matched to generated type curves. Only the fluorescein data are matched to the type curves because fluorescein was the only tracer utilized in all the tracer experiments. The dye is believed to act as a conservative tracer which is one of the requisites for the curve matching analysis. The input parameters necessary to solve for equations used in this chapter are the same as those listed in Chapter 6. A summary and comparison among the curve matching data concludes this chapter.

As described in Chapter 5, there are two curve matching methods applied to the data from the tests conducted at the UIGRS. Sauty (1980) methods were employed to the data from the nonrecirculating tests and nonrecirculating well pairs in the recirculation tests, and the Brenner solution method was used for the recirculating experiments.

RECIRCULATION TESTS

Test I-1

Fluorescein data from well V16D in Test I-1 are compared to type curves generated using the Brenner solution (Figure 39). A family of type curves were created with a porosity of 0.004 based on an arbitrarily estimated aquifer thickness of 1.5 feet and graphed with the experimental data. This porosity value was chosen because the experimental data peak is similar in timing to those of the type curves.

The experimental data on Figure 39 have very low relative concentrations and fall below the type curves causing the data points to appear in a horizontal line near zero. The C/Co values for the field data are orders of magnitude lower than the Brenner solution curves.
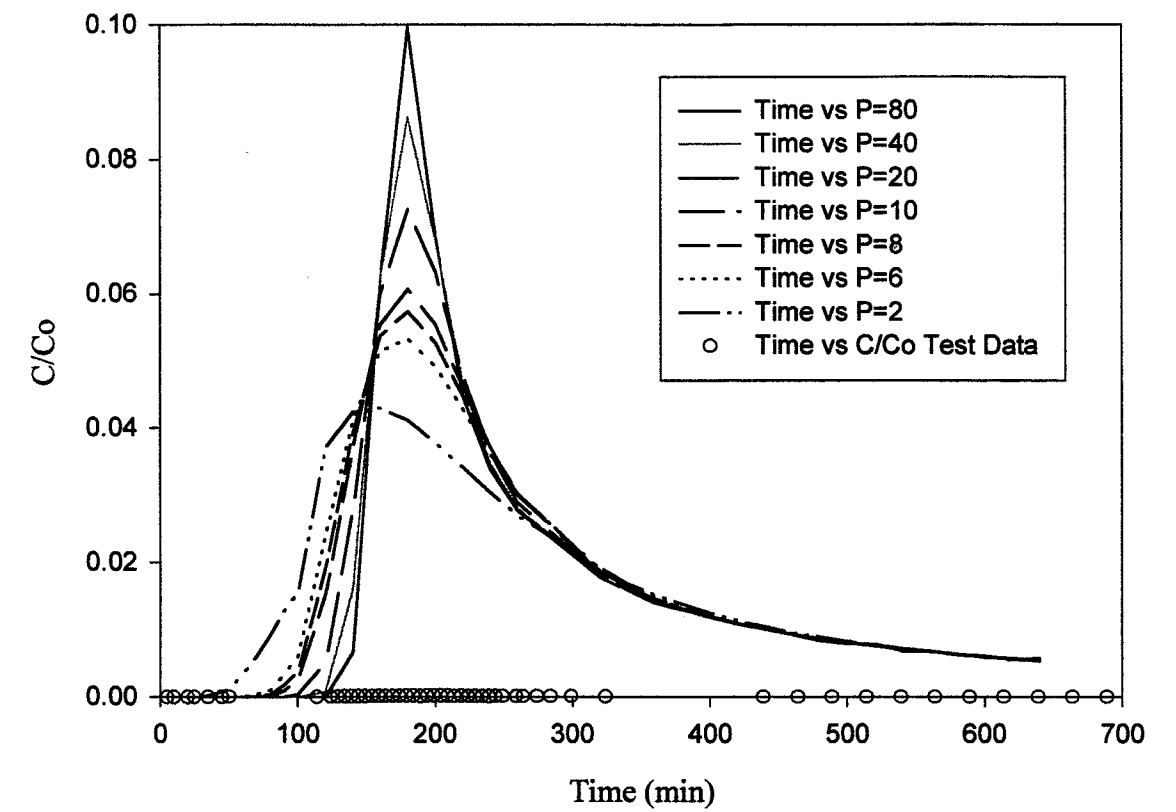
Figure 39. Curve Matching with the Brenner Solution to Data from Well V16D in Test I-1 (n=0.004)

Test I-2

The comparison of the data from well V16D in Test I-2 to the Brenner solution also does not yield a solution (Figure 40). A family of type curves is generated with a porosity of 0.003 based upon the same foundation as in Test I-1. The experimental data fall below the type curves and appear as a horizontal line near a C/Co of zero as in Test I-1.

The Sauty (1980) curve matching method is applied to the experimental data from well Q16D in Test I-2 (Figure 41). Axes and related titles of the experimental data are shown on the figure. The fluorescein breakthrough curve corresponds to a type curve with a Peclet number of 60. The early rise, peak and a section of the tail of the experimental breakthrough curve match the type curve fairly well. Table 21 lists the curve matching results.

	Q16D
Curve matching method	Sauty
Peclet number	60
Effective porosity	NA
Dispersivity (ft)	0.33
Dispersion (ft^2/min)	0.056

Table 21. Curve Matching Results for Test I-2.

Test I-3

Fluorescein data from well V16D in Test I-3 are matched to type curves generated using the Brenner solution (Figure 42). A family of type curves with a porosity of 0.002 is utilized for the same reasons discussed in Test I-1. As in the other two recirculating experiments using the Brenner solution the relative concentrations of the experimental data are much too small to be seen on the same axis. Thus no calculations can be conducted.

The Sauty (1980) method is used to analyze data from well T16D in Test I-3 (Figure 43). Axes and related titles of the experimental data are shown on the figure. The early data best match the type curve with a Peclet number of 8. However, the peak best fits the type curve with a Peclet number of 100. This number does not appear to be representative of most
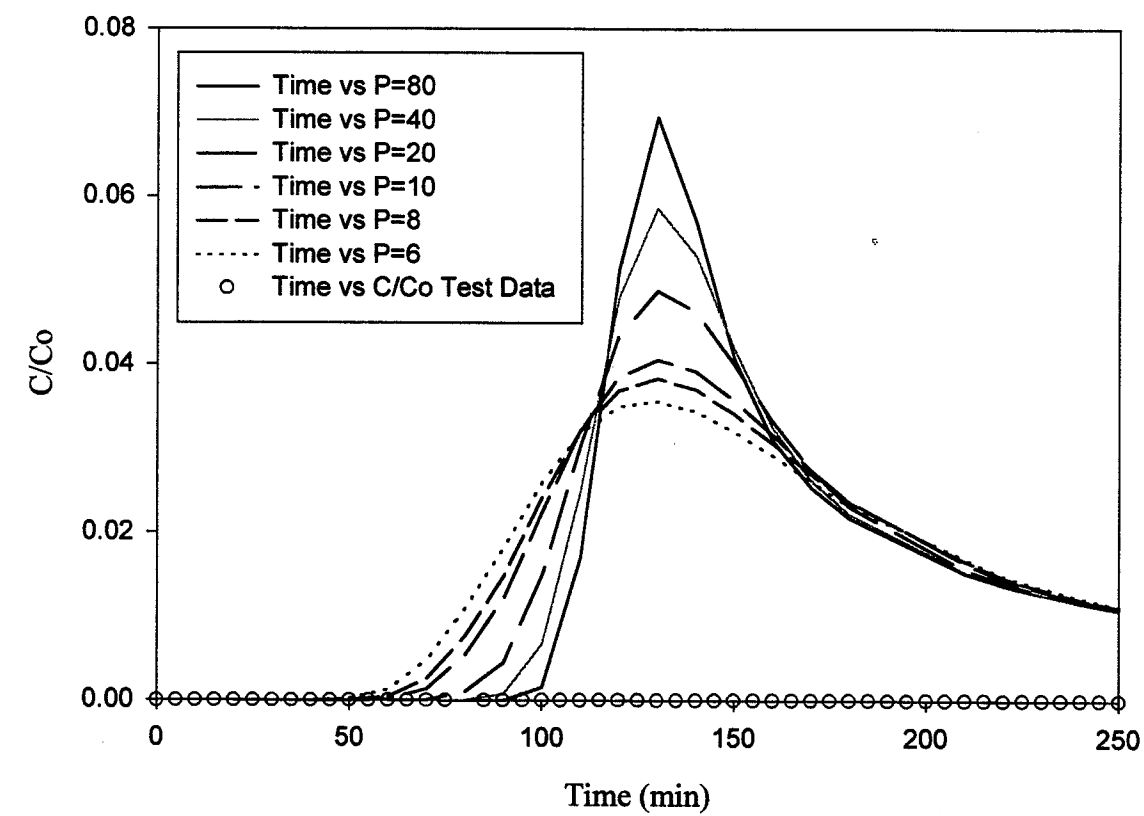
Figure 40. Curve Matching with the Brenner Solution to Data from Well V16D in
Test I-2 (n=0.003)
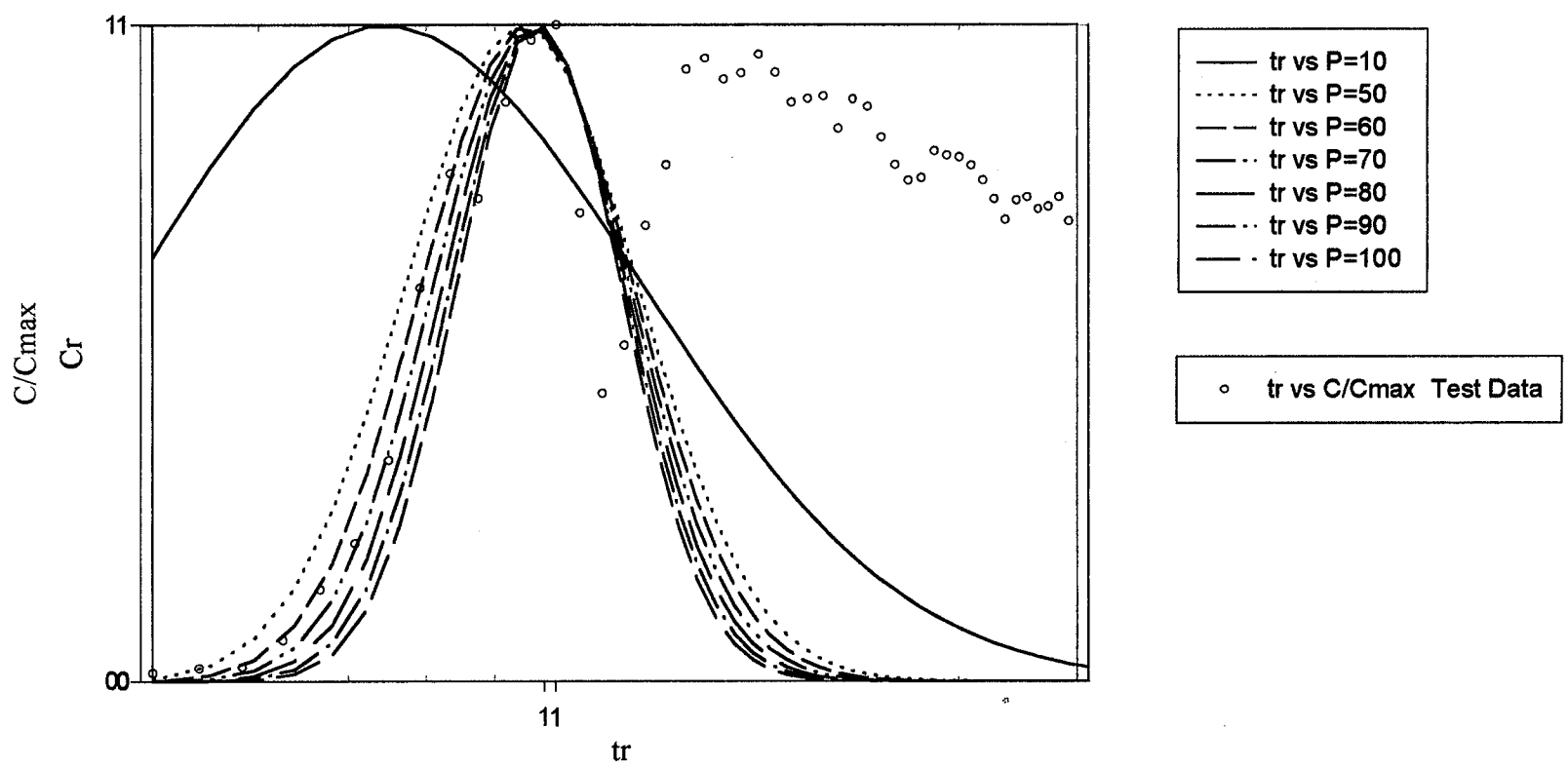
Figure 41. Curve Matching with The Sauty (1980) Method to Data From Well Q16D in Test I-2.
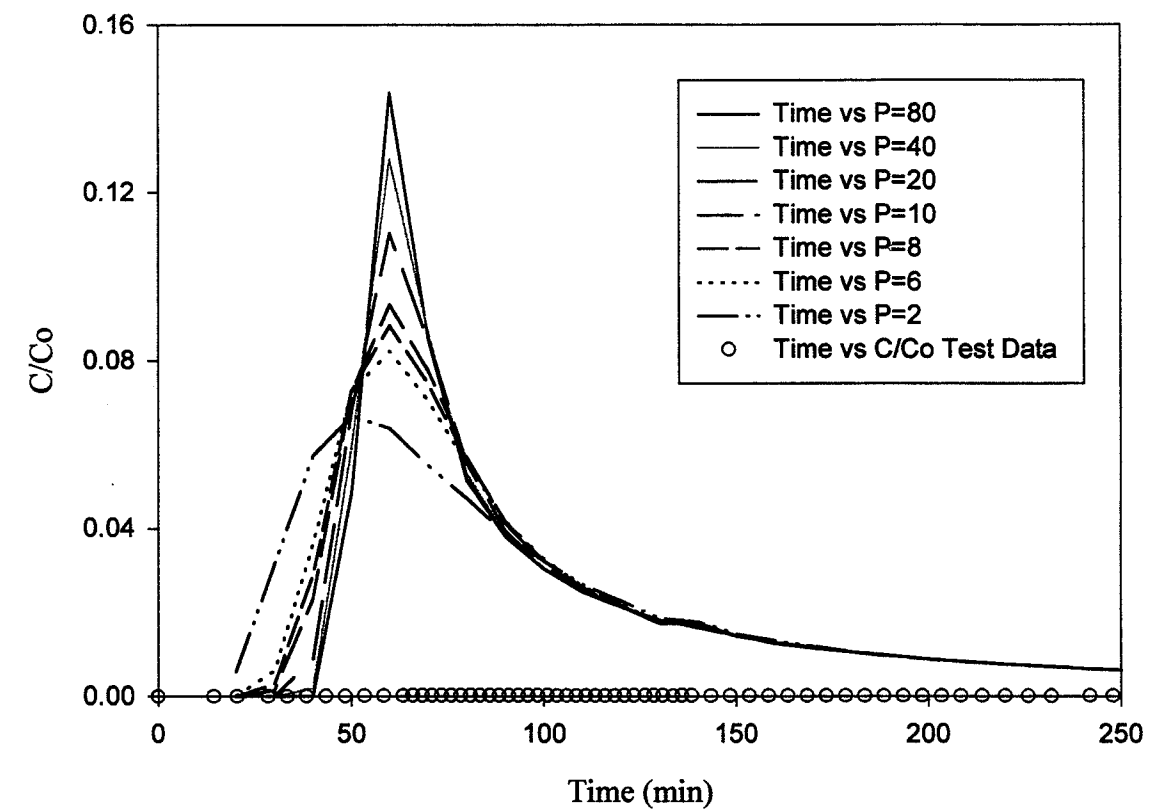
Figure 42. Curve Matching with the Brenner Solution to Data From Well V16D in Test I-3 (n=0.002)
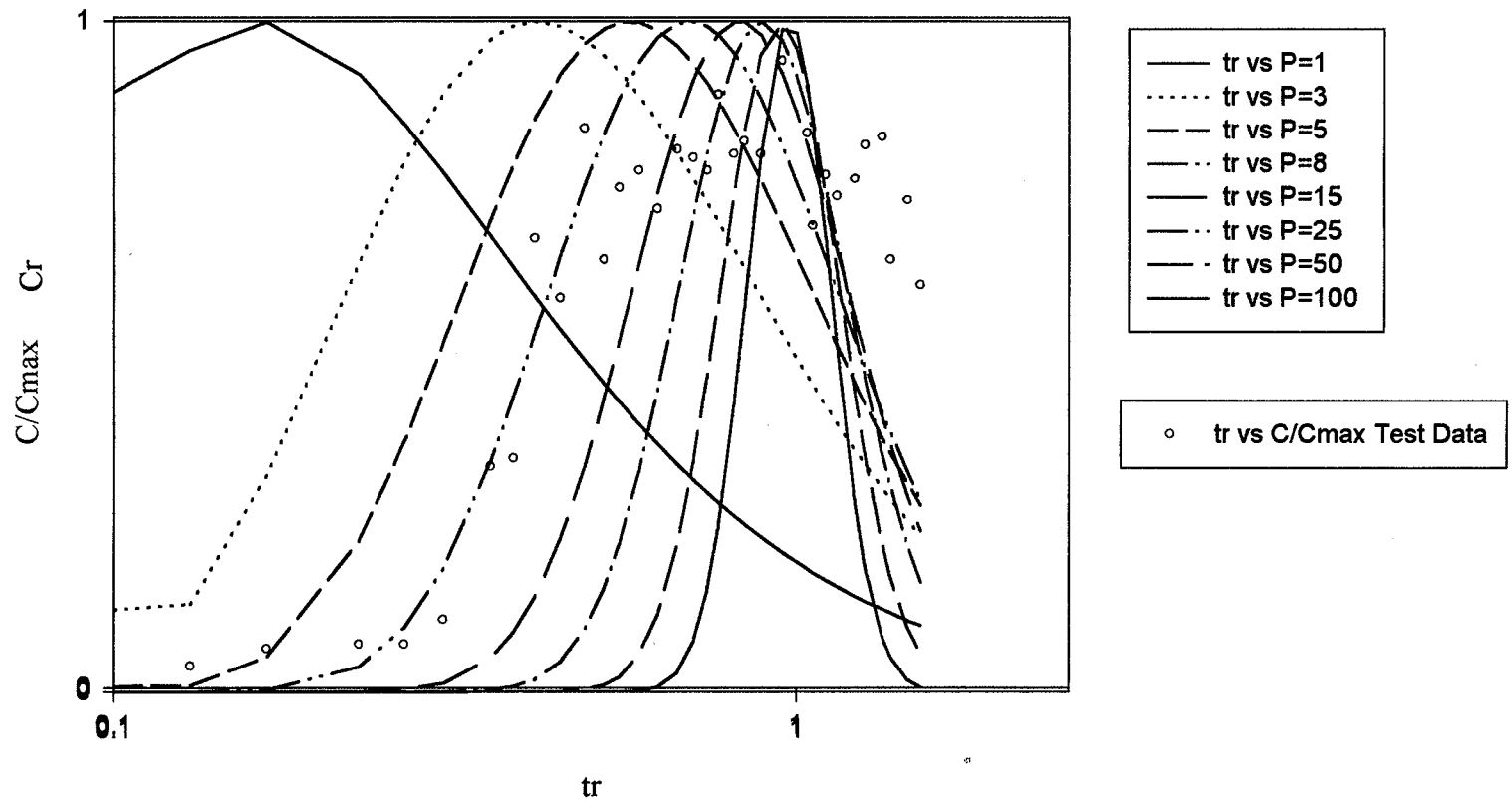
Figure 43. Curve Matching with the Sauty (1980) Method to Data From Well T16D in Test I-3.

of the data. The BTC tail lies above the curve. Calculated parameters are listed in Table 22.

Curve matching is not applied to data from well Q16D. The breakthrough curve peak is not defined well enough.

	T16D
Curve matching method	Sauty
Peclet number	8
Effective porosity	NA
Dispersivity (ft)	8.75
Dispersion (ft^2/min)	2.89

Table 22. Curve Matching Results for Test I-3.

NONRECIRCULATION TESTS

Test II-2

Data from well Q17D in Test II-2 are compared to type curves generated using the Sauty (1980) method (Figure 44). The experimental data axes and labels are shown on the figure. The early data and peak of the experimental data match a type curve with a Peclet number of 100. The tail of the experimental data lies above the type curve. Calculated parameters are listed in Table 23.

	Q17D
Curve matching method	Sauty
Peclet number	100
Effective porosity	NA
Dispersivity (ft)	0.2
Dispersion (ft^2/min)	0.034

Table 23. Curve Matching Results for Test II-2.
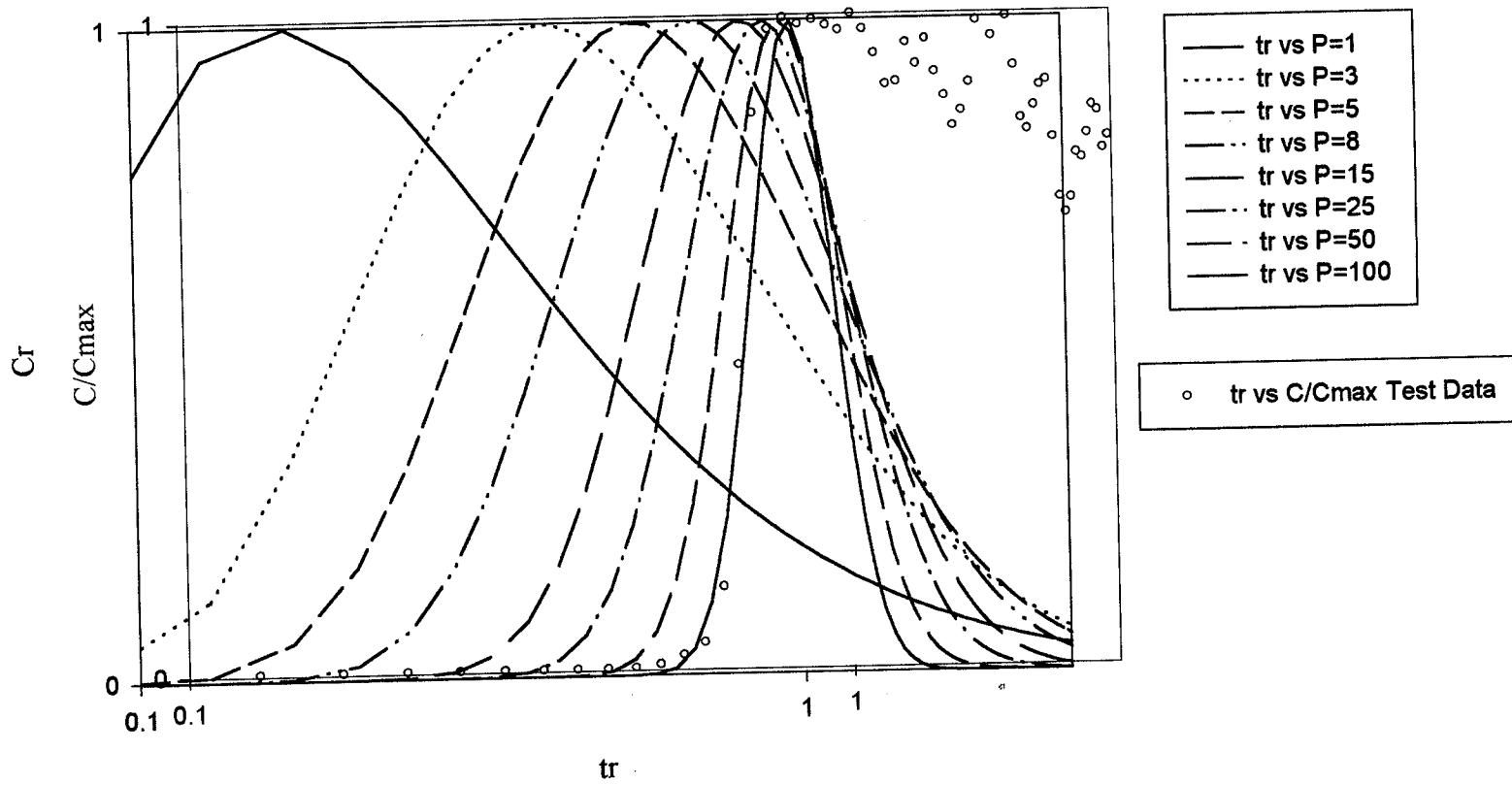
Figure 44. Curve Matching with the Sauty (1980) Method to Data From Well Q17D in Test II-2.

Test II-4

Curve matching analysis yields unlikely results using the Sauty (1980) method for data from well Q17D in Test II-4. A Peclet number of 1000 is calculated based on the main breakthrough curve peak. This is a highly unlikely value and probably does not represent the data or the aquifer. Therefore, no parameter calculations are carried out. The rise of the experimental data does not match any of the type curves. This provides additional support for the supposition that the fluorescein breakthrough curve was affected by the pumping of the injection well the evening prior to Test II-4 by drawing fluorescein from previous experiments back into the flow field.

SUMMARY AND COMPARISONS

A summary of the calculated aquifer values for each experiment by curve matching are listed in Table 24. Wells Q16D, Q17D and T16D each have one data set which varies widely. Well V16D yielded no data. Dispersivity and mechanical dispersion are highest in well T16D, followed by Q16D and lowest in well Q17D. Well T16D has a much lower Peclet number which generates a much higher dispersivity value and dispersion coefficient.

Confidence in the calculated values from the curve matching process is low. Only a small percentage of the data match the type curves. The deviations from the type curve occur most with the data that comprise the tail of the breakthrough curve. The transport processes that cause the tail of the breakthrough curve are not represented in the Sauty (1980) method. A more in-depth discussion of the reliability of the curve matching data is provided in chapter 8.

	RECIRCULATING		NONREC.
Test	TEST I-2	TEST I-3	TEST II-2
Distance between inj. and monitoring wells (ft)	20	70	20
Observation well	Q16D	T16D	Q17D
Curve matching method	Sauty	Sauty	Sauty
Peclet number	60	8	100
Dispersivity (ft)	0.33	8.75	0.2
Dispersion (ft^2/min)	0.057	2.89	0.034

Table 24. Summary of Calculated Parameters from Curve Matching.

CHAPTER 8
DISSUSSION OF RESULTS

INTRODUCTION

This chapter describes the results from the tracer tests conducted at the UIGRS. A description is given of the general information gained from conducting tracer tests in fractured basalt and about the E-fracture aquifer, a comparison of results, and tracer migration by various transport processes. A discussion of the curve matching results is presented at the end of the chapter.

GENERAL DISCUSSION OF TRACER TEST RESULTS

The most important information learned from conducting tracer tests at the UIGRS is the need to carefully plan, imagine the consequences and to eliminate any possible human or mechanical error. A haphazardly conducted experiment will yield poor or ambiguous results. The interpretation of tracer tests in fractured rock is quite complex without having to incorporate anomalies from experimental problems. Fractured rock systems are heterogeneous by nature; however, most of the methods available for interpreting tracer test results are for homogeneous environments. This makes interpretation of the tests difficult.

The tracer test results provide considerable insight into the nature of the E-fracture aquifer. Five experiments were conducted successfully in four wells screened in the E-fracture aquifer. The results indicate this fracture zone is hydraulically continuous within the area of the four wells tested. It was also demonstrated that the fracture zone is able to transport particles of 6.0 μm size based on the data from Tests I-3 and II-4. The aquifer is heterogeneous based on the fact that none of the breakthrough curves have a bell shape as would be expected in a homogeneous environment and several curves have multiple peaks.

DISCUSSION OF RESULTS BY COMPARISONS

Comparison of Dissolved Tracers

A number of conservative tracers was desired for the tracer experiments conducted at the UIGRS; two of the experiments tested a variety of dissolved tracers. Fluorescein, veratryl

alcohol (VA), benzoic acid (BA) and bromide were the dissolved tracers injected in Test II-4; however, problems during the test and the degradation of VA and BA resulted in little information on these tracers. A number of dissolved tracers were also injected in Test I-3, including iodide, fluorescein and veratryl alcohol (VA). As discussed in Chapter 6 the breakthrough curves for these three tracers appear very similar in each of the wells. This indicates fluorescein and VA act as conservative tracers because their breakthrough curves are similar to iodide which is a known conservative tracer. The breakthrough curves have small variances that are caused by differences in tracer chemical properties, small velocity variations and slight alterations in their flow paths.

Comparison of Dissolved Tracers with Particulate Tracers

Two of the experiments utilized particulate tracers in addition to dissolved tracers; the peak breakthroughs for particulates occurred prior to the dissolved tracer breakthroughs'. These results are similar to those found by several authors (Brown, 1998; Pang et al., 1998; Sinton et al., 1997; Petrich, 1995; McKay et al., 1993; Champ and Schroeter, 1988; Sinton and Close, 1983, in Pang et al., 1998; Pyle, 1979, in Harvey et al, 1989; Wood and Ehrlich, 1979; Atkinson et al., 1973). The size of the particulates restricts them to the larger fractures, and as discussed in Chapter 2, particles follow the preferential pathways which have the highest velocities. This process is described by Enfield and Bengtsson (1988). By definition velocity is inversely proportional to effective porosity. Since particles cannot pass through smaller pore spaces or fractures the effective porosity is less, thus increasing the velocity. Theoretically, all the tracers should travel to the monitoring well at the same time but since the dissolved tracers both follow slower and faster pathways it takes longer for their peak concentrations to emerge. However, in well T16D in Test I-3 the bead peak arrived before any other tracer was detected.

Comparison of Breakthrough Curves Among Different Wells

Tests I-2 and I-3 were the only tracer experiments in which more than one well was monitored. Tracers were detected in wells V16D and Q16D for Test I-2 and in wells V16D, T16D and Q16D for Test I-3. Recirculation ceased in Test I-2 after 120 minutes causing

concentrations to drop in both wells within a few minutes. The peaks may be artificial and thus the results for wells V16D and Q16D are not compared.

Based on the hydraulic gradients in Test I-3, peak breakthrough of all the tracers should first arrive in well Q16D, followed by T16D and lastly by V16D; yet the reverse is seen for the dissolved tracers. Reasons for this include: the flow line regime generated by the recirculation of the pumped water, heterogeneities of the aquifer, fracture orientation and preferential pathways. More flow lines converge at the pumping well (V16D) and therefore the peak arrives first in this well and with lower concentrations. A longer time period is necessary for the breakthrough peak to occur in well T16D. Tracers are detected in well Q16D much later than the other two wells. Based on the data from Test I-2, breakthrough in well Q16D should have occurred much sooner. However, this well is located within a very low hydraulic conductivity area. Another explanation for the late arrival of the tracers in well Q16D is the blockage of certain flow paths caused by biofouling or the filtration of microbeads and spores from previous tests. The new flow paths may be longer, thus causing later breakthrough peaks.

The peak breakthrough of the microbeads occurs first in well T16D followed by well V16D, which follows the order of the hydraulic gradients. There are no data for well Q16D. Transport of the dissolved tracers is shown to be controlled by the pumping-recirculation array which should also control transport of the microbeads. The arrival of the earlier peak in well T16D may be explained by the longer flow paths leading to the pumping well where encounters of filtration are greater causing a later peak in well V16D.

The initial detection of the dissolved tracers in T16D and V16D should follow the same pattern as for the microbeads. For example, fluorescein and the microbeads are detected first in well T16D, VA arrives at approximately the same time to wells V16D and T16D, but iodide is first detected in well V16D. Iodide has a higher detection limit which may be the reason it is detected in another well first.

The sequence of the peak concentrations is not the same for all the wells, which may indicate a heterogeneous environment or variances in chemical properties and velocities. As expected, slightly higher fluorescein and much higher iodide concentrations are found in the closer down gradient well, T16D, compared to well V16D. The pumping well (V16D) has

lower concentrations caused by a greater dilution from radial flow. However, concentrations of VA are highest in well V16D which is unexpected. Veratryl alcohol has the greatest recovery, almost ten times higher than the other conservative tracers in V16D. It is unknown why this occurred. The number of microbeads collected from well V16D and T16D is nearly the same. Well V16D should have a greater breakthrough peak because more flow lines converge at the well; however, the flow paths may also be much longer in which the particles have a greater chance of encountering filtration.

Gradient Normalized Time Comparison of Tests

Comparisons among tracer tests are provided for similarly conducted tests and those with like curves. Fluorescein results are employed in the comparison because it is the tracer common to all tests.

There are two main comparisons among the results from the recirculation tests (I-1, I-2 and I-3) and the nonrecirculation tests (II-2 and II-4). The recirculation tests (I-1, I-2 and I-3) are compared because they were conducted in the same well pair and with the same basic setup. Finally, results from Tests II-2 and II-4, the nonrecirculation tests, are compared because the tests were conducted in a like manner (i.e. same well setup, same pumping rate, etc.).

The hydraulic gradient is the only alterable factor governing tracer travel time; therefore, the data were adjusted to subtract its effect when comparing test results with different gradients. The following equations show how the hydraulic gradient is associated with travel time:

$$v = \frac{-K\left(\frac{\partial h}{\partial l}\right)}{n_e}$$

and

$$t = \frac{l}{v}$$

therefore

$$t = \frac{(l)(n_e)}{(-K)\left(\frac{\partial h}{\partial l}\right)}$$

where:

v = velocity [L/T]

K = hydraulic conductivity [L/T]

$\frac{\partial h}{\partial l}$ = hydraulic gradient

n_e = effective porosity

t = travel time [T]

l = distance between wells [L]

The effective porosity, hydraulic conductivity and the distance between the wells remains constant throughout the tracer test; therefore, only the hydraulic gradient can be altered. Normalizing travel time to a single gradient when comparing two or more tracer tests with differing gradients should eliminate any variability in the travel time. The normalization of time is accomplished by the steps in the following example. Test A (gradient A) has a higher gradient than Test B (gradient B). Step 1 is to choose the test to be normalized. Test A is chosen. Step 2 is to divide gradient A by gradient B. This value is the normalization constant. Step 3 is to divide the time by the normalization constant for each data point in Test B. Step 4 is to re-plot the breakthrough curves.

Recirculation Tests

Results for well V16D in the recirculation tests are gradient normalized and graphed in Figure 45. The data for Tests I-1 and I-2 are normalized to Test I-3 because it had the highest gradient. The point at which recirculation stopped for each test is identified on the figure. The breakthrough curves in all three experiments should increase at the same time and with the same slope. The breakthrough curves of Tests I-2 and I-3 begin to increase at the same time and follow each other exactly until a time where recirculation stopped in Test I-2. The increase in concentration for Test I-1 is slightly later than the other two tests which may be caused by a small error in the gradient calculation. No samples were collected between t=19 min and t=44 min because a storm occurred during this time; the fraction collector was re-
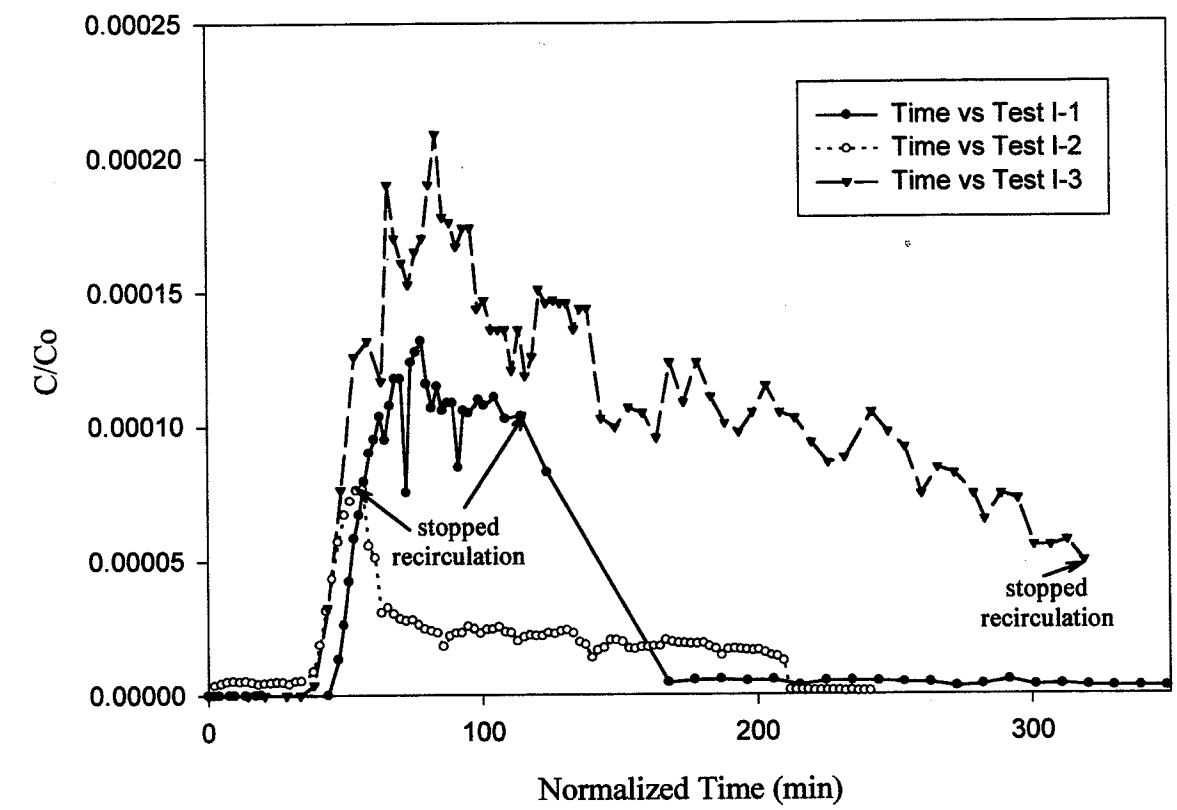
Figure 45. Relative Fluorescein Concentrations vs Normalized Time for
Recirculation Tests (Tests I-1, I-2 and I-3) for Well V16D
(Normalized to I-3).

programmed after the storm passed. It is possible that t=44 min could be in error and the sample may have been collected at an earlier time. The curves for Test I-1 and I-3 follow the same pattern during approximately the first 100 minutes of normalized time.

The magnitude of relative concentrations vary among the recirculation tests for well V16D. Test I-2 relative concentrations may be different because well Q16D was also pumping which may have altered the flow regime and captured more of the tracer. The different sampling methods for Tests I-1 and I-3 may account for their differences. Test I-1 samples were collected by allowing water to drip into test tubes which were moved automatically by a fraction collector, whereas grab samples were taken in Test I-3.

Nonrecirculation Tests

Tests II-2 and II-4 were conducted in a similar fashion, but four operational differences may have caused the dissimilar results. Following the fluorescein injection in Test II-2, water chased the tracer for nearly 45 minutes; in Test II-4 the water chase was only for one minute. Second, in Test II-4 the tracer was circulated within the injection well but was not in Test II-2. The third difference is the sampling method. In Test II-4 grab samples were collected by hand and in Test II-2 a fraction collector was used. The samples collected by a fraction collector are not grab samples but a composite of five minute intervals. The fourth difference, and probably the most significant, was that the injection well in Test II-4 was pumped the evening prior to the test (described in Chapter 6).

The breakthrough curves for Tests II-2 and II-4 appear to be quite different. Figure 46 is a graph of the relative concentrations of fluorescein breakthrough curves for Tests II-2 and II-4 in which Test II-2 is normalized. The concentrations for Test II-4 are almost 10 times higher than those in Test II-2. Fluorescein was detected in Test II-4 samples prior to those for Test II-2. The Test II-2 breakthrough curve increases very rapidly and peaks a few hundred minutes earlier than the peak for Test II-4. The increase of both curves has the same slope. The curve for Test II-4 has a few fluctuations prior to peaking. The tail of the curve for Test II-2 retreats to only half its peak concentration, while for Test II-4 the tail retreats to a much lower concentration and eventually drops off at about t=1650 minutes (t=0 at each tracer injection). This drop is explained previously as caused by the air injection/explosion.
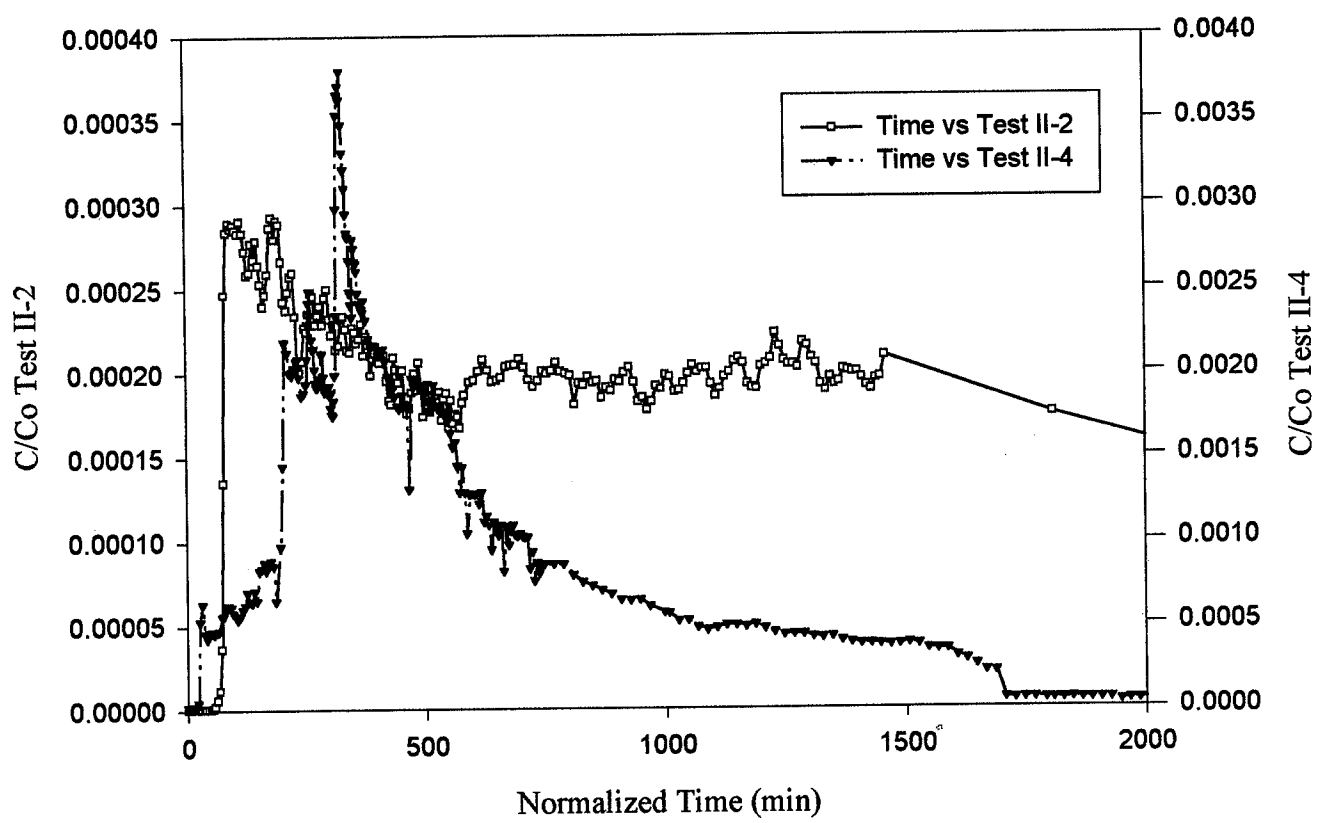
Figure 46. Relative Fluorescein Concentrations vs Normalized Time for
the Nonrecirculation Tests, II-2 and II-4, for Well Q17D.
(Normalized to II-4).

After the main peak for Test II-4, both curves follow a downward trend with similar slopes until about t=600 minutes. The curve increases and stabilizes for Test II-2, but for Test II-4 the downward trend towards a residual concentration continues.

Residual Fluorescein Effects

Residual fluorescein appears to have a mixed effect on the results of the tracer experiments. The shape and peak time of the fluorescein breakthrough curve are very similar to that of iodide and veratryl alcohol in Test I-3, yet fluorescein had been injected several times prior to this test. The similarities of the curves suggest residual fluorescein did not significantly affect the fluorescein results in Test I-3. However residual effects appear to be great in Test II-4. In the comparison with Test II-2 the curves and peak times are very different. The hydraulic gradients are very similar and the tests were conducted in a similar fashion. Residual fluorescein in Test II-4 is the only explanation for the large differences. The skewness of the breakthrough curve is caused by the pumping of the injection well, Q16D, the evening prior to the experiment which disrupted and flushed the system. Fluorescein was injected five times prior to Test II-4 and was thereby drawn from pore spaces and fractures that would otherwise have been allowed to remain. In addition, the scale of Test I-3 was much greater than Test II-4. Well Q16D is located in a very low hydraulic conductivity zone which possibly allows a greater tracer retention. It is unknown the extent of which residual fluorescein affected the other experiments; although, it is probably not a significant problem.

Based on the results of Test I-3 it is determined fluorescein can be used multiple times with success. The successes of the experiments at the UIGRS can be attributed to low amounts of fluorescein injected (except for Test II-2), large time gaps between experiments, the use of different well pairs and the aquifer system itself.

Test Reproducibility

Reproducibility of the tracer tests is quite good as shown by comparison of the recirculation experiments. Test I-1 was the first test conducted and Test I-3 was the last. It was anticipated the results of Test I-3 would not be very similar because of differences in the way they were conducted and the alterations of flow paths resulting from filtered microbeads

and spores. Despite the obstacles the results of the recirculation tests are quite similar, indicating the manner in which tracer experiments are conducted may not significantly affect the outcome (i.e. packers or no packers, etc.).

DISCUSSION OF TRACER MIGRATION BY TRANSPORT PROCESSES

Tracer transport in fractured rock is governed by a number of complicated processes. These include advection, dispersion, diffusion, aquifer heterogeneity, flow in multiple channels, channeling, sorption (and desorption), biodegradation and density effects. Particulate transport may in addition be affected by filtration and predation. Table 25 lists these processes and the pattern of responses in the breakthrough curves. Information is provided for ionic, organic (including fluorescein), microbial and particle transport.

There are several similarities among the results of the tracer tests provided in Chapter 6 of this thesis which provide an insight into the E-fracture aquifer. These include low tracer recovery, and for the dissolved tracers' breakthrough curves, a rapid rise in concentration, multiple peaks and shoulders (fluctuations) and long tails. Also, the breakthrough of the particulate tracers occurs prior to the conservative tracers.

The recovery was low for many of the tracers, particularly for the particulate tracers. For example, the recovery of fluorescein was only 3.71% for well V16D in Test I-1, and 1.54% for the same well in Test I-2. The recovery of the particulates was less than 1% for Tests I-3 and II-4. The low retrieval of the tracers may be attributed to loss within dead end fractures and pore spaces, borehole storage, sorption, biodegradation, density effects, dilution, dispersion and diffusion. The particulates are probably lost to density effects and filtration. Spores may also be lost by sorption and predation. The dissolved tracers are considered to act conservatively based on the findings in Test I-3; therefore, sorption probably does not affect their transport. They are also not likely to biodegrade; although, VA will degrade when stored without proper preservation. Unlike the spores, the microbeads are probably not affected by sorption because they do not have a surface charge. The loss of spores may also be attributed to problems with the analysis methods and the analyses themselves. Harvey (1991) in Harvey et al. (1993) stated the major mechanisms immobilizing bacterial transport

TRANSPORT PROCESS	PATTERNS OF RESPONSE	IONIC TRANSPORT	ORGANIC TRANSPORT	MICROBIAL TRANSPORT	PARTICLE TRANSPORT
advection	tracer spreading - bell shaped BTC	yes	yes	yes	yes
dispersion	tracer spreading - bell shaped BTC	yes	yes	yes	yes
molecular diffusion	long tail in BTC	yes	yes		
matrix diffusion	long tail in BTC	yes	yes		
aquifer heterogeneity	fast BTC rise, multiple BTC peaks, long BTC tail, and tracer loss	yes	yes	yes	yes
transport in different channels	multiple peaks and long BTC tail	yes	yes	yes	yes
channelized transport	faster BTC peak, fewer physical and chemical reactions (eg. sorption, biodegradation)	yes	yes	yes	yes
reversible sorption	long BTC tail	yes?	yes	yes	yes
irreversible sorption	tracer loss	yes?	yes	yes	yes
reversible and irreversible sorption	long BTC tail and attenuated BTC peak		yes	yes	yes
biodegradation	tracer loss		yes		
density effects	tracer loss (and/or long BTC tail for dyes)	yes?	yes	yes	yes
filtering	tracer loss			yes	yes
predation	tracer loss			yes	
motility	tracer loss and earlier BTC peak			yes	
death	tracer loss			yes	
starvation	faster BTC peak, less sorption			yes	
microbial growth	scewed BTC results and more tracer recovered than injected			yes	

BTC = breakthrough curve   Table 25. Summary of Fractured Rock Transport Processes and Effects on Breakthrough Curves.

are straining and irreversible sorption. Whereas McKay et al. (1993) found *phage* attenuation is caused mainly by sorption and diffusion (diffusion is not considered a transport mechanism for particulate tracers because diffusion is movement under a chemical gradient).

The dissolved tracer breakthrough curves have a fairly rapid rise, which may be the result of channeling. Channeling is caused by areas of faster movement within a fracture resulting from tortuous flow through rough walled fractures.

Nearly all of the dissolved tracer breakthrough curves have shoulders (fluctuations) and multiple peaks. These may result from flow through different channels or fractures (Claasen and Cordes, 1975; Pang et al., 1998). Each peak may represent breakthrough within a single fracture. The multiple peaks and shoulders also demonstrate the aquifer is heterogeneous. In a homogeneous environment the breakthrough curve is smooth and bell shaped.

Many of the breakthrough curves have significant tails. Tailing is caused by borehole storage, dispersion, matrix and molecular diffusion, transport in different channels and desorption. Tracer remaining in the injection borehole may act as a continuous source. In the early portion of the experiment the tracers diffuse from their "flow channel" into the eddies, dead-end fractures and pore spaces and the block matrix. The long tail is a result of the reverse of this process. Matrix diffusion is probably not a major mechanism because the experiments were short in duration. Flow through different channels causes tailing by a combination of lower velocities in some channels and faster velocities in other channels (NRC, 1996). As stated previously, none of the dissolved tracers were affected by sorption; they therefore were not affected by desorption.

DISCUSSION OF CURVE MATCHING RESULTS

The Sauty (1980) curve matching method provided results for non-dipole wells in the recirculation tests and wells in the nonrecirculation tests; however, curve matching by the Brenner Solution for the dipole well pair in the recirculation experiments did not yield any calculated aquifer parameters. In the Sauty (1980) method, the experimental data are presented as C/C_{max} where C_{max} is the maximum concentration in the monitoring well instead of C/Co where Co is the initial concentration in the injection well as in the Brenner Solution.

The very low relative concentrations of the experimental data are magnitudes less than those predicted by theory of the Brenner Solution causing the experimental data to fall significantly below the type curves; thus a curve match could not be performed using this method.

A wide range of Peclet numbers was estimated for the E-fracture aquifer by the Sauty (1980) method. Peclet numbers varied from 8 to 100. A high Peclet number indicates mixing is dominated by mechanical dispersion or advection whereas a lower number indicates mixing is dominated by diffusion. A Peclet number above seven indicates transport is controlled by advective dispersion and the effects of diffusion can be ignored (Fetter, 1993). The results from the curve matching indicates this is true for transport in the E-fracture.

The dispersivity values calculated from the fluorescein data increase with increasing distance. Wells Q16D and Q17D show evidence of low dispersivity and dispersion values, nearly 100 times less than well T16D which is further from the injection well. Sauty (1980) found dispersivity increases with distance and stabilizes at a characteristic value dependent upon the factor which controls heterogeneity. Fetter (1993) explained as the length of the flow path increases the heterogeneity also increases which in turn enlarges the plume. Pang et al. (1998) however, stated the dispersivity value should be constant.

The dispersivity values calculated from the fluorescein data are similar to those listed in the literature. Domenico and Schwartz (1990) stated that dispersivities range from 0.1 to 2 m (0.33 to 6.56 ft) over relatively short distances. The values calculated for the E-fracture vary from 0.20 to 8.75 ft.

The reliability of the curve matching results may be low based on conclusions by Gelhar et al. (1992). They conducted a critical review of data on field-scale dispersion in aquifers and determined that none of the fractured media data they analyzed are of high reliability. The Brenner solution and Sauty methods are two of the methods analyzed in Gelhar et al. (1992). These techniques do not account for an increasing dispersivity with distance. The distances between the wells used in the experiments at the UIGRS are not large enough for dispersivity to be constant. Gelhar et al. (1992) stated dispersivity may be constant at distances of hundreds of meters but not at tens of meters. In addition, Sauty (1980) stated the accuracy of the values calculated from his method is dependent upon the

extent of the heterogeneity which is not known. For these reasons the results presented from the curve matching are estimations only.

Failure of more than 50% of the data to match the type curves also reduces the reliability of the results. Most of data comprise the breakthrough curve tail which lies above the Sauty (1980) type curves. The processes that cause tailing are not incorporated into the Sauty (1980) method. Gelhar et al. (1992) determined that radially convergent tests were not of high reliability because the data often exhibit tailing and are accurate to within one or two orders of magnitude only.

CHAPTER 9
CONCLUSIONS AND RECOMMENDATIONS

The general conclusions of this study are: 1) the E-fracture zone is a heterogeneous aquifer as seen by multiple peaks and shoulders in the breakthrough curves and differences in peak breakthrough times for the different wells and experiments and 2) conducting recirculating and nonrecirculating tests with multiple tracers (dissolved and particulate tracers) provides an abundance of information about the aquifer, transport in fractured basalt and individual tracer characteristics. More specific conclusions from conducting the tracer experiments are discussed.

1. The E-fracture aquifer is hydraulically continuous within the area of four wells (V16D, T16D, Q16D and Q17D) used in the tracer experiments.
2. Fluorescein and veratryl alcohol (VA) act as conservative tracers denoted by their similar breakthrough curve shape and peak timing with iodide, a known conservative tracer, in Test I-3.
3. Particles and conservative tracers in the same tracer experiment help identify the existence of preferential flow paths in a fractured rock environment as seen by the early arrival of the microbeads and spores relative to the conservative tracers.
4. Fractures with apertures greater than 6 μm connect the wells in the E-fracture based on the breakthrough of the microbeads (6μm diameter) in wells V16D, T16D, Q17D and Q16D.
5. Overall, *Bacillus thermoruber* spores did not yield successful results and may therefore not be a useful tracer. Filtration, density effects, sorption, and problems stimulating them in the laboratory are likely to have prevented the spore recovery.
6. Recovery of the tracers was quite low. One explanation is borehole storage in the injection well which may contain much of the tracer throughout the experiment. Another explanation is the length of the flow paths. More than 99.999% of the particulate tracers are not recovered and are therefore relatively unsuccessful in this type of environment at

these well spacings. The particulates are lost mainly by filtration and density effects. Spores may also be lost by sorption and predation.

7. Small amounts of residual fluorescein does not appear to significantly affect subsequent tests, demonstrated by the similarities of the fluorescein breakthrough curves of the recirculation tests.

8. There is field reproducibility of the tracer tests based on the similarity of the fluorescein results of the recirculation tests.

9. Several transport processes may affect dissolved tracer transport in fractured rock, including flow through different channels, dispersion, channeling, molecular and matrix diffusion, flow into dead-end fractures, borehole storage and density effects.

10. Curve matching by the Sauty (1980) method for the nonrecirculation experiments and the nonrecirculation wells in the recirculation experiments produced results; although, curve matching by the Brenner Solution did not.

11. High Peclet numbers were calculated by the Sauty (1980) method of curve matching which indicate transport is governed by advective dispersion and not diffusion. The Peclet numbers produced dispersivity values which increased with increasing distance.

12. Reliability of the curve matching results is likely to be low because the aquifer is heterogeneous, anisotropic and is in fractured rock, and because a majority of the experimental data do not match the type curves . Both curve matching methods are for experiments conducted in a homogeneous, isotropic medium which the E-fracture zone is not.

There are several recommendations of additional studies that should be conducted to better understand these tracer experiments, the E-fracture zone and transport in fractured rock.

1. A transport model incorporating processes that may have caused the deviations from the bell-shaped curve may prove useful to simulate the tracer tests at the UIGRS to verify aquifer parameters (i.e. dispersivity and dispersion), calculate others (i.e. effective porosity) and to obtain a better understanding of transport of the E-fracture network.

2. Laboratory studies should be conducted on the *Bacillus thermoruber* spores to determine their sorption capacity and their optimum growth environment because there was almost no spore recovery.

3. Push-pull tests ought to be conducted in the same wells as the tracer experiments to verify calculated aquifer parameters, to study the microbial activity and to gain a better understanding of the E-fracture.

4. Additional wells drilled within the transect between Q17D and V16D are suggested for supplementary aquifer and tracer tests. This would provide additional information about the E-fracture network.

5. A microbial analysis should be conducted of the E-fracture and compared to the results conducted by Zheng (1992) to determine what effect the tracers had on the aquifer.

REFERENCES

Abelin, H., L. Birgersson, J. Gidlund, and I. Neretnieks. 1991a. A large-scale flow and tracer experiment in granite, 1. Experimental design and flow distribution. Water Resources Research, Vol. 27, No. 12, pp. 3107-3117.

Abelin, H., L. Birgersson, L. Moreno, H. Widén, T. Ågren, and I. Neretnieks. 1991b. A large-scale flow and tracer experiment in granite, 2. Results and interpretation. Water Resources Research, Vol. 27, No. 12, pp. 3119-3135.

Aris, R. 1959. The longitudinal diffusion coefficient in flow through a tube with stagnant pockets. Chem. Eng. Sci. Vol. 10, pp. 194-198.

Atkinson, T.C., D.J. Smith, and R.J. Whitaker. 1973. Experiments in tracing underground waters in limestones. Journal of Hydrology. Vol. 19, pp. 323-349.

Aulenbach, D.B., J.H. Bull, and B.C. Middlesworth. 1978. Use of tracers to confirm ground-water flow. Ground Water, Vol. 16, No. 3, pp. 149-157.

Bales, R.C., C.P. Gerba, G.H. Grondin, and S.L. Jensen. 1989. Bacteriophage transport in sandy soil and fractured tuff. Applied Environmental Microbiology, Vol. 55, pp. 2861-2967.

Bear, J., C.F. Tsang, and G. de Marsily. 1993. Flow and Contaminant Transport in Fractured Rock. Academic Press, Inc., New York, NY, 560p.

Berkowitz, B., J. Bear, and C. Braester. 1988. Continuum models for contaminant transport in fractured porous formations. Water Resources Research, Vol. 24, No. 8, pp. 1225-1236.

Boggs, J.M., and E.E. Adams. 1992. Field study of dispersion in a heterogeneous aquifer, 4. Investigation of adsorption and sampling bias. Water Resources Research, Vol. 28, No. 12, pp. 3325-3336.

Brenner, H. 1962. The diffusion model of longitudinal mixing in beds of finite length, numerical values. Chemical Engineering Science. Vol. 17, pp. 229-243.

Brock, T.D., M.T. Madigan, J.M. Parker. 1994. Biology of Microorganisms. Prentice Hall, Englewood Cliffs, NJ.

Brown, P.A. 1998. Spore, microsphere and encapsulated cell transport in a heterogeneous subsurface environment. M.S. Thesis, University of Idaho, Moscow, Idaho.

Brown, S.R. 1987. Fluid flow through rock joints: the effect of surface roughness. Journal of Geophysical Research, Vol. 92, No. B2, pp. 1337-1347.

Brown, S.R. 1989. Transport of fluid and electric current through a single fracture. Journal of Geophysical Research, Vol. 94, No. B7, pp. 9429-9438.

Bush, J.H., and M. McFadden. 1994. Generalized discussion of Latah County Geology. Unpublished. 33p.

Bush, J.H. 1998. Personal communication.

Champ, D.R., and J. Schroeter. 1988. Bacterial transport in fractured rock - a field-scale tracer test at the Chalk River Nuclear Laboratories. Water Science and Technology. Vol. 20, No. 11/12, pp. 81-87.

Chapelle, F.H. 1993. Ground-Water Microbiology and Geochemistry. John Wiley and Sons, Inc., New York, New York.

Claassen, H.C., and E.H. Cordes. 1975. Two-well recirculating tracer test in fractured carbonate rock, Nevada. Hydrological Sciences - Bulletin. Vol. XX, No. 3, pp. 367-383.

Cliffe, K.A., D. Gilling, N.L. Jefferies, and T.R. Lineham. 1993. An experimental study of flow and transport in fractured slate. Journal of Contaminant Hydrology, Vol. 13, pp. 73-90.

Coats, K.H., and B.D. Smith. 1964. Dead end pore volume and dispersion in porous media. Soc. Pet. Eng. J. Vol. 4, pp. 73-84.

Davis, S.N., G.M. Thompson, H.W. Bentley, and G. Stiles. 1980. Ground-water tracers - A short review. Ground Water, Vol. 18, No. 1, pp. 14-23.

Davis, S.N., D.J. Campbell, H.W. Bentley, and T.H. Flynn. 1985. Ground-Water Tracers. National Water Well Association. Robert S. Kerr Environmental Research Laboratory. U.S. Environmental Protection Agency. 200p.

Domenico, P.A., and F.W. Schwartz. 1990. Physical and Chemical Hydrogeology. John Wiley & Sons, Inc., New York, NY, 824p.

Dverstorp, B., J. Andersson, and W. Nordqvist. 1992. Discrete fracture network interpretation of field tracer migration in sparsely fractured rock. Water Resources Research, Vol. 28, No. 9, pp. 2327-2343.

Enfield, C.G., and G. Bengtsson. 1988. Macromolecular transport of hydrophobic contaminants in aqueous environments. Ground Water, Vol. 26, No. 1, pp. 64-70.

Everts, C.J., and R.S. Kanwar. 1994. Evaluation of rhodamine WT as an adsorbed tracer in an agricultural soil. Journal of Hydrology, Vol. 153, pp. 53-70.

Fetter, C.W. 1993. Contaminant Hydrogeology. Macmillan Publishing Company, New York, NY. 458p.

Fetter, C.W. 1994. Applied Hydrogeology. Macmillan Publishing Company, New York, NY. 691p.

Fontes, D.E., A.L. Mills, G.M. Hornberger, and J.S. Herman. 1991. Physical and chemical factors influencing transport of microorganisms through porous media. Applied and Environmental Microbiology, Vol. 57, No. 9, pp. 2473-2481.

Freeze, R.A., and J.A. Cherry. 1979. Groundwater. Prentice Hall, Englewood Cliffs, NJ. 604p.

Gannon, J.T., U. Mingelgrin, M. Alexander, R.J. Wagenet. 1991. Bacterial transport through homogeneous soil. Soil Biol. Biochem., Vol. 23, No. 12, pp. 1155-1160.

García Pardo, B. 1993. Relation between ground water and surface water at the University of Idaho Groundwater Research Site. M.S. Thesis, University of Idaho, Moscow, Idaho.

Ge, S. 1997. A governing equation for fluid flow in rough fractures. Water Resources Research, Vol. 33, No. 1, pp. 53-61.

Gelhar, L.W., C. Welty, and K.R. Rehfeldt. 1992. A critical review of data on field-scale dispersion in aquifers. Water Resources Research, Vol. 28. No. 7, pp. 1955-1974.

Grisak, G.E., and J.F. Pickens. 1980. Solute transport through fractured media; 1. The effect of matrix diffusion. Water Resources Research, Vol. 16, No. 4, pp. 719-730.

Grove, D.B., and W.A. Beetem. 1971. Porosity and dispersion constant calculations for a fractured carbonate aquifer using the two well tracer method. Water Resources Research, Vol. 7, No. 1, pp. 128-134.

Harvey, R.W., L.H. George, R.L. Smith, and D.R. LeBlanc. 1989. Transport of microspheres and indigenous bacteria through a sandy aquifer: results of natural- and forced-gradient tracer experiments. Environmental Science Technology, Vol. 23, No. 1, pp. 51-56.

Harvey, R.W., and S.P. Garabedian. 1991. Use of colloid filtration theory in modeling movement o bacteria through a contaminated sandy aquifer. Environmental Science Technology, Vol. 25, No. 1, pp. 178-185.

Harvey, R.W., N.E. Kinner, D. MacDonald, D.W. Metge, and A. Bunn. 1993. Role of physical heterogeneity in the interpretation of small-scale laboratory and field observations of bacteria, microbial-sized microsphere, and bromide transport through aquifer sediments. Water Resources Research, Vol. 29, No. 8, pp. 2713-2721.

Hendry, M.J., J.R. Lawrence, and P. Maloszewski. 1997. The role of sorption in the transport of klebsiella oxytoca through saturated silica sand. Ground Water, Vol. 35, No. 4, pp. 574-584.

Istok, J.D., M.D. Humphrey, M.H. Schroth, M.R. Hyman, and K.T. O'Reilly. 1997. Single-well, "push-pull" test for in situ determination of microbial activities. Ground Water, Vol. 35, No. 4, pp. 619-631.

Kanwar, R.S., J.L. Baker, and P. Singh. 1997. Use of chloride and fluoresceint dye as tracers in measuring nitrate and atrazine transport through soil profile under laboratory conditions. J. of Environ. Sci. Health, Vol. A32, No. 7, pp. 1907-1919.

Keswick, B.H., D-S. Wang, and C.P. Gerba. 1982. The use of microorganisms as ground-water tracers: A review. Ground Water, Vol. 20, No. 2, pp. 142-149.

Kopp, W.P. 1994. Hydrogeology of the upper aquifer of the Pullman-Moscow Basin at the University of Idaho Aquaculture Site. M.S. Thesis, University of Idaho, Moscow, Idaho.

LaBlanc, D.R., S.P. Garabedian, K.M. Hess, L.W. Gelhar, R.D. Quadri, K.G. Stollenwerk, and W.W. Wood. 1991. Large-scale natural gradient tracer test in sand and gravel, Cape Cod, Massachusetts 1. Experimental design and observed tracer movement. Water Resources Research, Vol. 27, No. 5, pp. 895-910.

Li, T. 1991. Hydrogeologic characterization of a multiple aquifer fractured basalt system. PhD. Dissertation, University of Idaho, Moscow, Idaho.

Lum, W.E., J.L. Smoot, and D.R. Ralston. 1990. Geohydrology and numerical model analysis of ground-water flow in the Pullman-Moscow area, Washington and Idaho. U.S. Geological survey Water-Resources Investigations Report 89-4103, 73p.

Mackay, D.M., D.L. Freyberg, P.V. Roberts, and J.A. Cherry. 1986. A natural gradient experiment on solute transport in a sand aquifer, 1. Approach and overview of plume movement. Water Resources Research, Vol. 22, No. 13, pp. 2017-2029.

Maloszewski, P., and A. Zuber. 1992. On the calibration and validation of mathematical models for the interpretation of tracer experiments in groundwater, Advances in Water Resources, Vol. 15, pp. 47-62.

McDowell-Boyer, L.M., J.R. Hunt, and N. Sitar. 1986. Particle transport through porous media. Water Resources Research, Vol. 22, pp. 1901-1921.

McKay, L.D., J.A. Cherry, R.C. Bales, M.T. Yahya, and C.P. Gerba. 1993. A field example of bacteriophage as tracers of fracture flow. Environ. Sci. Technol. Vol. 27, No. 6, pp. 1075-1079.

Moreno, L., Y.W. Tsang, C.F. Tsang, F.V. Hale, and I. Neretnieks. 1988. Flow and tracer transport in a single fracture: a stochastic model and its relation to some field observations. Water Resources Research, Vol. 24, No. 12, pp. 2033-2048.

Moreno, L., and I. Neretnieks. 1993. Flow and nuclide transport in fractured media: the importance of the flow-wedded surface for radionuclide migration. Journal of Contaminant Hydrology, Vol. 13, pp. 49-71.

National Research Council (NRC). 1994. Alternative for Ground Water Cleanup. National Academy Press, Washington D.C., 314p.

National Research Council (NRC). 1996. Rock Fractures and Fluid Flow. National Academy Press, Washington D.C., 551p.

Neretnieks, I. 1980. Diffusion in the rock matrix: an important factor in radionuclide retardation. Journal of Geophysical Research, Vol. 85, No. B8, pp. 4379-4397.

Neretnieks, I., T. Erikson, and P. Tähtinen. 1982. Tracer movement in a single fissure in granitic rock: Some experimental results and their interpretation. Water Resources Research, Vol. 18, No. 4, pp. 849-858.

Neretnieks, I. 1983. A note on fracture flow dispersion mechanisms in the ground. Water Resources Research, Vol. 19, No. 2, pp. 364-370.

Neretnieks, I. 1993. Solute transport in fracture rock - applications to radionuclide waste repositories, in Flow and Contaminant Transport in Fractured Rock. Academic Press, Inc., New York, NY, pp. 39-127.

Novak, C.F. 1993. Modeling mineral dissolution and precipitation in dual-porosity fracture-matrix systems. Journal of Contaminant Hydrology, Vol. 13, pp. 91-115.

Novakowski, K.S., G.V. Evans, D.A. Lever, and K.G. Raven. 1985. A field example of measuring hydrodynamic dispersion in a single fracture. Water Resources Research, Vol. 21, No. 8, pp. 1165-1174.

Novakowski, K.S., and P.A. Lapcevic. 1994. Field measurement of radial solute transport in fractured rock. Water Resources Research, Vol. 30, No. 1, pp. 37-44.

Ostensen, R.W. 1998. Tracer tests and contaminant transjport rates in dual-porosity formations with applications to the WIPP. Journal of Hydrology, Vol. 204, pp. 197-216.

Pang, L., M. Close, and M. Noonan. 1998. Rhodamine WT and *Bacillus subtilis* transport through an alluvial gravel aquifer. Ground Water, Vol. 36, No. 1, pp.112-122.

Pankow, J.F., R.L. Johnson, J.P. Hewetson, and J.A. Cherry. 1986. An evaluation of contaminant migration patterns at two waste disposal sites on fractured porous media in terms of the equivalent porous medium (EPM) model. Journal of Contaminant Hydrology, Vol. 1, pp. 65-76.

Petrich, C.R. 1995. Microsphere and encapsulated cell transport in a heterogeneous subsurface environment. PhD. Dissertation, University of Idaho, Moscow, Idaho.

Pierce. J.L. 1998. Geology and hydrogeology of the Moscow East and Robinson Lake quadrangles, Latah County. M.S. Thesis, University of Idaho, Moscow, Idaho.

Provant, A.P. 1995. Geology and hydrogeology of the Viola and Moscow west quandrangles, Latah County, Idaho and Whitman County, Washington. M.S. Thesis, University of Idaho, Moscow, Idaho.

Ptak, T., and G. Schmid. 1996. Dual-tracer transport experiments in a physically and chemically heterogeneous porous aquifer: effective transport parameters and spatial variability. Journal of Hydrology, Vol. 183, pp. 117-138.

Ralston, D.R. 1998. Personal communication.

Rasmuson, A., and I. Neretnieks. 1986. Radionuclide transport in fast channels in crystalline rock. Water Resources Research, Vol. 22, pp. 1247-1256

Raven, K.G., K.S. Novakowske, and P.A. Lapcevic. 1988. Interpretation of field tracer tests of a single fracture using a transient solute storage model. Water Resources Research, Vol. 24, No. 10, pp. 2019-2032.

Reimus, P.W., B.A. Robinson, H.E. Nuttall, and R. Kale. 1994. Simultaneous Transport of Synthetic Colloids and a Nonsorbing Solute Through Single Saturated Natural Fractures. Los Alamos National Laboratory, U.S. Department of Energy, LA-UR-94-TSA-11-94-R104.

Reeves, M., G.A. Freeze, V.A. Kellel, J.F. Pickens, D.T. Upton, and P.B. Davies. 1991. Regional Double Porosity Solute Transport in the Culebra Dolomite Under Brine-Reservoir-Breach Release Conditions: An Analysis of Parameter Sensitivity and Importance. SAND89-7069, Sandia National Laboratories, Albuquerque, NM.

Sabatini, D.A., and R.A. Austin. 1991. Characteristics of rhodamine WT and fluorescein as adsorbing ground-water tracers. Ground Water, Vol. 29, No. 3, pp. 341-349.

Sauty, J.P. 1980. An analysis of hydrodispersive transfer in aquifers. Water Resources Research, Vol. 16, No. 1, pp. 145-158.

Sauty, J.P. 1977. Interpretation of tracer tests by means of type curves: application to uniform and radial flow. First International Well Testing Symposium, U.S. Dep. Of Energy, Div. Geothermal Energy, Berkeley, CA, Oct. 19-21, 1977, pp. 82-90.

Schmotzer, J.K., W.A. Jester, and R.R. Parizek. 1973. Groundwater tracing with post sampling activation analysis. Journal of Hydrology, Vol. 20, pp. 217-236.

Shiau, B-J., D.A. Sabatini, and J.H. Harwell. 1993. Influence of rhodamine WT properties on sorption and transport in subsurface media. Ground Water, Vol. 31, No. 6, pp. 913-920.

Sinton, L.W., R.K. Finlay, L. Pang, and D.M. Scott. 1997. The transport of bacteria and bacteriophages in irrigated effluent into and through an alluvial gravel aquifer. Water, Air, and Soil Pollution, Vol. 98, No. 3-4, pp. 17-48.

Skilton, H., and D. Wheeler. 1988. Bacteriophage tracer experiments in groundwater. Journal of Applied Bacteriology, Vol. 65, pp. 387-395.

Smart, P.L., and I.M.S. Laidlaw. 1977. An evaluation of some fluorescent dyes for water tracing. Water Resources Research, Vol. 13, No. 1, pp. 15-33.

Streltsova, T.D. 1976. Hydrodynamics of groundwater flow in a fractured formation. Water Resources Research, Vol. 12, No. 3, pp. 405-414.

Sudicky, E.A., and E.O. Frind. 1982. Contaminant transport in fractured porous media: analytical solutions for a system of parallel fractures. Water Resources Research, Vol. 18, No. 6, pp. 1634-1642.

Tang, D.E., E.O. Frind, and E.A. Sudicky. 1981. Contaminant transport in fractured porous media: analytical solution for a single fracture. Water Resources Research, Vol. 17, No. 3, pp. 555-564.

Thompson, M.E. 1991. Numerical simulation of solute transport in rough fractures. Journal of Geophysical Research. Vol. 96, No. B3, pp. 4157-4166.

Thompson, M.E., and S.R. Brown. 1991. The effect of anisotropic surface roughness on flow and transport in fractures. Journal of Geophysical Research, Vol. 96, No. B3, pp. 21,923-21,932.

Tsang, Y.W., and C.F. Tsang. 1987. Channel model of flow through fractured media. Water Resources Research, Vol. 23, No. 3, pp. 467-479.

Tsang, Y.W., C.F. Tsang, I. Neretnieks, and L. Moreno. 1988. Flow and tracer transport in fractured media: a variable aperture channel model and its properties. Water Resources Research, Vol. 24, No. 12, pp. 2049-2060.

Tsang, Y.W., and C.F. Tsang. 1989. Flow channeling in a single fracture as a two-dimensional strongly heterogeneous permeable medium. Water Resources Research, Vol. 25, No. 9, pp. 2076-2080.

Tsang, C.F., Y.W. Tsang, and F.V. Hale. 1991, Tracer transport in fractures: Analysis of field data based on a variable-aperture channel model. Water Resources Research, Vol. 27, No. 12, pp. 3095-3106.

Turner, G.A. 1958. The flow structure in packed beds. Chem. Eng. Sci., Vol. 7, pp. 156-165.

Wood, W.W., and G.G. Ehrlich. 1978. The use of baker's yeast to trace microbial movement in ground water. Ground Water, Vol. 16, No. 6, pp. 398-403.

Zheng, M. 1992. Microbial ecology of a basalt aquifer. M.S. Thesis, University of Idaho, Moscow, Idaho.